Geotechnical Engineering

Project Day 2020

Organised by the
SRI LANKAN GEOTECHNICAL SOCIETY

SLGS

Message from the President - SLGS

From its inception, Sri Lankan Geotechnical Society has provided a forum for disseminating new knowledge in the field of geotechnical engineering and promoting research. It has organized many conferences, workshops and field visits in this context.

The Project Day competition is an annual event held among Sri Lankan undergraduates doing projects in the field of geotechnical engineering. It commenced in year 2000 with the objective of encouraging them to do good research and publish. Participants are expected to present their findings in a concise four paged paper and make a 15-minute oral presentation. The best paper and the second paper will receive cash awards and certificates.

Many winners in the past years have proceeded to do higher studies and established good carriers in the field of Geotechnical Engineering as both academics and practicing engineers.

It is encouraging to note that there are eleven papers on a wide variety of topics this year. I thank all the authors for their interest and commitment and hope they will continue with the habit of presenting their research in written form. It is only when one starts to write his findings, he would realize the gaps in his work or knowledge and would be able to rectify them.

I also wish to convey my sincere gratitude to the panel of evaluators; Prof. U. G. A. Puswewala, Dr. J. J. P. Ameratunga and Dr. J. S. M. Fowze.

Prof. Athula Kulathilaka
President – SLGS

Content

Develop a Relationship between 1-D Consolidation Parameters and Index Properties for Residual Soil

P.H.T.N. De Silva, S. Abeygunawardana and D. de S. Udakara
Department of Civil Engineering, University of Peradeniya, Sri Lanka

ABSTRACT: In the general engineering sense, residual soil is defined as the soil remains at the location of their geologic origin when they are formed by weathering of parent rock. The properties of these soils always affect to the design in construction and lack of understanding of these properties can lead construction errors. Therefore it is essential to know the suitability of a soil for a particular use based on its engineering characteristics. The determination of Compression Index (C_C) from consolidation tests is complex, expensive and time consuming. Tests for the determination of index properties such as Atterberg limits, water content and specific gravity are comparatively easier and take lesser time to obtain in the laboratory. Because of these factors, this study is carried out to predict the Compression Index using index properties. Under this study Compression Index and index properties of ten different undisturbed and disturbed samples obtained from Gampola to Bambarakale, Sri Lanka were determined by using Oedometer tests and index property tests. From the results of these laboratory tests correlations have been developed between Compression Index and index properties by using linear and multiple regression analyses. The study indicates that Compression Index relates better with the plasticity index than with the liquid limit. According to multiple regression analysis, compression index has a better correlation with both plasticity index and liquid limit. Also the results showed the same trend as with the results from the past studies.

1 INTRODUCTION

Settlement of soil under certain loads is a main consideration in construction design. This settlement can be defined as the decrease in volume due to rearrangement of soil particles under the effect of pressure. As a parameter to estimate the settlement of soil, Compression Index (C_C) can be used.

Compression index value of a soil can be obtained by laboratory Oedometer tests. But those tests are expensive, complex and time consuming. Even a very small disturbance also can affects to the settlement of soil sample. Because of these reasons many correlations were developed in the past to predict compressibility characteristics using index properties, the properties which are obtained by conducting index property tests comparatively easy and economical with respect to Oedometer tests.

Ibrahim *et al.* (2012) have given equation correlating compression index with plasticity index of soils at Perlis [1]. Kumar *et al.* (2016) made correlations in terms of liquid limit (LL), plastic limit (PL), optimum moisture content (OMC), maximum dry density (MDD) and differential free swell (DFS) to predict compression index for fine grained remolded soil [2]. Soibam *et al.* (2015) developed correlations to predict coefficient of consolidation (C_v) for soft clay in Manipur valley in terms of shrinkage index (I_s), plastic index (I_p) and moisture content (W_L) [3]. Sridharan and Nagaraj (2000) also proposed an equation to predict compression index for fine grained remolded clay in terms of shrinkage index (I_s), as given by $C_C = 0.007(I_s+18)$ [4]. Vikas *et al.* (2015) proposed their equation for compression index taking into account the plasticity index of remolded soil in India [5]. Vinod and Bindu (2010) studied on compressibility characteristics of high plasticity clay in State of Kerala, India and proposed correlations to predict compression index [6]. Among those equations, they discovered that the compression index correlates best with shrinkage index and plasticity index than the other parameters.

The existing relationships were developed mainly for remolded soils. Considering that, this study was carried out to find a correlation of Compression Index with index properties of residual soil in Sri Lanka.

2 METHODOLOGY

2.1 *Soil classification*

Ten disturbed soil samples were chosen at the area from Gampola to Bambarakale, Sri Lanka for soil classification tests like Atterberg limit tests and grain size analysis. Grain size analysis was done according to British Standard (BS 1377: part 2: 1990) by wet sieving 100 g of air dried soil using a 63 μm sieve. The soil passing through 63 μm sieve

was carefully collected and performed the grain size analysis using hydrometer method as per British Standards. The liquid limit of soils was determined using cone penetrometer method as specified in British Standard (BS 1377: part 2: 1990). The plastic limit (PL) of the soils was determined by rolling thread method specified in BS 1377: part 2: 1990. The plastic index (PI) was calculated as the numerical difference between liquid limit and plastic limit. With the use of particle size distribution curves, plasticity chart and British Soft Classification System for Engineering Purposes (BSCS), the soil samples were classified according to British Standard System. Understanding the soil type is important before conducting the 1-D consolidation test to check the suitability of soil for the consolidation test. The classification of all the ten soils is given in table 1.

Table 1. Soil classification

Sample no:	Location	Soil type
1	Gampola	Sandy clay of intermediate plasticity (CSI)
2	Atabage	Sandy clay of intermediate plasticity (CSI)
3	Wahugupitiya	Sandy silt of high plasticity (MSH)
4	Katukithula	Sandy silt of high plasticity (MSH)
5	Ramboda	Sandy silt of very high plasticity (MSV)
6	Labukale	Sandy silt of intermediate plasticity (MSI)
7	Labukale	Sandy silt of high plasticity (MSH)
8	Kuda Oya	Sandy clay of intermediate plasticity (CSI)
9	Pundalu Oya	Sandy silt of high plasticity (MSH)
10	Bambarakale	Silty sand of intermediate plasticity (MSI)

2.2 *Index property tests*

In this study, water content (W_n), spesific gravity (Gs) and Atterberg limits were considered as index properties. The water content of the soils was determined using oven drying method as specified in BS 1377: part 2: 1990. But the water content was not considered to develop the relationships since those values are varying with the environmental conditions. The specific gravity of soils was determined using pycnometer method specified in BS 1377: part 2: 1990. Stoppered bottle with a capacity of 50 ml was used. The variation between the specific gravity values was limited. Therefore those values were not used to predict the Compression Index. The liquid limit and plasticity index mentioned in section 2.1 were used as index properties to predict the Compression Index of soils.

2.3 *One-dimensional consolidation tests*

Ten undisturbed soils were tested by one-dimensional consolidation tests as specified in BS 1377: part 5: 1990 using oedometers with brass rings. A lubricant such as grease was used inside of the rings to minimize the friction between the ring and the soil specimen. Filter papers were placed on the top and the bottom of the soil specimen to prevent soil particles from being forced into the pores of the porous plates. Porous plates were kept on both sides of the specimen. The ring with the sample was placed in a consolidation cell and fixed the metal jacket on top of the cell. Then the cell was correctly positioned on the loading frame and dial gauge was adjusted to give a proper dial gauge reading under the applied load. The cell was inundated with distilled water and it was allowed to saturate for 24 hrs. Each soil specimen was subjected to five loading increments. (1 lb, 2 lb, 4 lb, 8 lb and 16 lb). The obtained parameters are given in table 2.

Table 2. Obtained parameters

Sample no:	W_n	G_s	LL	PI	C_C
1	16	2.60	43	20	0.1063
2	17	2.61	35	16	0.0617
3	13	2.62	58	24	0.1395
4	32	2.56	52	21	0.1006
5	24	2.60	73	26	0.1258
6	22	2.55	44	12	0.0682
7	9	2.64	58	23	0.1341
8	15	2.63	37	14	0.0905
9	21	2.57	53	18	0.0905
10	18	2.63	40	14	0.0653

3 RESULTS AND DISCUSSION

Using the data in table 2, the correlations are obtained using single and multiple regression analysis and correlations are given below in table 3.

Table 3. Correlations developed in the study

Index parameters	Correlations developed	R^2
LL	C_C=0.0019LL+0.0057	0.603
PI	C_C=0.0053PI+0.0021	0.799
LL and PI	C_C=0.005027PI+0.000149LL-0.00361	0.800

Different empirical relationships were proposed by many researchers to predict compression index using index property parameters such as liquid limit, plastic limit, plasticity index, shrinkage index, water content and specific gravity. Likewise a relationship is developed to predict compression index using liquid limit. Figure 1 shows the variation of Compression Index with liquid limit and this rela-

tionship is linear with a regression coefficient (R^2) of 0.603 as given by;

C_C=0.0019LL+0.0057 (1)

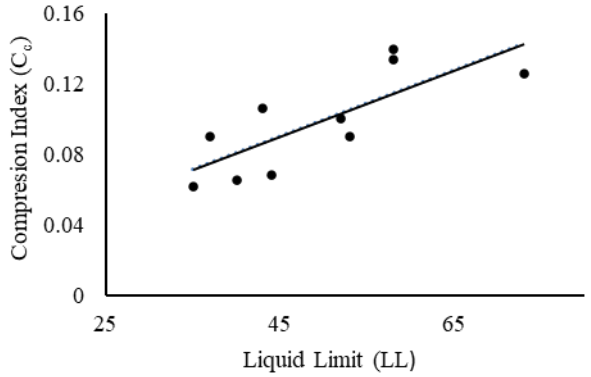

Fig. 1 Variation of compression index with liquid limit

According to figure 1, it can be seen that the soils with a higher liquid limit undergo more compression than soils with a lower liquid limit.

Another relationship between compression index and plasticity index was developed as shown in figure 2 using the data in table 2. According to this figure, it shows that the soils with higher plasticity index undergo more compression than soils with a lower plasticity index. This relationship is also linear with a regression coefficient (R^2) of 0.799 as given by;

C_C=0.0053PI+0.0021 (2)

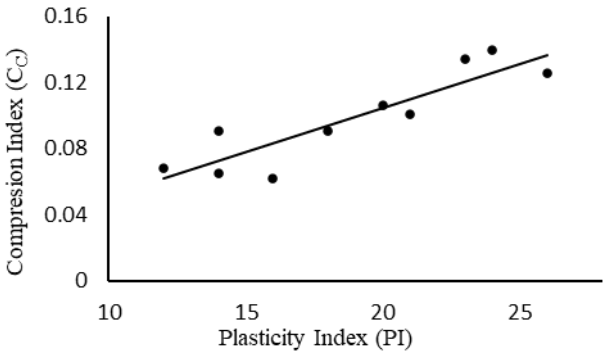

Fig. 2 Variation of compression index with plasticity index

Multiple regression analysis was used under this study to check the variation of compression index with liquid limit and plasticity index and that relationship is given by the following equation with a reasonable value of regression coefficient. (R^2 = 0.800)

C_C=0.005027PI+0.000149LL-0.00361 (3)

The predicted correlation between compression index and liquid limit is compared with the proposed correlations by various researchers. The figure 3 shows the comparison between the present study and previous studies.

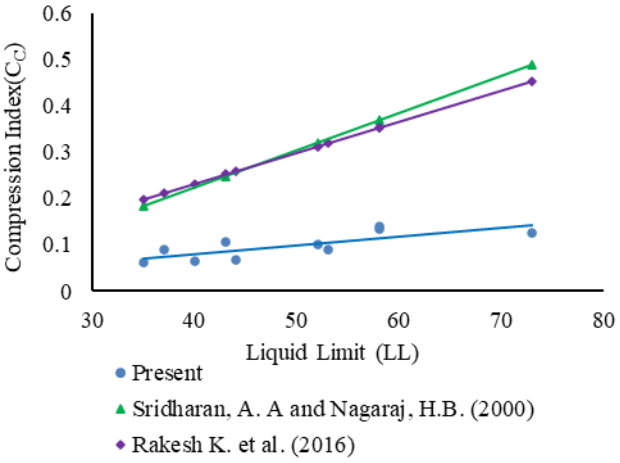

Fig. 3 Comparison of proposed relationship with relationships proposed by Sridharan and Nagaraj (2000) and Rakesh et al. (2016)

The figure 4 shows the comparison of predicted correlation between compression index and plasticity index with past studies. Here the relationships developed by Vikas K. et al. (2015) and Sridharan and Nagaraj (2000) are considered.

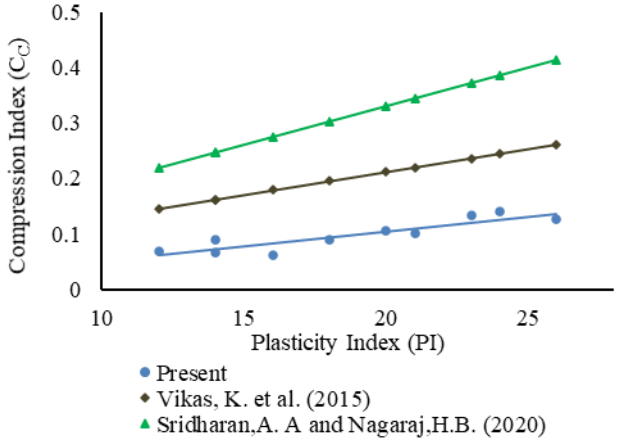

Fig. 4 Comparison of proposed relationship with relationships proposed by Sridharan and Nagaraj (2000) and Vikas et al. (2015)

The above relationships of past studies are for remolded soils. The settlement of undisturbed in-situ soil is considered in the present study. The settlement of undisturbed soil may be different as compared to remolded soil because compressibility depends on its boundary conditions. Also the boundary conditions are altered in remolded soils.

But the both present and past studies follow the same trend.

4 CONCLUSIONS

This research presents a method to predict the compression index (C_c) for residual soil in Sri Lanka with basic soil properties such as liquid limit and plasticity index. Linear and multiple regression analysis were carried out to develop relationships between compression index and index property parameters. Ten undisturbed soil samples were used to obtain the compression index and ten disturbed soil samples were used for the estimation of index properties.

The equations (1) and (2) show that the compression index of soils has a better correlation with the plasticity index than the liquid limit. The equation (3) represents the effect of both liquid limit and plasticity index on compression index and that equation has the greatest value of coefficient of determination.

However, these equations can be used conveniently, in accordance with the requirement. These findings help to predict compression index without conducting 1-D consolidation test which is complex, time consuming and expensive. Although there is a difference between predicted and existing relationships, both follow the same trend.

5 REFERENCES

Amat, C., Ariffin, N.A., Ibrahim, N.M., Rahim, N.L., and Salehuddin, S., (2012)., Determination of plastic index and compression index of soil at Perlis, APCBEE Procedia 4, pp.94-98

Bindu, J., Vinod, P., and Jain, V.K., (2010)., Compression index of high plasticity clay – an empirical correlation, J.indian terotechnology, 40:174-180

Devi, K.R., Devi, S.P., Prasad, D.S.V., and Raju, G.V.R.P., (2015)., Study on consolidation and correlation with index properties of different soils in Manipur valley, J. engineering research and development, 11:57-63

Dwivedi, P., Jain, P.K., and Kumar, R., (2016)., Prediction of compression index (C_C) of fine grained remoulded soils from basic soil parameters, J. applied engineering research, 11:592-598

Nagaraj, H.B., and Sridharan, A., (2015). Compressibility behavior of remoulded fine grained soils and correlation with index properties, J. can. geotech, 37:712-722

Chitra, R., Dixit, M., and Jain, V.K., (2000)., Correlation of plasticity index and compression index of soil, internatioal journal of innovations in engineering and technology (IJIET), 5

Comparison of strength properties of sand obtained from direct shear test and triaxial test

S.M.I.S. Bandara, M.S.N.V. Mohottala and D.de.S. Udakara
Department of Civil Engineering, University of Peradeniya, Sri Lanka

ABSTRACT: Shear strength is the most important mechanical property which heads the stability and resistance of a soil mass. It is also known that the shear strength of the soil will vary depending on the state of stress and strain. In general, soil stress states at failure are more often subscribed by the Mohr-Coulomb failure criterion with two shear strength parameters: ϕ – the angle of internal friction and c – cohesion. But for sand, there is no cohesion. This study is to be carried out to present a comparison of the strength properties of sand obtained from the direct shear test and triaxial test because those are the most commonly using laboratory tests to determine the shear strength of the soil and it is difficult to find a comparison between shear strength obtained from those tests for sand under drained conditions.

1 INTRODUCTION

The triaxial test and direct shear test have been used to determine the shear strength parameters of soil for over 70 years. Triaxial shear tests are commonly used to determine the strength characteristics of soils subject to a wide range of stress paths and loading conditions. And the Direct Shear Test is used for determination of the consolidated drained (or undrained) shear strength of soils and performed by deforming a specimen at a controlled rate on or near a single shear plane. The deflection of the sample of the direct shear test is laterally restricted but the sample of the triaxial test is not restricted because of the membrane. Because of that failure plane of the direct shear test maybe not the weakest failure plane although failure plane of the triaxial become the weakest failure plane. This is the main difference between direct shear tests and triaxial tests.

Sarunas et al. (2015) have studied the comparison of the internal friction angle of sand using 3 types of laboratory tests including the triaxial test and direct shear test. They focused on the same density of the sand sample by varying applying pressures according to the test to obtain results. They have found out that results obtained from the direct shear test and triaxial test are very close.

Cioara *et al.* (2014) have conducted a comparative study regarding results obtained from the direct shear test, triaxial compression test, and biaxial compression test. Pells et al. (1975) have considered the cohesive soil and cohesionless soil for comparison by both laboratory tests. They have researched by varying density indexes and applying pressures to obtain the results.

Castellanos and Brandon (2013) have studied the comparison between triaxial test and direct shear test for soil by varying soil sample types such as remolded, undisturbed, and also by direct the composition furthermore by varying the drained condition. It was found that the friction angle obtained from the direct shear apparatus is normally about 2 to 5 degrees lower than that obtained using the triaxial apparatus.

Jurgis et al. (2016) have carried out the direct shear test and triaxial test on sandy soil to perform stress-strain behavior. Here they found out values for internal friction angle obtained from direct shear tests are higher than values obtained from the triaxial test. Alias et al. (2014) have compared the cohesion values and values for the angle of internal friction angle obtained from both tests on remolded granite residual soil. It shows that the direct shear test gave lower values than the triaxial test for the angle of internal friction. But for the cohesion, CD triaxial gave a higher value than CD direct shear test and CU triaxial gave a lower value than the direct shear test.

Abdul Naser Abdul Ghani et al. (2009) have investigated the shear strength characteristics of sand-waste material mixtures using the direct shear test for two different waste materials namely tire shred and rubber shred. This study mentioned the density indexes of the samples and how they obtained them. Maccarini (1992) carried out tests by using a series of undisturbed samples of residual soil which were taken from a slope from Rio de Janeiro. In his study, drained triaxial tests and drained direct shear tests were carried out to examine stress-strain behavior.

Considering the above, sand with variable density index values was used in this current study to compare the internal friction angle of sand and the stress-strain behavior from both Direct shear tests and Triaxial tests under drained conditions.

2 METHODOLOGY

Figure 1 shows the research methodology of the research.

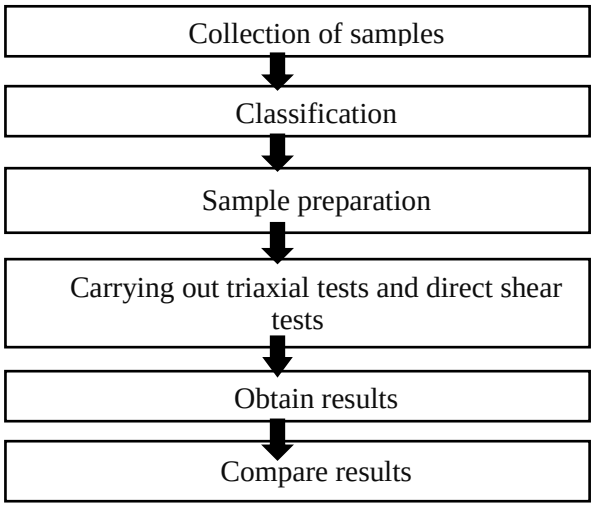

Fig. 1 Research methodology

The required amount of soil samples has been collected to do both laboratory tests from Mahaweli River near to Ramboda falls. To do the soil classification, firstly dry sieving analysis was done as specified in BS 1377: Part 2 – Clause 9. Then soil classification was done according to British Soil Classification System (BSCS). The following equation is used to determine the density index, I_d and required density for tests.

$$Id = \frac{\frac{1}{(\gamma_d)\min} - \frac{1}{\gamma_d}}{\frac{1}{(\gamma_d)\min} - \frac{1}{(\lambda_d)\max}} \quad (1)$$

Where, I_d is the density index, $(\gamma_d)_{min}$ is the minimum dry unit weight, $(\gamma_d)_{max}$ is the maximum dry unit weight and γ_d is the required dry unit weight.

The maximum dry unit weight and the minimum dry unit weight of sand were determined by referring clause 4.2 of BS 1377: Part 4: 1990 to obtain the required density for the tests. Then a subset of 3 CD triaxial test series and a subset of 3 CD direct shear test were carried out for loose, medium dense and dense states of compaction of the sand as specified in section 8 of BS 1377: Part 8: 1990 and section 4 of BS 1377: Part 7:1990 respectively. Each test series consisted of four individual tests conducted at different confining pressures 50kPa, 100kPa, 150kPa, 200kPa, and maintained the shear rate at 0.1016 mm/min during the tests. The relationship between measured shear stress at ultimate failure and applied normal stress was obtained to calculate the ultimate friction angle according to Mohr-Coulomb criteria.

3 RESULTS AND DISCUSSIONS

3.1 *Soil classification*

The classification was carried out on two soil samples to confirm the results. Since sand content was higher than 50% and the coefficient of curvature is between 1 to 3, this soil is classified as the well-graded sand according to British Soil Classification System (BSCS).

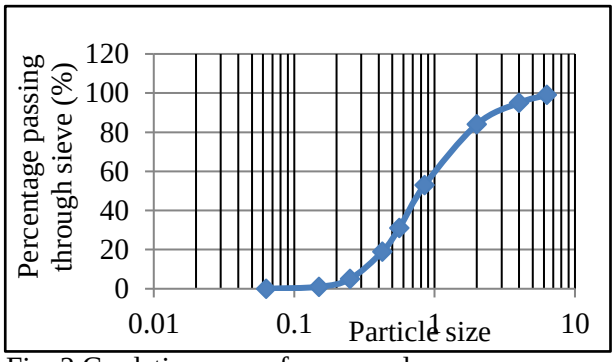

Fig. 2 Gradation curve for a sample

3.2 *Sample preparation*

The minimum dry density of sand was determined as 1369.8 kg/m^3 and the maximum dry density of sand was determined as 1765.10 kg/m^3. Density indices were taken specified in BS EN ISO 14688 - 02: 2004. Then required density ranges were calculated as in Table 1.

Table 1. Required density ranges

State of compaction	Density Index (%)	Density range (kg/m^3)
Loose	15-35	1417.41-1486.30
Medium dense	35-65	1486.30-1603.17
Dense	65-85	1603.17-1691.81

3.3 *Comparison of direct shear test and triaxial test results*

Using Mohr-Coulomb theorem ultimate friction angles and peak friction angles were calculated for sand. Then the dilation angles were calculated using the Mohr-coulomb model and Taylor's model for the dense state of compaction of the sand. Stress-strain curves obtained from both tests were compared.

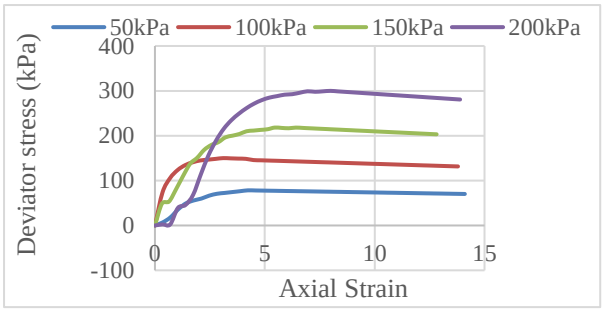

Fig 3. Deviator stress with axial strain for loose sand obtained from the triaxial test

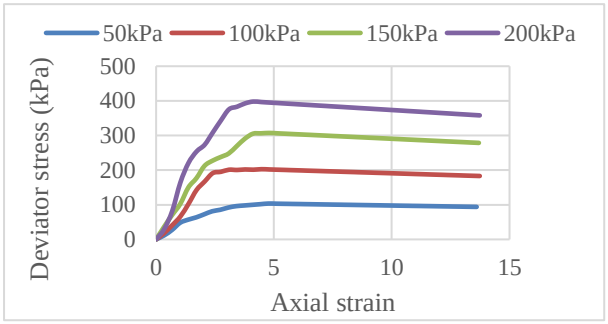

Fig 4. Deviator stress with axial strain for medium dense sand obtained from the triaxial test

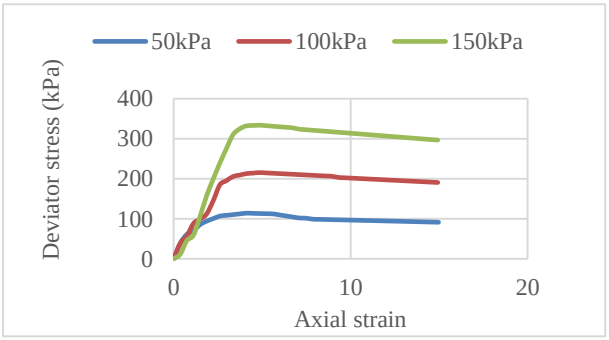

Fig 5. Deviator stress with axial strain for dense sand obtained from the tri-axial test

The results of the triaxial tests are illustrated in figs. 3-5. And it clearly shows the higher stresses for higher confining pressures and higher states of compaction.

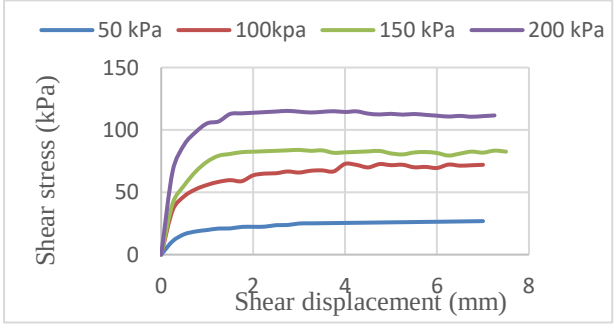

Fig 6. Shear stress with shear displacement for loose sand obtained from direct shear test

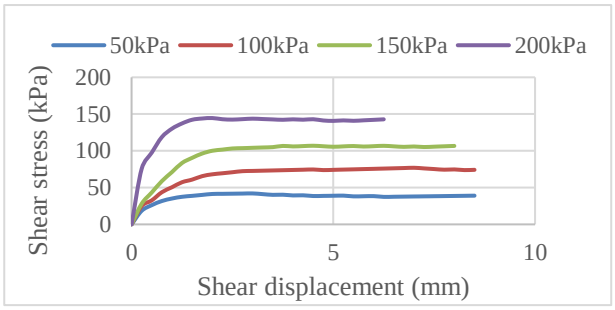

Fig 7. Shear stress with shear displacement for medium dense sand obtained from direct shear test

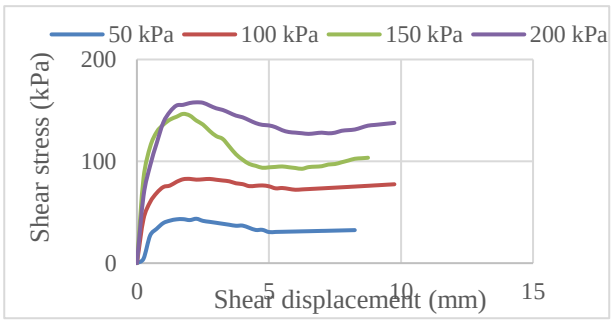

Fig 8. Shear stress with Shear displacement for dense sand obtained from direct shear test

The results of the direct shear tests are illustrated in figs. 6-8. And it clearly shows the higher stresses for higher normal pressures and higher states of compaction. After obtaining those graphs ultimate and peak friction angles were calculated and shown below in table 2 and table 3 using Mohr-Coulomb theorem.

Table 2. Ultimate friction angles (ϕ'_{ult}°)

State of compaction	Triaxial test	Direct shear test
Loose	24	29.76
Medium dense	28.5	34.61
Dense	30	35.42

Table 3. Peak friction angles (ϕ'_{peak}°)

State of compaction	Triaxial test	Direct shear test
Loose	26	29.76
Medium dense	30	35.75
Dense	32	40.60

Dilation angles at the peak shear stresses were calculated for direct shear tests and triaxial tests separately at a dense state of compaction. For that, the Mohr-Coulomb model and Taylor's model are used, as in the equations 2 and 3.

The angle of dilation from Mohr Coulombs' model,

$$\psi = \phi'_{peak} - \phi'_{ult} \quad (2)$$

The angle of dilation from Taylor's model,
$\psi = \tan^{-1}\{(\sigma/\tau)peak - \tan(\phi'_{ult})\}$ (3)

The dilation effect is due to particle arrangements and mineralogy. Ultimate friction angle accounts for the mineralogy and it is an intrinsic property of the soil. Here in the models, peak friction angle is taken as the secant friction angle at peak shear stress.

Table 4. Dilation angles (ψ°) obtained using the Mohr-Coulomb model

State of compaction	Triaxial test	Direct shear test
Loose	2.19	5.28
Medium dense	1.69	4.18
Dense	1.74	8.92

Table 5: Dilation angles (ψ°) obtained using Taylor's model

State of compaction	Triaxial test	Direct shear test
Loose	3.01	9.1
Medium dense	1.70	6.63
Dense	1.74	4.89

The dilation angles calculated using both models are shown in table 4 and table 5. From these results too it can be seen that direct shear test results showed higher dilation effect compared to triaxial tests.

4 CONCLUSION

Based on the results obtained from the series of both tests, it is observed that ultimate internal friction angles obtained from direct shear tests are about 6° higher than the ultimate internal friction angle obtained from the triaxial test for sand confirming the observations of the literature. And also peak friction angles obtained from direct shear tests are about 3º- 9° is higher than triaxial test results. The deflection of the sample of the direct shear test is laterally restricted although the sample of the triaxial test is not restricted because of the membrane. Because of that failure plane of the direct shear test maybe not the weakest failure plane although failure plane of the triaxial become the weakest failure plane. This may be the main reason to occur in higher internal friction angles obtained from the direct shear test.

Stress-strain curves are broadly similar in shape for both obtained from direct shear tests and triaxial tests. And it can be observed that higher stress values are given for higher applied normal pressure or cell pressure and lowest stress values are given for lower applied pressures.

In this study, dilation angles were calculated using the Mohr-Coulomb model and Taylor's model for the dense state of compaction of the sand. Observing those results it can be determined that dilation angles obtained using direct shear tests are higher than triaxial tests for both models.
When comparing with the past studies carried out on the coarse and fine sand, the results obtained in this study where the well-graded sand is used are very much similar in behavior between Triaxial and Direct Shear tests.

REFERENCES

Abdul Naser Abdul Ghani, Chow Shiao Huey, Norshida Ismail 2009, Shear Strength Characteristics of Sand-Waste Material Mixture. The journal of the Institution of Engineers, Malaysia, Vol. 70, No.1

Alias, R., Kasa, A., & Taha, M. R. 2014, Effective shear strength parameters for remolded granite residual soil in direct shear and triaxial tests. Electronic Journal of Geotechnical Engineering, 4559–4569

Bajestahsa Shafaeini, M., Yazdani, M. and Golshani, A., 2018, Experimental Determination of Shear Strength Properties of Lightweight Expanded Clay Aggregates Using Direct Shear and Triaxial Tests, 12(2), pp. 107–113.

Bolton, M. D. (1986). GCotechnique 36, The strength and dilatancy of sands, No. I.65578

Castellanos, B. A., & Brandon, T. L. 2013, A comparison and triaxial devices on undisturbed and remolded soils. 18th International Conference on Soil Mechanics and Geotechnical Engineering: Challenges and Innovations in Geotechnics, 1, 317–320.

Cioara, S., Stanciu, A., and Lungu, I. 2014, Comparative Study on Determining the Internal Friction Angle for Sand, (Lxiv).

Craig, R.F., 1986, Craig's soil mechanics, Seventh edition

Maccarini, M. 1993, A comparison of direct shear box tests with triaxial compression tests for a residual soil. Geotechnical and Geological Engineering, 11(2), 69–80. https://doi.org/10.1007/BF00423336

Lini Dev, K., Pillai, R. J., and Robinson, R. G. 2016, Drained angle of internal friction from direct shear and triaxial compression tests, International Journal of Geotechnical Engineering, 10(3), pp. 283–287. doi: 10.1080/19386362.2015.1133754

Pells, P.J.N., Maurenbrecher, P.M. and Elges, H.F.W.K. 1975, Validity of results from the direct shear test, International Journal of Rock Mechanics and Mining Sciences & Geomechanics Abstracts, 12(5–6), p. 73. doi: 10.1016/0148-9062(75)91280-2.

Sarunas Skuodis, Arnoldas Norkus, Neringa Dirgeliene and Liudvikas Rimkus 2016, Determining characteristic sand shear parameters of strength via a direct shear test, 22(2), pp. 271–278

Feasibility of using geopolymers to stabilize expansive soil

S. Kanjana, S. Sajiththijan and M.C.M. Nasvi
Department of Civil Engineering, University of Peradeniya, Sri Lanka

ABSTRACT: In the construction industry, ordinary Portland cement (OPC) based binders have been used to stabilize soft soils, and however the production of OPC emits significant amount of carbon dioxide to the environment. This study aims to use low calcium Class F fly ash (FA) based geopolymer as a novel binder to stabilize expansive soil. The effect of activator, binder and NaOH molarity on the strength and swell characteristics of expansive soil-geopolymer (ES-GP) were analyzed. ES-GP samples with different activator/binder (0.2-0.5), binder/soil (0.1-0.4) ratios and NaOH molarity (6M-12M) were prepared and the samples were cured under ambient temperature conditions. Unconfined compressive strength, swell pressure and scanning electron microscopy tests were conducted to analyze the strength, swell characteristics and to predict the microstructural changes. Based on the findings, the optimum mix ratios for high strength and low swell characteristics include activator/binder of 0.4, binder/soil of 0.3 and NaOH molarity of 8M. It is concluded that low calcium FA based geopolymers can be a promising alternative to OPC based binders to stabilize soft soils.

1 INTRODUCTION

Expansive soil has been considered as problematic soil and unsuitable for civil engineering constructions due to its swelling and shrinkage characteristics. The ground improvement is necessary for the problematic soils. In the chemical method of ground improvement, the soft soil is stabilized with cementitious materials through hydration or pozzolanic reaction. Ordinary Portland cement (OPC) and lime have been extensively used to stabilize the problematic soils. However, the production of OPC is an energy intensive process as the manufacture of OPC emits significant amount of CO_2 to the environment. Geopolymers are produced by the synthesize of aluminosilicate source materials with a strong alkaline solution. This research aims to predict the feasibility of using geopolymer prepared with ASTM class F fly ash to stabilize expansive soil in Sri Lanka.

There has been few research (Seco et al., 2011; Puppala et al., 2013) on the use of geopolymer for stabilizing the soil. Geopolymer is an inorganic aluminosilicate material formed through polycondensation of tetrahedral silica (SiO_4) and alumina (AlO_4) (Davidovits, 1991). It is synthesized by alkaline activation of materials rich in alumina (Al_2O_3) and silica (SiO_2). The chemical structure of geopolymer can generally be expressed as follows (Davidovits, 1991; Zhang et al., 2013).

$$M_n[-(Si-O_2)_z(Al-O_2)_n.wH_2O \quad (1)$$

where M is the alkaline element such as potassium, sodium, or calcium, – indicates the presence of a bond, z is ratio of Si/Al, and n is the degree of polymerization.

Geopolymer shows the properties such as resistance to heat, organic solvents and acids, low shrinkage potential and excellent adhesion to aggregates (Zhang et al., 2013). Also, it can be synthesized from fly ash, which is a waste from the combustion of coal in thermal power plants.

2 MATERIALS AND METHODOLOGY

2.1 *Expansive soil sample*

Expansive soil sample was collected from Digana, Sri Lanka. The soil was analyzed to determine its index properties and the results are given in Table 1. Based on the particle size analysis of the tested soil, the composition of the soil includes 37% sand, 35% silt and 28% clay. According to Unified Soil Classification System, the soil type is 'ML' (low-plastic silty soil). Free swell test was conducted to determine the swell potential of the expansive soil and the result was 1.5 indicating that it is moderately expansive.

Table 1. Index properties and compaction conditions of expansive soil

Index Properties	Values
Bulk density	1797 kg/m^3
Moisture content	16.0%
Specific Gravity	2.69
Plastic limit (PL)	24.7%
Liquid limit (LL)	32.4%
Plasticity index (PI)	07.7%
Optimum moisture content (OMC)	23.0%

2.2 *Fly ash (FA)*

FA used was obtained from Lakwijaya coal power plant, Norochcholai. The FA produced at this plant is ASTM Class F, containing more than 70% SiO_2, Al_2O_3 and Fe_2O_3 and very low in lime (< 12%).

2.3 *Alkaline Activator*

The alkali activator used for the synthesis of geopolymer was a combination of Sodium Silicate (Na_2SiO_3) and Sodium Hydroxide (NaOH) solution. The ratio of Na_2SiO_3 to NaOH was maintained at 2.5 obtained from researches. (Lazarescu et al., 2017)

2.4 *Expansive Soil - Geopolymer (ES-GP) sample preparation*

This research consisted of three parts. In the first part, the activator/binder ratio was changed from 0.2 to 0.5 (in 0.1 intervals) keeping both the binder/soil ratio and molarity of NaOH constant at 0.3 and 8M, respectively. In the second part, the binder/soil ratio was changed from 0.1 to 0.4 (in 0.1 intervals) and the molarity of NaOH was kept constant at 8M. The optimum activator/binder ratio was used to prepare the ES-GP samples. In the third part the molarity of the NaOH was changed from 6 to 12 M (in 2M intervals) and the optimum activator/binder and binder/soil ratios were used to prepare the ES-GP samples.

The following procedure was adapted to prepare the ES-GP samples. The raw expansive oven dried soil sample passing 2 mm sieve and the FA was mixed. The alkaline activator that was prepared 24 hours prior to the synthesis of geopolymer was added to the soil - FA mixture and was mixed in a Hobart mechanical mixer for a period of 4 minutes. Water was then added and mixed well. The final mix was poured into the Proctor compaction mould in three layers and each layer was statically compacted using the Proctor compaction apparatus. The optimum compaction conditions of expansive soil were established based on standard Proctor compaction test is listed in Table 1. All the geopolymer stabilized samples were prepared assuming that the stabilization does not change the compaction criteria. Cylindrical specimens of 38 mm diameter and 76 mm height were extruded from the moulded sample for unconfined compression testing. All the samples were wrapped with vinyl sheet immediately after the preparation to prevent any moisture loss and were then cured at ambient temperature condition for a period of 7 and 28 days until being tested.

3 RESULTS AND DISCUSSION

3.1 *Effect of Activator /Binder ratio and Binder/ Soil ratio on the strength*

Variation of UCS with activator/binder and binder/soil ratio for geopolymer stabilized soil for 7 and 28 days curing period is shown in Fig. 1. Accordingly, both 7 and 28 days UCS values increase with activator/binder ratio up to 0.4 and then it slightly decreases towards 0.5, resulting in optimum ratio of 0.4.

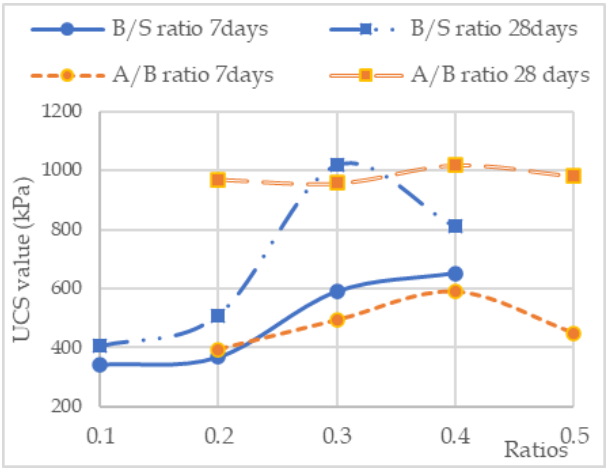

Fig. 1 Variation of UCS with activator/binder and binder/soil ratio

The initial increase in the UCS with the increase in activator/binder ratio to 0.4 is due to the increase in polycondensation reaction that reorganizes silica and alumina leached from the fly ash into a strong Si-O-Al structure (Cristelo et al., 2011) and increase in activator content increases the amount of Na that combines with alumina and silica to form sodium aluminosilicate hydrate gel (N-A-S-H) (Phummiphan et al., 2015) that forms a dense mixture. Also, it is due to increase in activator content that facilitates the particles to move past one another and voids in the expansive soil samples are filled with solid particles thus increasing the density of the mixture. Beyond an activator/binder ratio of 0.4, the alkaline liquid replaces the soil and fly ash particles forming voids that reduces the density of the mixture.

Based on Fig. 1, it can be noticed that UCS value increases with the increase in binder/soil ratio from 0.1 to 0.3. For a given binder/soil ratio, 28 days UCS values of the stabilized samples are higher than that of the 7 days UCS. This is due to the enhanced rate of geopolymerization at 28 days as 7 days is not sufficient for the dissolution of alumino-silicate materials to produce a homogeneous geopolymer matrix.

With the increase of fly ash content, more alumino-silicate materials are available leading to en-

hanced rate of geopolymerization and formation of calcium silicate hydrate (C-S-H) gel which contributes to the high strength towards 0.3 ratio (Murmu et al., 2018). With any further addition of fly ash beyond an optimum value, the reaction is entering an inert zone with time where the excess amount of fly ash leads to more unreacted particles hindering the rate of geopolymerization. This leads to reduce the UCS of 28 days cured samples stabilized with binder to soil 0.4 (Arulrajah et al., 2015).

Variation of swell pressure with the binder/soil ratio is shown in Fig. 2, where swell pressure decreases with the increase in binder content and it can be explained as follows. Fly ash in the geopolymer samples consists of silicate, aluminium and iron oxide that have potential to provide multivalent cations, such as Ca^{2+}, Si^{4+}, Al^{3+}, Fe^{3+} and promotes flocculation of clay particles by cation exchange resulting in the reduction of surface area and water affinity. Increase in the fly ash content increases the flocculation rate reducing the surface area and water affinity leading to reduced swell potentials.

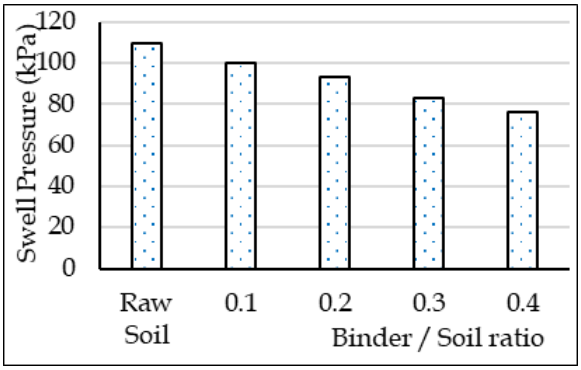

Fig. 2 Variation in swell pressure with fly ash content

3.2 *Effect of NaOH molarity on strength and swell characteristics*

Fig. 3 shows the variation of UCS with the NaOH molarity. It can be seen that, for both 7 and 28 days curing periods, UCS increases with the NaOH molarity up to 8M and then it reduces beyond the optimum value. When the NaOH concentration increases from 6M to 8M, it dissolves more aluminosilicate particles from fly ash to react with Na_2SiO_3 and increases the rate of geopolymerization (Arulrajah et al. 2015). This leads to higher strength at 8M NaOH than the 6M NaOH samples. On the contrary, when the NaOH concentration is increased beyond 8M, UCS reduces although previous researchers found that strength increases with molarity. During the preparation of the samples, it was noted that the geopolymer stabilized soil samples with 10 and 12 M NaOH molarity values were highly viscous compared to those of 6M and 8M samples and less workable. This would have led to poor reaction rate between the soil and geopolymer due to non-uniform mixing during sample preparation. This would have caused the strength reduction at high NaOH molarity values. However, use of 8M NaOH geopolymer for soil stabilization work is economically feasible compared to high NaOH molarity values and this is anyway a favorable outcome as long as the application of these precursors for soil stabilization works are considered.

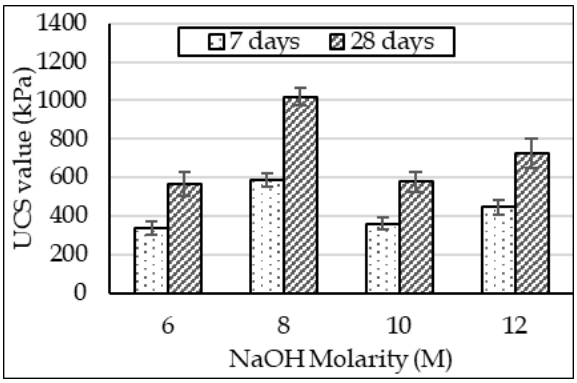

Fig. 3 Variation of UCS value with molarity of NaOH

Swell pressure decreases with the increase in NaOH molarity as shown in Figure 4. The particles are bound well and the gaps among the particles are thoroughly filled with geopolymer products from the pozzolanic reaction so that there are no voids to allow the expansion of soil particles and the bonds are tight enough to prevent the expansion due to penetration of water. (Nalbantoglu 2004)

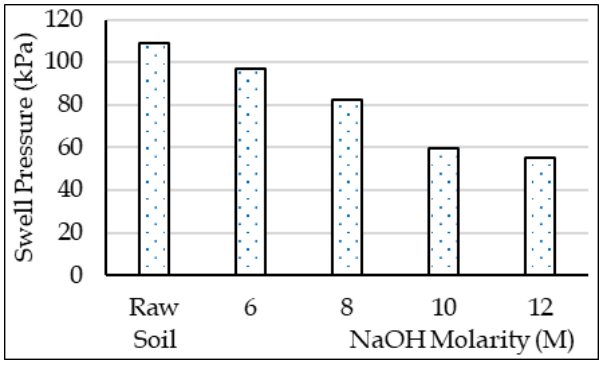

Fig. 4 Variation of swell pressure with molarity of NaOH

3.3 *Microstructural Analysis*

The morphology of 28 days cured geopolymer stabilized expansive soil samples at various binder/soil ratios (0.2, 0.3 and 0.4) were tested to analyze the effect of geopolymer on the structure of the ES-GP sample. For all these mixes, both the activator/binder ratio and the molarity of NaOH were

kept constant at their optimum values of 0.4 and 8M respectively. Fig. 5 shows the SEM images of the ES-GP samples at different binder/soil ratios. Fig. 5(a) shows the morphology of expansive soil sample and it contains mostly fine particles. In Figs. 5(b), (c) and (d), cementitious products resulting from pozzolanic reaction can be clearly observed. At a binder/soil ratio of 0.3, a compacted and homogeneous microstructure is observed with uniform geopolymer products, explaining the reason for the high compressive strength values obtained at a binder/soil ratio of 0.3. In the mixture with binder/soil ratio of 0.4 (Fig. 5d), more unreacted FA particles can be seen compared to ES-GP samples with other binder/soil ratio values, justifying the low strength values obtained at a binder/soil ratio of 0.4.

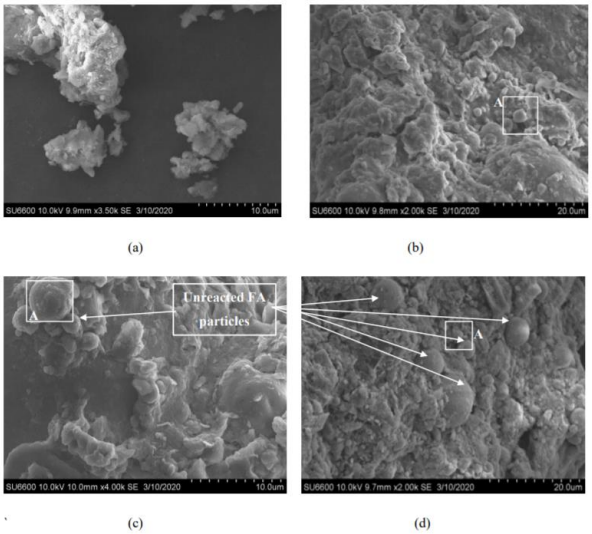

Fig. 5 SEM image of (a) raw expansive soil and ES-GP sample at various binder/soil ratios of (b) 0.2, (c) 0.3 and (d) 0.4

4 CONCLUSIONS

The following conclusions are drawn based on the outcome of this research study,

- Unconfined Compressive Strength (UCS) of fly ash treated samples increases with the increase in activator/binder ratio from 0.2 to 0.4 and then it reduces towards a ratio of 0.5.
- The optimum binder/soil ratio for high UCS of the treated samples was 0.3. With the increase of fly ash content, more alumino-silicate materials are available for geopolymerization leading to enhanced rate of geopolymerization.
- Swell pressure decreases with the increase in binder content as the fly ash have potential to provide multivalent cations and promotes flocculation of clay particles resulting in the reduction of surface area and water affinity.
- UCS increases with the NaOH molarity up to 8M and then it reduces beyond the optimum value. However, 8M is favorable outcome for optimum value considering the health and economic feasibility.
- Swell pressure decreases with the increase in NaOH molarity as the particles are bound well and the gaps among the particles are thoroughly filled with geopolymer and the bonds are tight enough to prevent the expansion due to penetration of water.
- The optimum mix composition for high strength and low swell characteristics for expansive soil include activator/binder 0.4, binder/soil 0.3 and NaOH 8M. The findings of this research show that geopolymers can be successfully applied to stabilize soft soils.

REFERENCES

Arulrajah, A., Kua, T., Phetchuay, C., Horpibulsuk, S., Mahghoolpilehrood, F., and Disfani, M., (2015)., Spent Coffee Grounds–Fly Ash Geopolymer Used as an Embankment Structural Fill Material, Journal of Materials in Civil Engineering, 28:04015197.

Cristelo N, Glendinning S, Pinto A (2011). Deep soft soil improvement by alkaline activation, Proceedings of the Institution of Civil Engineers - Ground Improvement 164:73-82.

Davidovits, J., (1991)., Geopolymers: Inorganic polymeric new materials, J. Thermal Analysis, 37:1633-1656

Lazarescu V, Szilagyi H, Baera C, Ioani, A (2017). The Effect of Alkaline Activator Ratio on the Compressive Strength of Fly Ash-Based Geopolymer Paste, Materials Science and Engineering, 209:1-6.

Murmu A, Dhole N, Patel A (2018). Stabilisation of black cotton soil for subgrade application using fly ash geopolymer. Road Materials and Pavement Design 21(3):867-885.

Nalbantoglu Z (2004). Effectiveness of Class C fly ash as an expansive soil stabilizer. Construction and Building Materials, 18(6):377-381.

Phummiphan I, Horpibulsuk S, Sukmak P, Chinkulkijniwat A, Arulrajah A, Shen S (2015). Stabilization of marginal lateritic soil using high calcium fly ash-based geopolymer. Road materials and pavement design 17:877-891.

Puppala A, Manosuthikij T, Chittoori B (2013). Swell and shrinkage characterizations of unsaturated expansive clays from Texas, Engineering Geology, 164:187-194.

Seco A, Ramírez F, Miqueleiz L, García B (2011). Stabilization of expansive soils for use in construction. Applied Clay Science 51(3):348-352.

Zhang M, Guo H, El-korchia T, Zhang G, Tao M (2013). Experimental feasibility study of geopolymer as the next-generation soil stabilizer. Construction and building materials 47:1468-1478.

The Effect of Fouling Materials on Permeability Behaviour of Large Size Granular Materials

J.M.M.Y Karunarathna, M.M.N. Gimhani, and S.K. Navaratnarajah
Department of Civil Engineering, University of Peradeniya, Sri Lanka

ABSTRACT: In civil engineering constructions, large size granular materials are frequently used. In this study, the focus is on railway substructure where large size granular materials are used to place rail track on it. This layer, also known as ballast should have proper drainage capacity to avoid any damage to the rail track. Due to fouling, drainage is disturbed and causes several problems. To avoid such situations track maintenance should be done at appropriate stages. This study mainly focuses on the permeability behavior of fouled ballast with different levels of fouling in Sri Lankan railways. Clay is used as the fouling material and the Indian standard of ballast gradation is used. Constant head permeability tests have been conducted by using large scale permeameter built in the laboratory. A finite element model analysis was conducted using SeepW (2012) to quantify the drainage capacity of ballast under different degrees of fouling. This study analyses the permeability behavior of fouled ballast and evaluating the critical fouling percentage to propose the ballast cleaning work at the rail track site.

1 INTRODUCTION

Granular materials are discontinuous, highly heterogeneous materials that are randomly assembled. Accumulation of fine particles in granular materials causes complications to the engineering properties of granular materials which leads the engineering applications to descend their scope.

Ballast is a coarse granular medium that is placed above the sub-ballast and below the rails and sleepers. The main reason to use ballast in railway construction is that it is less expensive and the high abundancy. Because of its highly irregular shape ballast has a high load-bearing capacity and self-locking ability. High permeability value is an important property of ballast that makes water fallen onto rail tracks to drained out without obstructing its functions.

The phenomenon of fine particle accumulation which is called ballast fouling can be occurred due to many reasons such as ballast degradation, mud pumping, wind, and infiltration from the top. Aggregation of these fine materials of sand, clay, coal, and quarry dust in ballast for a long time causes rail tracks to decrease its functions such as plastic strain and permeability.

1.1 *Quantification of Fouling*

Void Contamination Index (VCI) introduced by Tennakoon et al. (2012), was used as an indication of the fouling level. The VCI defined as shown below.

$$VCI = \frac{V_f}{V_{vb}} \times 100$$

$$VCI = \frac{(1+e_f)}{e_b} \times \frac{G_{sb}}{G_{sf}} \times \frac{M_f}{M_b} \times 100$$

V_f - Volume of fouling materials, V_{vb} - Initial void volume of clean ballast, e_f - Void ratio of fouling material, e_b - Void ratio of clean ballast, G_{sb} - Specific gravity of ballast, G_{sf} - Specific gravity of fouling material, M_f - Mass of fouling material, M_b - Mass of clean ballast

The effect of fouling on permeability depends on the type of fouling materials (e.g., sand, clay, coal, etc). Therefore, the proper understanding of the nature of fouling materials should be given priority than the quantity of fouling. For example, sand and coal fouling may not decrease the overall permeability of the track significantly, whereas clay fouling can decrease the track drainage more dramatically (Selig and Waters 1994).

2 MATERIALS AND METHODS

2.1 *Materials*

Materials used in the study include railway ballast collected from the Nawalapitiya quarry and clay as the fouling material. The test sample was prepared according to the gradation of the Indian railway ballast standard (Figure 1), which is currently adopted in Sri Lankan railways.

According to Selig & Waters (1994), fouling materials are the materials passing 9.5mm sieve. Therefore clay was sieved using a 9.5mm sieve. The gradation curve of fouling material and some of the properties of ballast and clay fouling are presented in Figure 1.

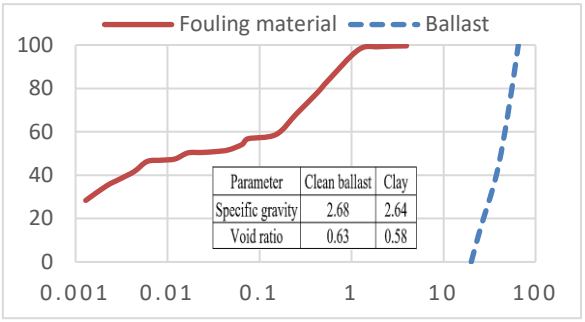

Figure 1-Gradation curves of ballast and clay fouling

Liquid Limit, average Plastic Limit, and Plasticity Index, Optimum Moisture Content and the Maximum Dry Density obtained for clay were 47%, 24%, 23%, 16.5, and 1674 kg/m^3, respectively.

2.2 *Large scale permeability apparatus*

Laboratory experiments to determine the permeability associated with different levels of fouling were conducted by the large scale permeameter built according to past researches and standards in the Geotechnical Laboratory. The schematic diagram of the large scale permeability apparatus and a photograph of the apparatus is shown in Figure 2.

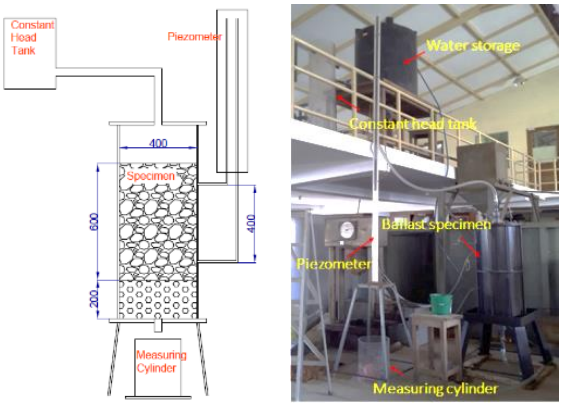

Figure 2 - Schematic diagram (Left) and Photograph (Right) of large scale permeability apparatus

The steel cylinder with 400mm diameter holds the ballast-filled up to a height of 800mm. The sample size ratio (diameter of the test sample to the maximum particle size of ballast) should be greater than 6 to minimize the effects of the sample size (Marachi et al., 1972, Indraratna et al., 1993). According to AS 1289.6.7.3-1999, the height of the specimen should be greater than at least 5 times the maximum particle size. Therefore in this study, a specimen height of 400 mm was considered.

To prevent the washout of fine particles, a filter membrane was placed at the base of the ballast specimen. A ballast layer of 200mm of size greater than 63mm was placed at the bottom of the cylinder to maintain a free drainage boundary.

2.3 *Laboratory test method*

To simulate uniformly fouled ballast, clean ballast was mixed with fouling materials (clay) and then poured into the apparatus. Prepared clean ballast was fouled with clay with the VCI values of 25, 50, 75, and 100. The fouled specimen was compacted in four equal layers to represent typical field density in the apparatus. After the apparatus was filled with water the specimen was kept one hour to get saturated. After ensuring that the specimen is saturated, piezometer readings for 5 different flow rates were taken and the head difference was plotted against flow rates.

2.4 *Finite element model analysis*

Since the water flow through a rail track would be both vertical and horizontal, a 2-D seepage analysis was conducted using the finite element software, SEEP-W (GeoStudio, 2012), to determine the drainage capacity concerning different fouling percentages and conditions. Permeability values for different VCIs were obtained from the experimental results (Figure 7) were used as input parameters in the analysis. Figure 3 shows a typical cross-section of a Sri Lankan ballast rail track. For the analysis, a finite element discretization of the one-half track is considered due to the symmetry.

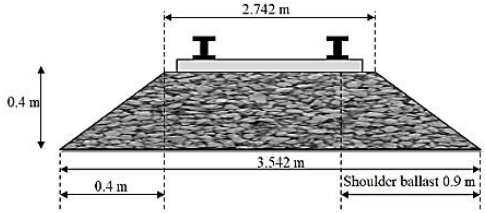

Figure 3 – Cross-section of a Sri Lankan Railtrack

For the analysis following boundary conditions were applied. An impermeable layer at the bottom, free drainage boundary condition on top of the shoulder ballast, and symmetric boundary condition at the centerline of the rail track. A hydraulic head similar to the height of the ballast layer was assigned to the top surface of the ballast layer. The analysis was carried out under steady-state flow conditions. The model was analyzed under three possible scenarios for ballast fouling with clay.

Model 1: A newly constructed track is simulated. The entire track is divided into three equal horizontal layers (133 mm each) and the permeability values concerning different VCI values are used (Figure 4a).

Model 2: A fouling track which is subjected to undercutting is simulated. The track is divided into two horizontal layers. The top layer consists of clean ballast and the bottom layer has 100 VCI ballast (Figure 4b). The thickness of the layer of clean ballast is varied.

Model 3: A track subjected to shoulder cleaning is simulated. The whole track is divided into 4 parts including shoulder ballast and 3 horizontal ballast layers with different values of VCI (Figure 4c).

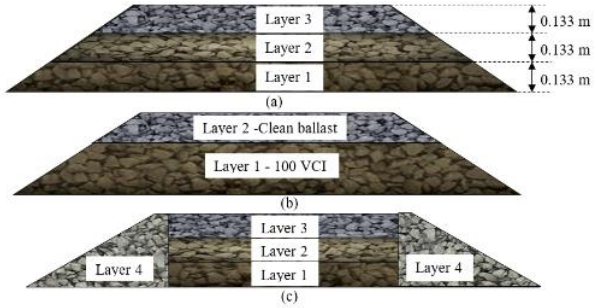

Figure 4 - Fouled ballast patterns (a) Model 1, (b) Model 2 and (c) Model 3

2.5 *Drainage classification*

In this study, maximum rainfall intensity was considered which is corresponded to a critical flow rate (Q_c) of 0.0008 m^3/s over the unit length of the track. From the FEM analysis, the maximum drainage capacity (Q) of the ballast was obtained for various levels and conditions of fouling. Figure 5 shows a typical output of numerical analysis using SEEP-W software.

When the track drainage capacity is equal to or less than the critical flow rate, then the fouled track is considered to be impermeable. To identify this condition, a non-dimensional parameter Q/Qc is considered. The drainage condition of the rail track was classified according to the drainage criteria specified by Terzaghi and Peck in 1967 (Table 1).

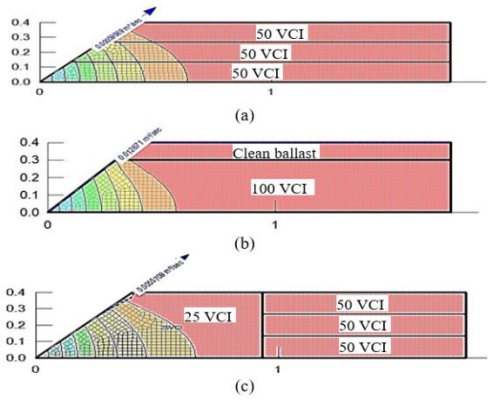

Figure 5 - The output of numerical analysis using SEEP/W (a) Model 1, (b) Model 2 and (c) Model 3

Table 1 - Drainage Capacity Criteria

Drainage classification	Range
Free drainage	$Q/Q_c > 100$
Good drainage	$10 < Q/Q_c < 100$
Acceptable drainage	$1 < Q/Q_c < 10$
Poor drainage	$0.1 < Q/Q_c < 1$
Very poor	$0.001 < Q/Q_c < 0.1$
Impervious	$Q/Q_c < 0.001$

RESULTS

2.6 *Permeability Test Results*

Results of permeability tests for clean ballast (VCI=0%) and ballast with VCI values 25%, 50%, 75%, and 100% are presented in Figure 6.

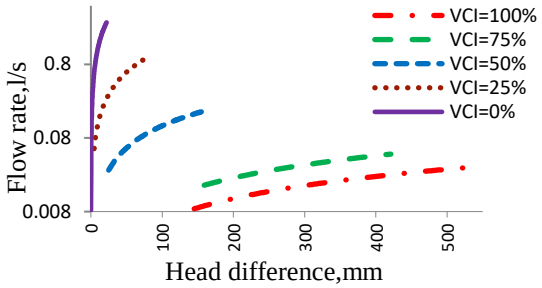

Figure 6-Flow rate vs Head Difference for different VCI

Gradients obtained from the graphs in figure 6 were used to calculate the respective permeability values (Figure 7) using linear Darcy's law.

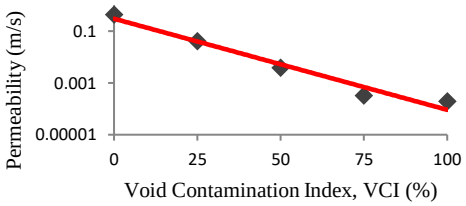

Figure 7 Variation of Permeability with VCI

The results confirmed that the hydraulic conductivity decreased with the increase in VCI.

2.7 *Layer Profiles*

Photographs of the specimen cross-sections were taken while unloading the materials from the apparatus after conducting the tests. Figure 8 shows the layer locations where photographs were taken and illustrations of layer profiles. It can be seen that most of the fines washed out to the bottom of the specimen.

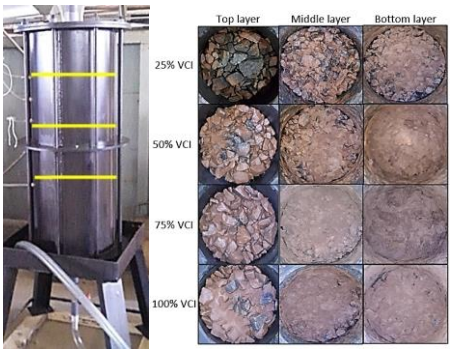

Figure 8 - Ballast specimen layer profile

2.8 *Finite Element Model Results*

From the numerical model, drainage capacity (Q) related to the respective fouling condition and lev-

el, were obtained. Drainage was classified according to drainage capacity criteria and selected data from each of the 3 cases are presented in tables 2, 3 and 4 concerning the critical flow rate (Q_c).

Table 2 - Track drainage classification based on Model 1

Case	VCI %			Q/Qc	Drainage classification
	Layer 1	Layer 2	Layer 3		
1-2	25	0	0	58.088	Good Drainage
1-6	50	25	25	5.398	Acceptable
1-9	50	50	50	0.745	Poor Drainage
1-12	100	100	100	0.037	Very Poor
1-13	100	50	0	27.164	Good Drainage
1-15	100	50	50	0.505	Poor Drainage
1-17	100	25	25	5.154	Acceptable
1-22	0	0	100	0.966	Poor Drainage

In most of the cases when VCI of the layer 3 (top layer) exceeds 50% drainage condition was classified as 'poor drainage'

Table 3-Track drainage classification based on Model 2

Case	Clean ballast layer thickness(m)	Q/Q_c	Drainage Classification
2-1	0.01	1.380	Acceptable
2-3	0.025	4.000	Acceptable
2-5	0.05	6.322	Acceptable
2-6	0.1	15.839	Good Drainage

Table 4 Track drainage classification based on Model 3

Case	VCI %				Q/Q_c	Drainage Classification
	Layer 1	Layer 2	Layer 3	Layer 4		
3-4	50	50	0	0	75.110	Good Drainage
3-10	100	100	100	0	74.853	Good Drainage
3-16	50	0	0	25	7.344	Acceptable
3-28	25	0	0	50	0.685	Poor Drainage
3-34	50	50	25	50	0.678	Poor Drainage
3-42	50	0	0	100	0.034	Very Poor
3-48	100	50	0	100	0.034	Very Poor
3-49	100	100	50	100	0.034	Very Poor

Based on the results shown in Table 4, in most cases when shoulder ballast exceeds 50% VCI, the track drainage is classified as 'poor drainage', even if the other layers are relatively clean.

3 CONCLUSION

Rail tracks are usually positioned on ballast for several reasons. One of them is the ability to provide rapid drainage. A series of large-scale constant head permeability tests were conducted with different fouling levels to calculate the permeability value of fouled ballast corresponding to the VCI value. The test results were used for investigating how the levels of fouling impact the permeability values of fouled ballast. The results delivered that the permeability of fouled ballast decreases with the increase of the VCI.

A two-dimensional finite element seepage analysis was conducted to simulate actual track geometry. The drainage capacity of the track, which has different levels of fouling in several layers, including the shoulder ballast, was estimated using this numerical model. The results of this analysis showed that both the location and fouling levels have a considerable effect on the general drainage capacity of the track. The analysis confirmed that cleaning the ballast with the undercutting technique should be adopted when the VCI of the top 100mm of the ballast exceeds 50% and when the shoulder ballast is fouled to more than 50% VCI, it should be cleaned or replaced to have sufficient drainage.

ACKNOWLEDGMENT

This research is funded by the University of Peradeniya Research Grant (Grant No: URG-2017-29-E) and Accelerating Higher Education Expansion and Development (AHEAD) Operation of the Ministry of Higher Education funded by the World Bank (Grant No: AHEAD/RA3/DOR/STEM/No.63) is also appreciated for their support in continuing this research. We would like to thank the technical staff of the laboratory for helping with lab testings.

REFERENCES

GeoStudio (2012). "Seepage Modeling with SEEP/W", An Engineering Methodology, July 2012 Edition, GEO-SLOPE International Ltd.

Indraratna, B., Nimbalkar, S.S., and Tennakoon, N. (2010). "The Behaviour of Ballasted Track Foundations: Track Drainage and Geosynthetic Reinforcement," Proceedings of Florida 2010 Conference on Advances in Analysis, Modeling, and Design," Feb. 20–24, ASCE, Orlando, FL.

Parson. B.K. (1990). "Hydraulic conductivity of railroad ballast and track substructure drainage. " Geotechnical report: University of Massachusetts.

Ranatunga, D.G.L. (2001). "Towards more efficient hydraulic and hydrological design of cross drainage structures using new developed intensity duration frequency equations." Hydrology Division, Irrigation Department. Transactions of The Institute of Engineers, Sri Lanka, 1-12

Selig, E., and Waters, J. (1994). "Track geotechnology and substructure management". London, England: Thomas Telford.

Tennakoon, N., Indraratna, B., Rujikiatkamjorn, C., Nimbalkar, S., and Neville, T. (2012). "The Role of Ballast-Fouling Characteristics on the Drainage Capacity of Rail Substructure", Geotech. Testing Journal, Vol. 35, No. 4

Terzaghi, K. and Peck, P.B., (1967). "Soil Mechanics in Engineering Practice." New York., John Willey & Sons.

Wallace, A.J. (2003). "Permeability of Fouled Rail Ballast." UG Thesis, School of Civil, Mining and Environmental Engineering, University of Wollongong, Wollongong.

Combined Effect of Temperature and Salinity on the Tri-axial Mechanical Behaviour of Geopolymers

M.M.A.L.N. Maheepala, R.L. Hewavitharana and M.C.M. Nasvi
Department of Civil Engineering, University of Peradeniya, Sri Lanka

ABSTRACT: Carbon Capture and Storage (CCS) is identified as the best solution to reduce anthropogenic greenhouse gases from the atmosphere and well cement provides the required wellbore integrity in a CCS project. Geopolymers have been recognized as a good alternative to OPC, which is currently used as well cement in sequestration wells. Well cement is exposed to a variety of temperatures, salinities and confinements with increasing depth. Hence, this research focused on the combined effect of temperature and salinity on the tri-axial mechanical behaviour of geopolymers. The research work comprised of, (1) experimental work where a series of uni-axial compressive strength (UCS) testing were performed on neat geopolymer paste samples cured at different temperature and salinity combinations for 7 and 28 days and, (2) numerical work where a model was devised using COMSOL multiphysics to predict the tri-axial behaviour of geopolymer. Based on the results, the failure strength of geopolymer increases with the temperature and salinity at all confinements. Hence, it is concluded that the combined effect of temperature and salinity acts favourably to provide excellent mechanical behaviour in downhole environs.

1 INTRODUCTION

Greenhouse gas emission is a major threat in the globe which is rapidly increasing due to the excessive usage of fossil fuel. Among the several mitigation methods for green-house gas emission, CCS method is identified as the best solution (Nasvi et al., 2012) where CO_2 is injected into deep underground reservoirs such as coal seams, saline aquifers and depleted oil and gas reservoirs via injection wells and held safely for several decades.

The material used to make the injection wells should maintain their integrity to prevent any leakages to the surrounding underground formations or to the atmosphere. Most sequestration projects use ordinary Portland cement (OPC) as well cement with different additives. It has been found that Portland cement is unstable in CO_2 rich environments as it undergoes degradation due to acidic attacks and is subjected to shrinkage due to high pressure and temperature. (Balinee et al., 2018). On the contrary, fly ash based geopolymers which are durable, anti-corrosive, chemically inert, less permeable and adaptive to pressure variations have been recognized as a good alternative to OPC, under aggressive curing temperatures and varying salinity concentrations (0-40%) in earth's down hole.

Many studies have focused on the mechanical behaviour of well cement. Balinee et al. (2018) studied the mechanical behaviour of geopolymer and OPC in saline water. It was found that the compressive strength of geopolymer increases with the salinity level due to the restricted alkaline leaching from the sample with the excess Na+ ions in the surrounding curing solution. Giasuddin et al., (2013) observed that geopolymer samples cured in saline water are associated with lower sorptivity, that indicates a lower level of porosity and micro-crack density.

Nasvi et al. (2015) conducted a numerical study on the triaxial mechanical behaviour of geopolymers at different curing temperatures (23–80 °C) using the COMSOL software. They concluded that the resulting failure strength increases with the confining pressure due to the closure of pore voids. The deviatoric strength also increased for all confinements up to 60 °C and then reduced beyond 60 °C to 80 °C. The initial strength increment was due to the increased reaction rates with the rapid dissolution of Si and Al in alkaline materials and the nucleation rates slow down beyond 60 °C, hence no further strength increment with the curing temperature was observed.

However, to date, no study has been carried out to determine the cumulative effect of temperature, salinity and the confinement on geopolymers. Hence, the aim of this research is to study the combined effect of temperature and salinity on the tri-axial mechanical behaviour of geopolymers.

2 EXPERIMENTAL WORK

2.1 *Materials*

ASTM Class F Low calcium-based fly ash (Ca < 10%) samples were collected from Lakwijaya coal power plant, Norochcholai, Puttalam, Sri Lanka. A combination of 15M Sodium hydroxide solution (Na_2O = 30.0%) and commercially available Sodium Silicate solution (Na_2O = 14.7%, SiO_2

= 29.4%) with a specific gravity of 1.53 were used to prepare the alkaline activator solution. Sodium hydroxide solution was prepared by mixing sodium hydroxide pellets with water and common salt was used in substitute of sodium chloride for the preparation of brine solutions for curing.

2.2 *Mix design*

An optimized reference mix design based on activator modulus (AM) was used to determine the proportions of each material to be mixed in order to acquire the desired strength parameters. The following ratios were maintained.

$$AM = \frac{SiO_2 \text{ in alkaline activator}}{Na_2O \text{ in alkaline activator}} = 1.25 \quad (1)$$

$$Na_2O \text{ dosage} = \frac{Na_2O \text{ in alkaline activator}}{\text{Mass of fly ash}} = 15\% \quad (2)$$

2.3 *Specimen preparation and curing*

PVC moulds with a diameter of 38 mm and a height of 100 mm, were used to cast the geopolymer samples. Alkaline activator solution was blended with fly ash in a mechanical mixer for 15 minutes to prepare the geopolymer paste. Immediately after mixing, the paste was placed in PVC moulds in 3 approximately equal layers where each layer was vibrated using a vibration table for 1 minute. Except for those cured at the room temperature (25 °C), the casted geopolymer samples were put in the oven for initial curing at respective temperatures (40, 60 ºC) for 24 hours followed by demoulding. The demoulded samples were immersed in brine solutions of varying concentrations (0, 10, 20, 30% NaCl) and oven cured again for 7 and 28 days. For each specific condition, four samples were tested to ensure reproducibility. The samples were covered with a polythene while being oven cured to prevent the excessive loss of moisture at elevated temperatures.

2.4 *Uni-axial compressive strength (UCS) testing*

UCS (zero confining pressure) was performed using a Universal testing machine (Avery, capacity = 60,000 lb) available at the Materials and Metallurgy Laboratory, by applying an approximately constant stress loading rate of 0.2 MPa/sec. The end faces of the samples were cut prior to testing, maintaining the length of the sample at 76 mm, to ensure purely axial loading during the test. UCS and Young's modulus were obtained via the experimental stress-strain curves.

3 NUMERICAL WORK

Due to the lack of lack of stiffness in the loading frame of the tri-axial apparatus available at the Geotechnical laboratory at University of Peradeniya, to apply higher confinements, a numerical model was developed using COMSOL multiphysics (version 5.5), finite element method-based software to simulate the tri-axial behaviour. UCS test results were used to validate the numerical model which was then extended to predict the tri-axial mechanical behaviour of geopolymers under different salinity, temperature and confining pressure combinations. COMSOL Multiphysics has a comprehensive simulation software environment with a wide range of applications from which we used the structural mechanics module, stationary study type and linear elastic material model for our numerical model. UCS, Young's modulus, Poisson's ratio (Nasvi et al., 2012), uni-axial tensile strength (UTS), bi-axial compressive (BCS) strength and density were used as the input material properties to the model. Several basic assumptions were incorporated for the model. (1) Geopolymer cement is linearly elastic, isotropic and a homogeneous material (no aggregates used), (2) UTS is 10% of UCS and BCS is 116% of UCS (Nasvi et al., 2015), (3) Poisson's ratio doesn't change with the %NaCl. A 2-D axisymmetric geometry was used with a fixed boundary at the bottom, a prescribed displacement on top, axial symmetry from left and a boundary load as the confining pressure (0 – 25 MPa) from right. Two parametric sweeps were used, (1) To apply a prescribed displacement from top up to the maximum displacement in steps of 0.05 starting from 0 mm, (2) To vary the confining pressure from 0 to 25 MPa in steps of 5 MPa.

4 RESULTS AND DISCUSSION

4.1 *Mechanical behaviour of geopolymer under uni-axial condition*

Variation of UCS of geopolymer with the salinity for 28 days is shown in Fig. 1. The standard deviation of the results varies in the range of 0 to 3.2 MPa. Generally, the UCS shows an increasing trend with the salinity levels. The percentage increase in the UCS with salinity at 7 and 28 days are 3 to 91% and 0.5 to 39% respectively depending on the curing temperature. During saline water curing, the abundance of Na+ ions in the curing solution, inhibits the leaching of cations from the geopolymer sample which actually promotes the geopolymerization reaction, thereby increasing the resulting strength at higher salinity levels (Nasvi et al., 2012). On the contrary, there has been a signif-

icant leaching of alkali activator solution and other useful reactants from the sample to the surrounding water in normal water cured samples, which leaves a considerable number of unreacted particles in the samples. (Balinee et al., 2018). Saline water cured samples have lower sorptivity test results than normal water cured samples which indicates less porosity or micro-crack density (Giasuddin et al., 2013) where as water cured samples have a relatively large number of unreacted particles and pores rooted in the geopolymer matrix which also testifies to the conclusions drawn above.

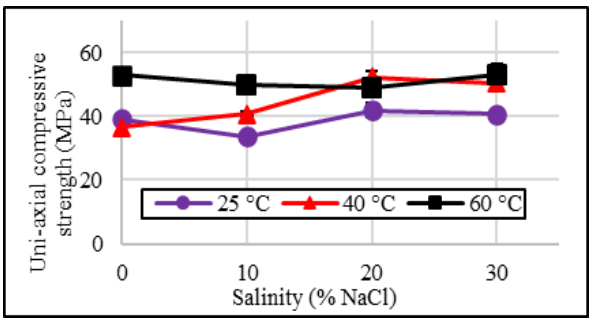

Fig 1. Variation of UCS with salinity level at 28 days

According to Fig. 2, UCS shows a generally increasing trend with the increasing temperature up to 60 °C for all salinity levels. In addition, it was also observed that UCS values increase with the curing period. At lower temperatures, the dissolution of Si and Al from the source materials takes place at a retarded pace and the geopolymer gel develops at a lower rate which is insufficient for polymerization. Elevating the curing temperature is associated with the increased dissolution of Si and Al and accelerated formation of a hard structure at the early stages of geopolymerization. As per Nasvi et al. (2012) the optimum curing temperature for low calcium fly ash based geopolymers is 60 °C, above which the compressive strength gradually reduces. When the curing temperature reaches around 80 °C to 100 °C, the viscosity of the mixture increases rapidly where Al and Si released by the dissolution of the source material reacts immediately. This increases the setting speed of geopolymer slurries from which the unreacted particles are covered, thereby restricting the further dissolution of the source material.

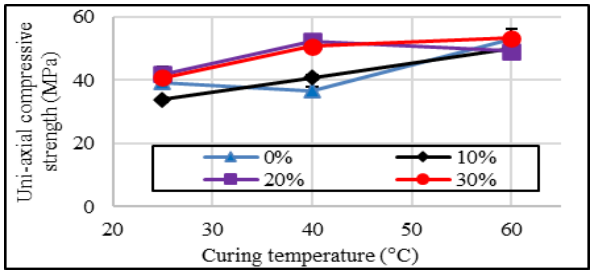

Fig 2. Variation of UCS with temperature at 28 days

There is also a possibility of breaking up of intergranular structure of geopolymer at very high temperatures (>100 °C) and hence it could lead to strength reductions at elevated temperatures. In addition, geopolymer needs moisture for polymerization and at elevated temperatures the rapid loss of water leads to the formation of micro cavities which cause an increase in porosity, contributing to the strength reduction. Overall, the effects from both the increasing temperature and the increasing salinity act favorably on the resulting UCS.

4.2 *Numerical results*

4.2.1 *Model validation*

The numerical model produced by COMSOL was validated against the existing results in order to assure the credibility of the new model, for which the experimental stress – strain curve values obtained for uni-axial compression were used as the reference.

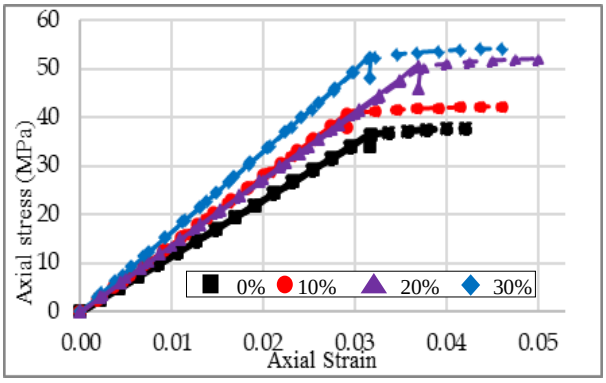

Fig 3. Axial stress-strain curves of geopolymer at 40 °C and 7 days (Solid – Experimental, Hollow – Numerical)

Fig. 3 shows the modelled and experimental axial stress-strain curves at 40 °C and 7 days. Due to the brittle nature of geopolymer, the stress-strain curves corresponding to the plastic region after the yield point, could not be obtained experimentally. Based on Fig. 3, it can be noticed that the experimental and modelled results are consistent up to the yield point after which the model assumes a perfectly plastic behaviour. Hence, the model was validated for the uni-axial results and was further extended to obtain the tri-axial mechanical behaviour of geopolymers.

4.3 *Tri-axial mechanical behaviour of geopolymers*

As per Fig. 4, failure strength increases with the confining pressure. The pores in the geopolymer paste act as a weakening agent of its micro structure, hence reducing the mechanical strength. But, with the increasing level of confinement, those pore voids tend to close, reducing the permeability

and the proportion of voids, thereby increasing the mechanical strength (Nasvi et al., 2013).

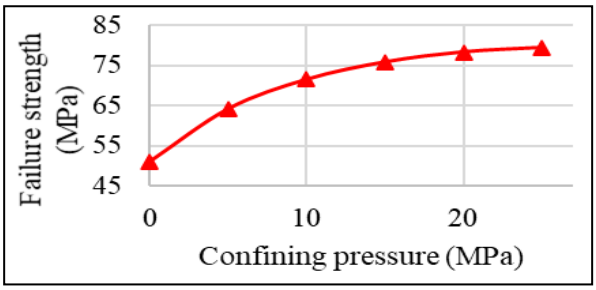

Fig 4. Variation of failure strength with confining pressures for geopolymer cured at 40 °C and 30% salinity level for 28 days

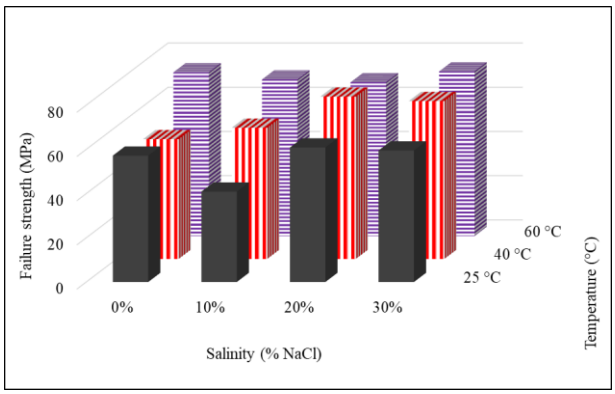

(a) P_c = 10 MPa

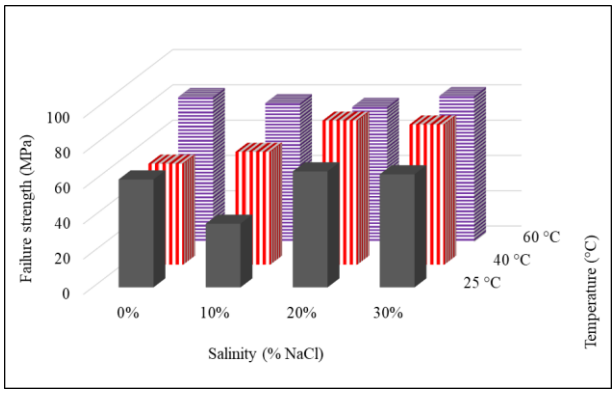

(b) P_c = 25 MPa

Fig 5. Failure strength at different salinity and temperature combinations at 28 days

According to Fig. 5, when the % NaCl increases from 0 to 30%, an average increment of failure strength by 4.1 and 4.5% compared to the normal water cured samples, could be observed for confining pressures of 10 and 25 MPa respectively. When the curing temperature increases from 25 to 60 °C, an average increase of failure strength by 18.6 and 26.4% compared to the strength of the samples cured at room temperature, could be observed for confining pressures of 10 and 25 MPa respectively. From the above rates it is evident that the rate at which the failure strength increases, tends to reduce with the increasing confinement as discussed previously and that the curing temperature plays a more dominant role than the salinity, in improving the failure strength of geopolymers.

5 CONCLUSIONS

The following conclusions are drawn based on the outcomes of this study.

1. UCS increases with the salinity level and the curing temperature due to the reduced leaching rates at higher salinity levels and improved geopolymerization at elevated temperatures.
2. At a given temperature, the resulting failure strength increases with the level of confinement due to the reduced permeability with the application of confinements.
3. At a given temperature, the resulting failure strength increases with the % salinity due to the resistivity provided by NaCl against the leaching of reactants from the samples.
4. At a given % salinity, the resulting failure strength increases with the temperature up to 60 °C due to the increased dissolution of Si and Al from the source material which accelerates the geopolymerization reaction.
5. On the whole, the combined effect of temperature and salinity acts favourably to provide excellent mechanical behaviour in saline conditions and at elevated curing temperatures with active confinements and can be a good replacement for OPC-based well cement in CO_2 sequestration wells.

REFERENCES

Balinee, B., Disaanth, P. and Nasvi, M.C.M., 2018. Comparison of Salinity Dependent Mechanical Behaviours of Geopolymer and OPC: An Application to CCS and Oil/Gas Wells. ENGINEER-JOURNAL OF THE INSTITUTION OF ENGINEERS SRI LANKA, 51(3), pp.13-20.

Giasuddin, H.M., Sanjayan, J.G. and Ranjith, P.G., 2013. Strength of geopolymer cured in saline water in ambient conditions. *Fuel*, *107*, pp.34-39.

Nasvi, M.C.M., Ranjith, P.G. and Sanjayan, J., 2012, January. Comparison of mechanical behaviors of geopolymer and class G cement as well cement at different curing temperatures for geological sequestration of carbon dioxide. In 46th US Rock Mechanics/Geomechanics Symposium. American Rock Mechanics Association.

Nasvi, M.C.M., Ranjith, P.G. and Sanjayan, J., 2013. The permeability of geopolymer at down-hole stress conditions: Application for carbon dioxide sequestration wells. *Applied energy*, *102*, pp.1391-1398.

Nasvi, M.C.M., Ranjith, P.G. and Sanjayan, J., 2015. A numerical study of triaxial mechanical behaviour of geopolymer at different curing temperatures: an application for geological sequestration wells. Journal of Natural Gas Science and Engineering, 26, pp.1148-1160.

Performance enhancement of rail track foundation using Geogrid and Rubber mats

T.H.V.P. Wickramasinghe, D.S.A. Wanigasekara and S.K. Navaratnarajah
Department of Civil Engineering, University of Peradeniya, Sri Lanka

ABSTRACT: Railroad transport is a popular mode of transportation in many countries including Sri Lanka. Ballasted rail tracks are the major infrastructure due to its resiliency to the repeated wheel loads, low construction cost, and ease of maintenance. Ballast is a prominent component of rail infrastructure that controls the stability and performance of the track. In this study, the stress-strain and degradation behavior of ballast and enhancement of ballast performance using geosynthetic materials (geogrids and rubber) were evaluated using a large-scale direct shear apparatus. Stress-strain behavior of ballast was evaluated with the laboratory experiment under three different normal stress conditions (30, 60 and 90 kPa) by placing: a rubber layer placed at bottom and top of ballast layer and a combination of Geogrid and Rubber layer. Ballast Breakage Index is evaluated to compare ballast degradation behavior. The laboratory results show the enhancement of rail track performance when using geosynthetics.

1 INTRODUCTION

The rail industry plays a major role in transporting of bulk freight and passenger transport in the world as well as in Sri Lanka. In recent years, the demand for higher speed and higher capacity trains is increased. In Sri Lanka ballasted rail tracks are the major infrastructures in railway networks. Even though the ballast has high lateral resistance property, large cyclic loads from those heavier and faster trains may induce rapid degradation and deformation of traditional railway foundation which is diversely affecting the stability of the rail track and causing frequent maintenance. In the recent times, Sri Lankan Railway is expected to upgrade the existing rail tracks to cater for higher speed and high hauling capacity trains.

To mitigate ballast damage, in some countries, the concept of adapting geosynthetics inclusions such as geogrids and rubber mats are practiced in rail tracks. Under Sleeper Pads (USP) and Under Ballast Mat (UBM), both are energy absorbing mats which are used to improve the performance of the rail track (Navaratnarajah et al., 2016). Nimbalkar et al. (2012) found that under the impact load with the use of rubber at the top and the bottom of ballast bed, the particle breakage was reduced by about 47% when using a stiff subgrade and by about 65% for a weak subgrade.

In this study, a large-scale direct shear test was carried out on ballast which was prepared according to the gradation of ballast material used in Sri Lankan tracks and tested by placing rubber layers placed at the top and bottom of the ballast layer under direct shear loading.

2 LITERATURE REVIEW

The sample size ratio is defined by the diameter of the apparatus divided by the mean diameter of the maximum particle size which was more than 5 in this study (Fagnoul and Bonnechere, 1969). Moreover, Sri Lankan railway is using the Indian standard for ballast gradation. Therefore, in this study Indian ballast gradation was used to prepare the ballast sample.

Large scale direct shear apparatus is commonly used to estimate the shear strength of coarser materials. According to Navaratnarajah et al., (2019) ballast material which was compacted to 16.1 kN/m^3 and 4 mm/min shearing rate was applied until a 60 mm maximum displacement which corresponds to 15% shear strain.

It is a known fact that ballast degradation is one of the major problems that affect the stability of the rail track. But this problem can be mitigated by limiting the generated stress on ballast using energy absorbing shock mats such as USP and UBM. Navaratnarajah, S.K., and Indraratna, B., (2017) showed that the ballast degradation decreased significantly when a rubber mat was placed on top of the hard-concrete base beneath the ballast layer and it was observed as average 35-45% reduction of breakage on the ballast.

To quantify the magnitude of ballast degradation, Ballast Breakage Index (BBI) is generally used. BBI value calculation was performed using the method proposed by Indraratna et al., (2005).

3 METHODOLOGY

The following step by step method was followed in this study as shown in figure 1.

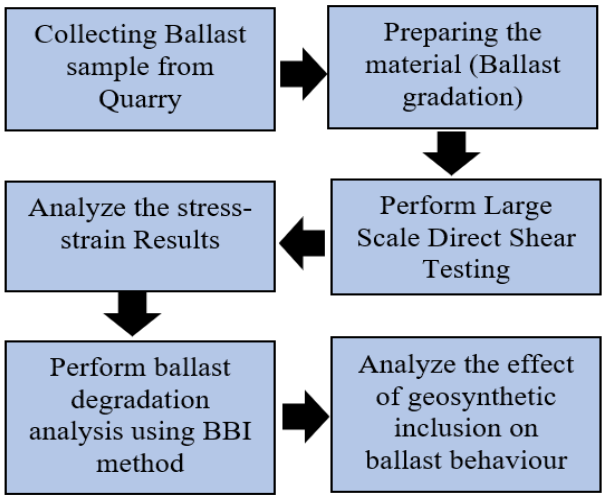

Figure 1 Summery of the methodology

3.1 *Materials*

3.1.1 *Ballast*

The particle size distribution (PSD) is shown in Figure 2, of the prepared ballast sample based on Indian standard which is currently adapted by Sri Lankan Railways.

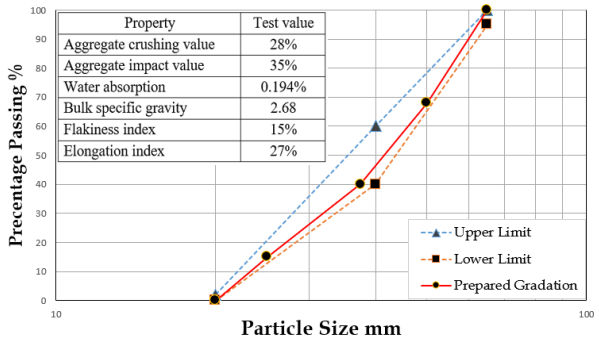

Figure 2 Particle size distribution of ballast sample

3.1.2 *Rubber mats*

The reduction of the amount of energy transferred to the ballast and other substructure components could be caused due to the ability of rubber mats in absorbing energy. Thereby the deformation and degradation in the tracks are minimized. With the use of USPs and UBMs on rail track foundation, the contact surface area of the ballast can be increased causing less settlement and reduced wear of the track substructure. Figure 3 shows the rubber mats used in this study and the mechanical properties are shown in Table 1.

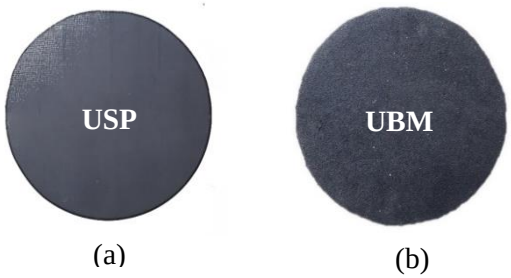

(a) (b)

Figure 3 Rubber mats

Table 1. Mechanical propertied of USP and UBM

Material Properties	USP	UBM
Thickness (mm)	10	10
Bedding Modulus (N/mm^3)	0.22	0.20

3.2 *Testing procedure*

In this study, a large-scale direct shear tests were carried out using the large-scale direct shear apparatus at the Geotechnical laboratory of the University of Peradeniya is shown in Figure 4.

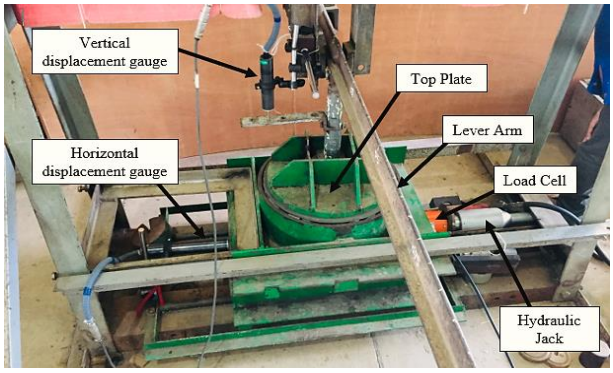

Figure 4 Large scale direct shear apparatus

A predetermined amount of dry ballast was placed in three 100mm thick layers and compacted to achieve the field unit weight of 16.1 kN/m^3. The ballast aggregates were compacted in layers by using a rubber-padded hammer to a typical field density. After filling the large-scale direct shear apparatus, a lever arm system of weights is used to apply the normal stress of 30 kPa, 60 kPa, and 90 kPa. In this study, fresh ballast, fresh ballast with UBM placed at the bottom, fresh ballast with USP placed on the top of ballast, fresh ballast with both USP and UBM and fresh ballast with geogrid and UBM placed at the bottom and USP at the top were tested under abovesaid three normal stresses. Figure 5 shows the placement of (a) fresh ballast, (b) UBM at the bottom of the ballast, (c) USP on the top of the ballast and (d) Geogrid on the top of the UBM.

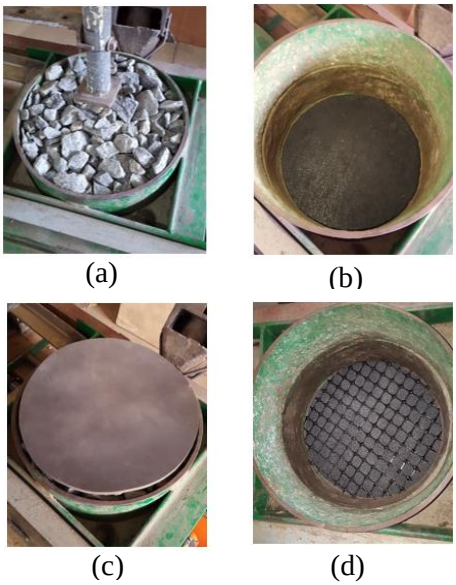

Figure 5 Sample placement; (a) Fresh ballast, (b) UBM at the bottom of the ballast, (c) USP on the top of the ballast and (d) Geogrid on top of UBM

4 RESULTS AND DISCUSSIONS

4.1 *Shear behavior of the ballast with various normal stresses*

Figure 6 shows the shear stresses for different samples for different normal stress. Based on the results, maximum shear stress has occurred in fresh ballast compared with UBM, USP, USP & UBM and combination of USP, UBM & Geogrid. And also, minimum shear stress has occurred in the USP & UBM sample. In most cases, it is observed that maximum shear stress kept increasing until 15% strain.

As discussed above, for the higher normal stress (60 kPa, 90kPa) fresh ballast has the highest shear stress. But the combination of USP, UBM & Geogrid sample has the second highest shear stress when compared to other rubber inclusions. This is because the geogrid provides an interlocking mechanism between ballast particles and which increases the shear resistance between ballast particles. The USP & UBM sample has the lowest shear stress on 30 kPa and 60 kPa normal stress. But in higher normal stress (90 kPa), the shear resistance of the sample with rubber inclusion at the top and bottom is high. This could be the reason that the-ballast particles were gripped on the rubber and give additional resistance. In 90 kPa normal stress the minimum shear stress has been observed in the ballast with USP sample. This clearly shows that the performance of rubber inclusion in rail track is depend on the application of deifferent wheel loads such as passanger to freight trains.

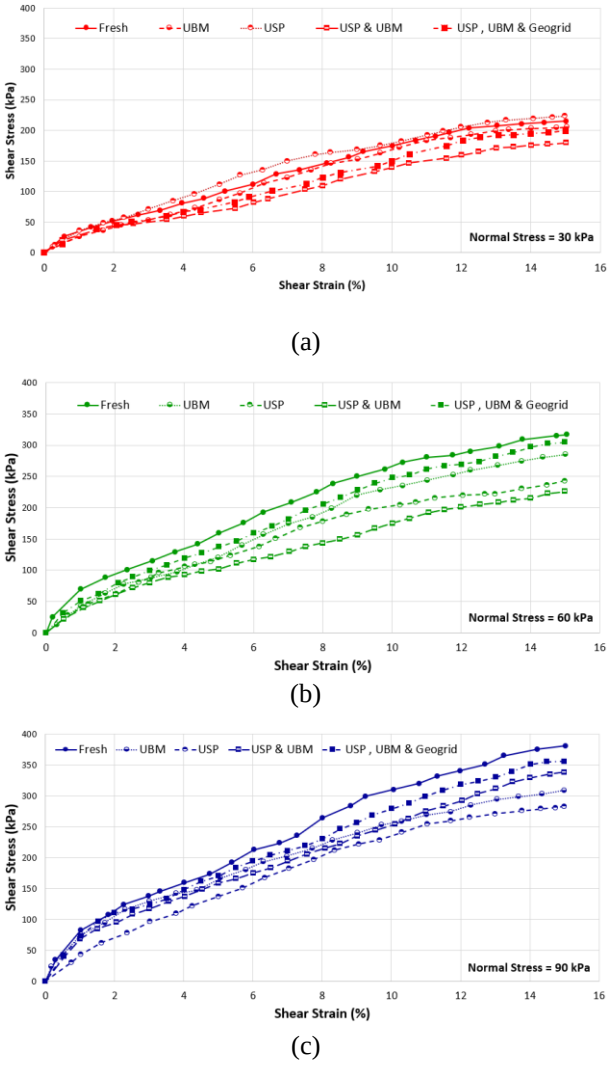

Figure 6 Different samples with; (a) 30kPa, (b) 60kPa and (c) 90kPa normal stress

4.2 *Degradation behavior of ballast with various normal stress*

Ballast particles experienced considerable breakage due to the application of normal loads and due to the shearing of particles. During the direct Shear loadings, ballast particles were undergone different types of degradation such as grinding, angular corner breakage and distinct splitting across the body of particles. Since the ballast breakage potential varies with depth due to changes in stress along with the depth of the ballast layer, the ballast mass was divided into top, middle, and bottom layers and analyzed separately where the direct shaer plane is in the center section of the middle layer. Figure 7 shows the photograps taken samples from three different layers which shows the fress ballast and degraded ballst before and after testing, repectivley.

(a) (b) (c)

Figure 7 Photographs of Coloured ballasts before and after the test: (a) top, (b) middle and (c) bottom layers

Figure 8 show the calculated BBI values of the three layers of different samples for 90 kPa normal stress. According to the results, ballast breakage has increased with the increase of normal stress due to the compression of ballast that leads to high breakage at higher normal stresses. The highest breakage occurred in fresh ballast and the lowest occurs in the USP & UBM sample and combination of USP, UBM & Geogrid sample.

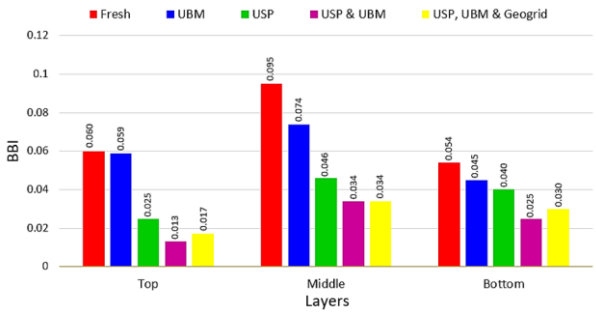

Figure 8 Ballast Breakage Index for different layers

When comparing the BBI value with the top, middle, and bottom layers, all the BBI results show comparatively larger BBI in the middle layer compared to the top and bottom layers. This is mainly because the shearing plane is fixed at the middle layer and where the ballast is experiencing more breakage on the shear plane. The minimum BBI value is occurred in USP & UBM sample and combination of USP, UBM & Geogrid sample of each layer with small variance. When considering the middle layer, BBI value of the fresh ballast has reduced more than twice with the use of USP &UBM and combination of USP, UBM & Geogrid in the ballast layer.

5 CONCLUSION

The large scale direct shear results of ballast stabilised with rubber and geogrid shows that the shear resistance of fresh ballast is high compared to ballast with geosynthetic inclusions. On the other hand, the ballast degradation higher for fresh ballast and it is significantly getting reduced when we introduce geogrid and rubber inclusions. Rubber inclusion reduces the ballast degradation however it also reduces the shear resistance. But inclusion of geosynthetic bring back some of the reduced shear strength. Based on this study, a combination of rubber and geogrid is better option enhancing the rail track performances in terms of stress-strain and degradation behaviour of ballast.
The scope of this study is limited to static load condition only.

ACKNOWLEDGMENTS

This research is funded by the University of Peradeniya Research Grant (Grant No: URG-2017-29-E) and Accelerating Higher Education Expansion and Development (AHEAD) Operation of the Ministry of Higher Education funded by the World Bank (Grant No: AHEAD/RA3/DOR/STEM/No.63) is also appreciated for their support in continuing this research. We would like thank our staff of the geotechnical laboratory for helping us in many ways.

REFERENCES

Fagnoul, A., and Bonnechere, F., “Shear strength of porphiry materials”, Proc. 7th International Conference on Soil Mechanics and Foundation Engineering, Mexico, 1969, pp. 61-65.

Indraratna, B., Lackenby, J., and Christie, D., “Effect of confining pressure on the degradation of ballast under cyclic loading”, *Geotechnique* Vol. 55, No. 4, 2005, pp. 325–328

Navaratnarajah, S. K., Indraratna, B. and Nimbalkar, S., “Application of Shock Mats in Rail Track Foundation Subjected to Dynamic Loads”, *Procedia Engineering*, Vol.143, 2016, pp. 1108-1119

Navaratnarajah, S.K., Gunawardhana, K.R.C.M., Gunawardhana. M.A.S.P., (2019), “Influence of type of interfaces on railway ballast behavior”, ICSECM2019-87

Navaratnarajah, S.K., Indraratna, B., “Use of rubber mats to improve the deformation and degradation behavior of rail ballast under cyclic loading”, *Journal of Geotechnical and Geoenvironmental Engineering*, Vol. 143, 2017

Nimbalkar, S., Indraratna, B., and Rujikiatkamjorn, C., “Performance Improvement of Railway Ballast using Shock Mats and Synthetic Grids”, GeoCongress 2012: State of the Art and Practice in Geotechnical Engineering, 2012, pp. 1622-1631

Investigation of Strength Behaviour in Soft Peaty Clays Stabilized with Calcium Carbide Residues, Fly Ash & Cement

A.K.G.M. Jayamal and A.S. Ranathunga
Department of Civil Engineering, University of Moratuwa, Sri Lanka

ABSTRACT: Due to unavailability of suitable land, many of the current infrastructure development projects in Sri Lanka, has to be constructed on lands underlain by soft peaty clay layers. These layers are highly compressible having a low shear strength and a high-water content. In situ deep mixing of soft peaty clay with a binder such as cement can improve strength and compressibility characteristics significantly in a short period of time. However, due to the higher cost and environmental impact for cement as the binder, reducing the cement content using industrial by-products such as Calcium carbide residue (CCR) and Fly ash (FA) is needed. This study focuses on usage of CCR and FA to substitute portions of cement as a binder. Improvements in strength for various proportions of CCR, FA and cement were assessed by conducting unconsolidated undrained triaxial tests for short-term (28 days) and long-term (90 days) curing. Adding only cement has the best improvement while 10% CCR, 15% FA with 5% cement mixture showed the best results among other mixtures. The CCR fixation point was 30% and had no effect with curing time. Further, moisture content of the soil plays a vital role in the strength improvement and having similar proportions for FA with CCR and cement mixtures provided better results.

1 INTRODUCTION

In the recent past, a number of highway projects commenced in Sri Lanka. These road projects sometimes had to be constructed through marshy lands which are underlain by thick peaty clay layers, having 30-40% organic content (Vitharana, 2019).

These thick layers of peaty clay have a low pH value, extreme water contents above 300% and shear strength as low as 2 kN/m^2 (Kulathilaka, 2015). Void ratio of peaty clay is relatively high compared to other soil types; hence a high-water content can be held in the soil resulting in a very low bulk density and low shear strength. When loads are applied on these layers, consolidation will take place and high secondary consolidation will occur. Therefore, before higher embankments are built over these lands, the soil needs to be stabilized.

In Southern Expressway and Colombo Katunayake Expressway projects, different techniques such as pre-consolidation with preloading; pre-consolidation with vacuum consolidation and heavy tamping followed by preloading; sand compaction piles and crushed stone piles; and excavation and removal have been used to enhance stiffness and shear strength of peaty clay soil (Kulathilaka, 2015).

Permeability of soil is very important for consolidation since the speed of the consolidation process depends on it. Previous studies revealed that peat is averagely porous and therefore has a medium state of permeability (Kolay & Pui, 2010). Therefore, even with perforated vertical drains, consolidation continues for a considerable time which makes the above methods ineffective when it comes to time constraints. Since the speed of construction is a major problem of current development projects, geotechnical engineers have to look for rapid methods. Deep mixing with cement, lime or with a mix of some other industrial binders in situ is another technique that can be adopted to improve the engineering properties of soft peaty clay in a short period of time.

The deep mixing process is beneficial over other techniques because when peaty clay is deep mixed in-situ with a binder like cement, a hydration process will cause followed by a subsequent pozzolanic reaction which increases strength and consolidation characteristics in a short period of time (around 28 days). However, laboratory studies done at University of Moratuwa have shown that a cement content of the order of 20-25% is required to achieve a desired level of improvement in peaty clay (Vitharana, 2019). This is comparable with the cement weights of 200-250 kg per cubic meter of peaty clay reported in literature (Kulathilaka, 2015). Hence, using cement is not economically and environmentally feasible for soil stabilization. Hence, several researchers have tested the use of industrial by-products as a full/partial replacement for cement to reduce the environmental impact and higher costs.

Fly ash (FA) is one such by-product produced at coal power plants and is successfully used as a cementitious material in many countries. FA mainly includes SiO_2, Al_2O_3, and Fe_2O_3 which makes FA a pozzolanic material. However, Sri Lanka has class "F" FA which is low in calcium (~6%) (Vitharana, 2019). Therefore, FA found in Sri Lanka needs to be mixed with a high calcium additive to generate better pozzolanic reactions such as Calcium Carbide Residues (CCR).

CCR is a by-product of the welding industry and agricultural industry which generates as a result of Calcium Carbide (CaC_2) reaction with water (refer to Eq. (1)).

$$CaC_2 + 2H_2O \rightarrow C_2H_2 + CCR \quad (1)$$

CCR has 50 – 75% calcium (CaO) content (Kampala & Horpibulsuk, 2013). When CCR is mixed with peaty clay, it reacts with pore water and makes a strong base medium. Natural pozzolanic materials (silica and alumina) in the soil dissolve in this base medium and react (pozzolanic reaction) with calcium ions to form a cementitious product as Calcium Silicate Hydrates (CSH), Calcium Aluminates Hydrates (CAH) and Hydrated Lime (refer to Eq. (2)) (Kampala & Horpibulsuk, 2013).

$$[SiO_2 + Al_2O_3 + H_2O] \text{ (from soil)} + CCR \rightarrow CSH + CAH + CASH + Ca(0H)_2 \quad (2)$$

The strength improvement in peaty clay due to above pozzolanic reaction can be classified into three zones: active, inert, and deterioration. In the *active zone*, strength increases with the CCR input. The optimum CCR content for the best strength improvement with the available natural pozzolanic materials in the soil is known as *CCR fixation point* and the active zone ends with CCR fixation point. Then the *inert zone* starts with a slower strength development due to the lack of natural pozzolanic materials in the soil to react with excess amount of CCR input. Adding another pozzolanic material rich source like FA, in this zone can accelerate the process again. In the deterioration zone strength decreases due to the loss of pozzolanic materials and unsoundness caused by excess free lime (Kampala & Horpibulsuk, 2013). Hence, using CCR and FA together should provide better strength improvement in peaty clay. However, Vitharana, (2019) proposed to use a smaller amount of cement with CCR and FA to improve soft peaty clay due to the lesser strength improvements observed with only CCR and FA.

Thus, the main objective of this study was to investigate the applicability of CCR and FA as a partial replacement of cement during dry mixing to improve the shear strength of soft peaty clay.

2 METHODOLOGY

Peaty clay samples were extracted from the Outer Circular Expressway at Kerawalapitiya. Impurities were removed and all the samples were mixed to prepare a homogeneous sample. The basic properties of peaty clay are presented in Table 1.

Soil samples were mixed with CCR (from Ovin Gas (pvt.) Ltd, Homagama) and FA (from Lakvijay Power Plant, Norochcholai) on a wet weight basis as in Table 2. The total additive percentage was kept at 30%. 5% cement content was selected as a fixed amount and remaining 25% was replaced with CCR and FA. Further, three samples were prepared with 15%, 30% and 45% of CCR in order to investigate the CCR fixation point of the soil. All the samples were mixed using a mechanical mixer and were cured under a surcharge of 10 kN/m^2 for 28 days (short-term) and 90 days (long-term) under submerged conditions.

Table 1. Basic properties of peaty clay

Basic Property	Value
Initial moisture content	614.12%
Initial pH	6.0
Organic content	39.64%
Specific gravity	1.514
Bulk density	1.0746 g/cm^3
Initial void ratio	5.44
Liquid limit	67.2%

Table 2. Mix proportions

Combination	Additives (% by weight)		
	CCR	FA	Cement
Peat only	-	-	-
Peat + Cement	-	-	30
Peat + CCR + FA+ Cement	20	5	5
	15	10	5
	10	15	5
	5	20	5
Peat + CCR + FA	15	15	
Peat + CCR	15, 30, 45		

After curing, undisturbed samples were obtained and Unconsolidated Undrained Triaxial test was conducted according to ASTM D2850 standards under 50 kPa, 100 kPa and 150 kPa cell pressures to investigate shear strength parameters of stabilized peaty clay samples.

3 RESULTS AND DISCUSSIONS

3.1 *CCR fixation point*

Strength behaviour of the short-term and long-term stabilized samples is represented in Fig. 1. The graphs were extended using best fit ($R^2 > 0.99$) polynomial trend lines to clearly observe the inert and the deterioration zones.

Similar to the findings in literature, shear strength of peaty clay has improved rapidly at the beginning. Because initially, pozzolanic reaction occurs rapidly and makes the cementitious material, which densify the peaty clay by filling pores in it. Next, an inert region is displayed, where increment slows down as the pozzolanic material in peaty clay gets depleted. However, further increase in CCR%, caused the shear strength to decline due to the excess lime created.

Compared to short-term, long-term curing exhibits around 3.5% increment in shear strength of peaty clay samples. In addition, the active region of both short-term and long-term curing falls up to 30% CCR.

Conversely, long-term curing displays a longer inert region (30% - 60%) while that for short-term curing is comparatively shorter (30% - 45%). These results indicate that long-term curing allows more room for the flocculation of peaty clay particles to densify the soil matrix. Therefore, in field application, we can expect higher strength improvement in peaty clay with time. However, a similar fixation point of 30% was observed for both short-term and long-term curing, indicating that the maximum adsorption capacity of Ca^{2+} ions by soft peaty clay will not change with time for curing.

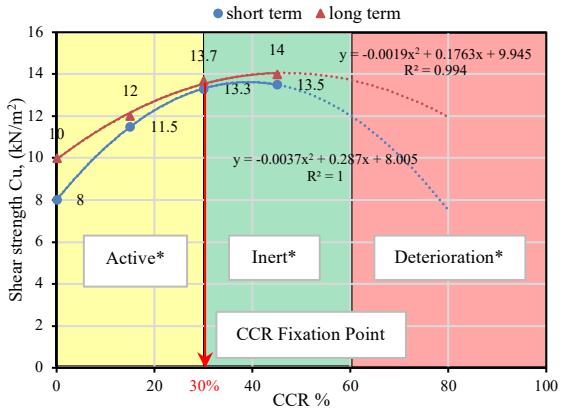

Fig. 1 Shear Strength variation with CCR

*shaded areas show the different stages of strength variation for long-term curing

3.2 *Strength behaviour of peaty clay with CCR, FA and cement*

Second objective was to investigate the best mixture of CCR and FA as a partial replacement of cement which gives the maximum improvement in shear strength of soft peaty clay samples and the shear strength behaviour of the soil samples are shown in Fig. 2.

According to Fig. 2, maximum improvement is achieved when 30% cement is added to the peaty clay. Among the other additive combinations, CCR 10%, FA 15% and 5% cement gave the highest shear strength. However, it is almost half of the shear strength obtained for 30% cement. In addition, when the curing period extends, all the soil samples

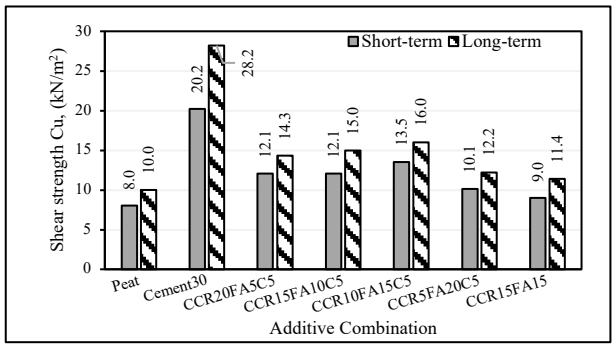

Fig. 2 Strength variation of soil samples with CCR, FA and cement

showed an increment ranging from 18% to 40% which is much higher than with only CCR. This explains the potential to improve the strength of the peaty clay with time when FA and/or cement is available which provides additional pozzolanic material for the excess lime generated by CCR to react. This can be further explained by the shear strength increment with the FA content of the samples (refer to Fig. 3).

Immediately after mixing stabilizers with soil, the hydration process of cement and pozzolanic reaction between CCR and FA has led to the stabilizing process. It is proven by the observation of immediate water content reduction of around 400% in mixtures. Therefore, the strength has improved considerably than when only CCR was mixed (average moisture content reduction when CCR was added is around 225%). Interestingly moisture content and the strength of stabilized soil has an inverse relationship.

Further, the strength has been increased with the increasing FA content up to 15% and then has reduced for 20% of FA. For 20% FA, there is only 5% cement and 5% CCR and the amount was not sufficient to generate enough pozzolanic reactions to strengthen the soil matrix. The maximum strength additive combination has an equal amount of FA (15%) and CCR (10%) with cement (5%). This observation suggests using an equal amount of FA with CCR and cement mixtures for better results.

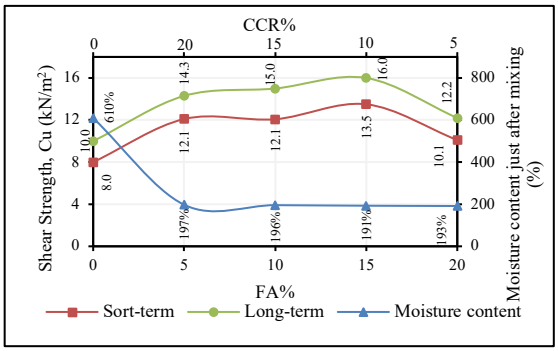

Fig. 3 Strength and moisture content variation of soil samples with FA

3.3 *Changes in the microstructure*

Microstructure of the stabilized samples were investigated through scanning electron microscope (SEM) and are shown in Fig. 4. Irregular shape of peaty clay particles and the voids among particles are clearly depicted in the figure. When the cement or CCR is mixed with soil, a rod-shaped structure (Ettringite) can be observed which makes a more aggregated and bonded structure hence increases the shear strength. The spherical shape of FA allows peaty clay to densify more than the CCR. Due to the high specific gravity of FA, it allows peaty clay to

be well compact and thus increase the shear strength.

However, the soil matrix with 30% cement is more densified and has higher ettringite formations compared to other mixtures. Hence, a higher cement percentage than 5% should be added for better improvement.

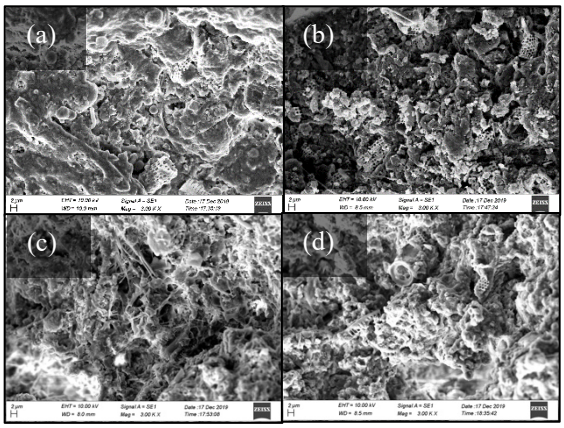

Fig. 4 SEM images of (a) peaty clay, (b) Peaty clay with 10% CCR 15% FA and 5% cement, (c) 30% cement and (d) 30% CCR (magnification of 3k and voltage of 10 kV)

4 COMPARISON WITH PREVIOUS STUDIES

Results of the present study were compared with Vitharana, 2019) who have used CCR, FA and cement as stabilizers with a surcharge of 10 kN/m^2 and are shown in Table 3. Both studies have similar organic content whereas, moisture content of present study's soil is twice as for Vitharana (2019)'s study. When peaty clay is treated only with cement, present study has around 34% lesser strength improvement despite using 10% higher cement for mixing. Thus, it further confirms the previous observation of the moisture content playing a vital role in the increment of the shear strength of peaty clay.

Table 3. Comparison with previous studies

Reference			Vitharana (2019)		Present Study	
Properties of Peaty clay		Moisture%	300%		614%	
		Organic%	40.5%		39.6%	
		G_s	1.8		1.5	
Shear Strength (kN/m^2)	Soil only		4.5		8	
	Additive combination (%)	Cement (C)	20		30	
			S-30	L-32	S-20	L-28.2
		CCR/ FA	CCR20+FA10		CCR15+C5+FA10	
			S-16	L-17	S-12	L-15
			CCR10+FA20		CCR10+C5+FA15	
			S-15	L-16	S-13.5	L-16
			CCR15		CCR15	
			S-11	L-17	S-11.5	L-12
CCR Fixation point			15%		30%	

S – Short-term (28 days); L – Long-term (90 days)

However, present study shows a higher improvement when FA and cement is added in 90 days compared to the previous study. We can conclude that adding cement provides more pozzolanic materials to continue the strengthening in the long run. Furthermore, CCR fixation point follows a similar pattern as for moisture content where the value is doubled in the present research. 15% CCR addition provides similar strength for both soils in short-term. Whereas, the long-term improvement of strength is hindered in present study due to the insufficient CCR content (CCR fixation point is 30%) for hydration process.

5 CONCLUSIONS & RECOMMENDATIONS

- Although cement is currently the best solution to stabilize peaty clay, CCR and FA combination has shown considerable strength development.
- The strength is increased with curing time, whereas, CCR fixation point will not change with curing time.
- Variation of moisture content plays a main role in the strength improvement of peaty clay.
- For better improvements, using similar proportions of FA with CCR and cement mixtures is suggested. And adding or replacing a portion of CCR with little amount of cement (> 5%) is also suggested.
- An extensive environmental study on the effect of heavy metal leachability from FA during soil stabilization should be conducted before any industrial application.

ACKNOWLEDGMENT

The assistance given by the Geotechnical Engineering and Materials Science and Engineering laboratory staff of University of Moratuwa are acknowledged.

REFERENCES

Kampala, A., & Horpibulsuk, S. (2013). Engineering Properties of Silty Clay Stabilized with Calcium Carbide Residue. Journal of Materials in Civil Engineering, 25(5), 632–644.

Kolay, P. K., & Pui, M. P. (2010). Peat stabilization using gypsum and fly ash. Journal of Civil Engineering, Science and Technology, 1(2), 1–5.

Kulathilaka, S. A. S. (2015). Experiences on Improvement of Soft Peaty Clays in Sri Lanka. ACEPS 2015, 10.

Maduransi, L.W.I., and Kulathilaka, S. A. S. (2015). Use of paddy husk ash as a binder in improvement of soft peaty clay. In International Conference on geotechnical Engineering (ICGE), pp .407 - 410.

Vitharana, T.H. (2019), Investigation of Strength Behaviour in Soft Peaty Clays Stabilized with Calcium Carbide Residues and Fly Ash, Bachelor's Dissertation, University of Moratuwa, Sri Lanka.

Reduction of Secondary Consolidation of Peaty Clay Due to Preloading with Extended Periods

D.R.I.S. Dasanayake, S.A.S. Kulathilaka
Department of Civil Engineering, University of Moratuwa, Sri Lanka

ABSTRACT: Peaty clays are with very high compressibility and very low shear strengths. Primary consolidation in peaty clays would be over in a short period and high secondary consolidation settlements would occur thereafter. Those high secondary consolidation settlements could lead to high settlements in the service period. In the construction of highway embankments in sites underlain by peaty clays, the reduction of in-service settlements is achieved by pre consolidation by preloading. Consolidation tests with loading, unloading and reloading increments in Oedometer and Rowe Cell apparatus have shown that, considerable reduction of secondary consolidation can be achieved by preloading. In construction on Peaty clay fill loading has to be done in stages allowing sufficient consolidation and gain in shear strength to prevent shear failures. Some of these loading stages may prolong in practice. In this research a prolonged loading stage was simulated by extending the duration of a selected loading increment. The results of the study confirmed the reduction of coefficient of secondary consolidation (C_α) due to preloading and showed that prolonging latter stages of loading will have additional benefits.

1 INTRODUCTION

Due to the scarcity of lands, Geotechnical engineers have to utilize lands underlain by weak soils improving them appropriately in the infrastructure development projects such as highways. Therefore, improvement and stabilization of thick layers of peaty clays with high compressibility and low shear strength is a major challenge.

Peat is formed by the decomposition and fragmentation of partially decayed vegetation or organic matter in anaerobic conditions. When peat is mixed with the alluvial clays it is termed peaty clay. Peaty clays can be usually found in marshy areas and flood plains where the water has accumulated over long periods. Peaty clays are with very high-water contents and high void ratios and low pH values. Water contents over 300% are recorded in extremely soft peaty clays. The organic contents of the peaty clays encountered in Sri Lanka are normally in the range of 20%-40%. Due to the organic matter peaty clays have low specific gravity. (Sarojini, 2014)

In order to overcome this issue numerous ground improvement techniques are applied to ensure that the construction is done without causing failures and the settlements of the ultimate structures are within the acceptable limits. Preloading is one such technique. Preloading process is designed to ensure that the peaty clay will remain in an over consolidated state during the service period. Due to the very low shear strength in peaty clay the construction fill is placed in stages allowing sufficient consolidation at each stage. Some of these loading stages could prolong due to various practical aspects in the construction projects.

2 BACKROUND

Previous laboratory studies by Fernando and Kulathilaka (2015) and Karunarathne (2018) with loading increments of 1 day and 3 days have shown that C_α values will reduce significantly with pre-loading. Research by Ahmed (2018) has shown that with much shorter loading increments (3 hour) also, the reduction of secondary consolidation is significant.

3 METHODOLOGY

This research was designed to study the effects of prolonged loading. As such, one load increment was extended to five days. All other increments were of one day's duration. In four identical samples extended load increment was done at 25, 50, 100 and 200kN/m^2. Thereafter sample was unloaded and reloaded. Behaviour of the pre-loaded peaty clay was simulated in reloading increments. Reloading increments were designed to obtain over consolidation ratios between 1 and 2 as the values achievable in the field are less than 2. Consolidation characteristics were evaluated in each increment using e vs log (time) plots and e vs log(σ) plots. The coefficient of secondary consolidation C_α corresponding to different stages was derived through these plots.

Consolidation tests were conducted in both Rowe Cell apparatus and Oedometer with identical samples of remoulded peaty clays. Peaty clay for this research was obtained from outer circular highway project in Sri Lanka. Non decayed pieces of wood and other impurities such as gravel were removed to obtain a remoulded sample of uniform density and water content.

Water content of peaty clay was determined by keeping the peaty clay sample in an oven at a maximum temperature of 60^0 and verified by keeping a sample at room temperature for about a week until there is no further weight loss. Basic properties of peaty clay used are summarized in Table 1.

Table 1. Basic Properties of Used Peaty Clay

Properties	Value
Water Content	647.57%
Organic Content	39.64%
Specific Gravity	1.504

Oedometer used in this research was 20mm in height and 50mm in diameter. Two-way drainage was permitted through porous disks at the top and the bottom and sample was kept as saturated using the water bath. Mechanical vertical load was applied to the sample.

Rowe Cell (Fig. 1) overcomes many limitations of the conventional Oedometer. Rowe and Barden (1966). The samples are loaded hydraulically by water pressure acting on the flexible diaphragm. Therefore, pressure distribution is uniform throughout the sample. Large diameter samples in Rowe Cell could be more representative. Drainage was provided only from the top. The pore water pressure was measured at the bottom.

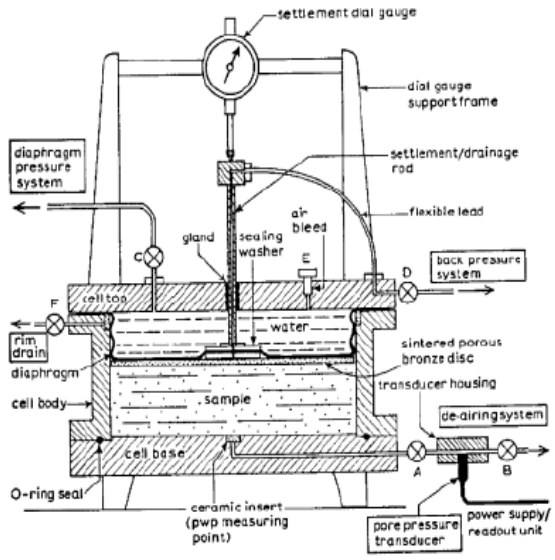

Fig. 1. Rowe Cell Setup

4 TEST RESULTS

4.1 *One day (24-hour) Long Increments*

Due to high secondary consolidation of peaty clays, reduction of the gradient of the void ratio vs log time curve after the completion of primary consolidation is not easily identified as in the curve of inorganic soils. This can be identified from Fig. 2.

The pore water pressure dissipation with time can be clearly identified in Fig. 2. Hence the beginning of secondary consolidation of the sample could be easily detected. Continuation of settlement even after the pore water pressure has dissipated to a small value is quite evident here. The coefficient of secondary consolidation can be calculated from the latter part of the plot. In the Rowe Cell the pore water pressure is measured at the impermeable bottom boundary. As some amount of time is required for pore pressure equilibration the full applied pore water pressure may not be recorded instantly at the bottom boundary. This is the reason for the increase of the measured pore water pressure observed at the commencement of a load increment.

4.2 *Extended consolidation increments*

The series of tests on the four identical samples included one loading increment extended for five days. This is to simulate a prolonged loading stage in the application of loading in stages in the field. The objective of the research is to study the effect of this in the further reduction of the coefficient of secondary consolidation (C_α) continuing from the previous research done. The following loading sequence was applied on the four-specimen used for series of tests. Thereafter unloading and reloading increments were applied as outlined in the preceding sections.

0 - 25kPa for 5 days – 50kPa – 100kPa – 200kPa
0 – 25kPa – 50kPa for 5 days – 100kPa – 200kPa
0 – 25kPa – 50kPa – 100kPa for 5 days – 200kPa
0– 25kPa – 50kPa – 100kPa – 200kPa for 5 days

The behavior of the specimen during the extended load increment of 25-50kN/m^2 in the Rowe Cell is presented in Fig. 2.

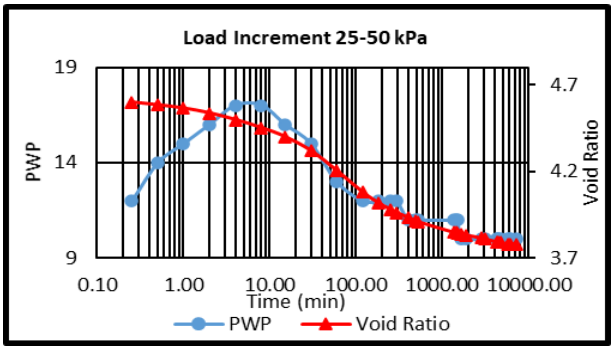

Fig. 2. Extended Load at 50kPa (Rowe Cell)

5 ANALYSIS

The e vs log (σ) plots for loading increments with extended loading increments for the Oedometer is presented in Fig. 3 and for the Rowe Cell is presented in Fig. 4. The gradients of the different segments of the e vs log (σ) plot are summarized in Table 2 for Oedometer and Rowe Cell. It is evident from the results the extended loading in lower stress levels did not lead to any significant further reduction of the C_c in the subsequent increments. However, when the extended loading is at 100kN/m^2, there is a significant reduction of gradient in the 200kN/m^2 increment. This was noted in both Oedometer and Rowe Cell.

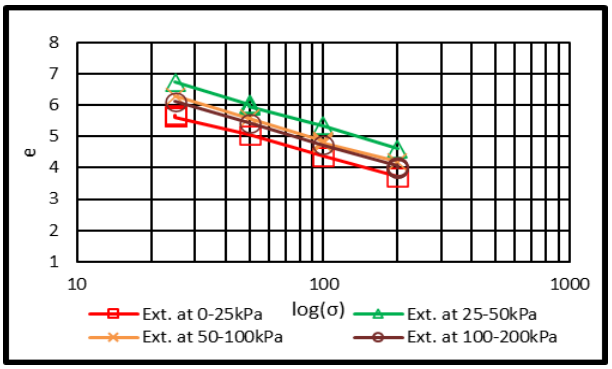

Fig. 3. Void Ratio vs Stress Level for Extended Loadings (Oedometer)

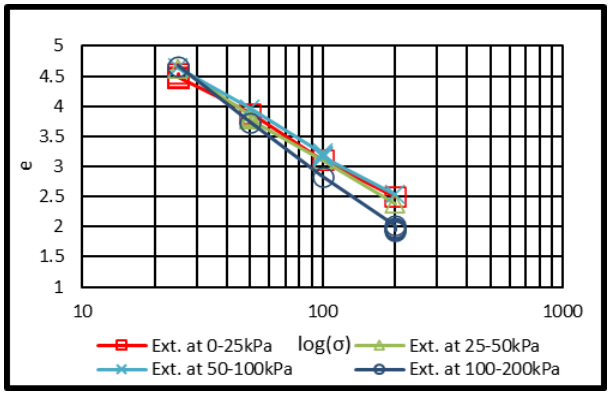

Fig. 4. Void Ratio vs Stress Level for Extended Loadings (Rowe Cell)

Table 2. Gradient of segments of Void Ratio vs Log(σ)

Sample		Gradient of e vs log (σ)		
		25-50	*50-100*	*100-200*
ELat 0-25kPa	OM	1.902	2.294	2.176
	RC	1.966	2.586	2.026
ELat 25-50kPa	OM	2.344	2.066	2.423
	RC	2.613	2.228	2.43
ELat 50-100kPa	OM	2.326	2.415	1.973
	RC	2.242	2.451	2.061
ELat 100-200kPa	OM	2.290	2.344	2.232
	RC	3.142	2.963	2.718

It should be noted that all four samples were prepared in the identical manner and thus the starting void ratio should be the same. Therefore except for the sample with extended loading at 25kN/m^2 the e values corresponding to other samples should be quite similar at the loading of 25kN/m^2. This is observed in the Rowe cell, but there are some deviations in the Oedometer samples. This is an indication of the practical difficulties in preparation of identical samples. The plots in Fig. 5 indicate that the C_α values of loading increments decrease with the stress level in Rowe Cell. The reduction after initial increment 0-25kPa is very high. This is a general feature normally seen in peaty clay. The C_α values of the reloading increments are quite low at initial increments where a high OCR value prevails. As the stress level increase and OCR approaches unity the C_α values increases. This feature is illustrated further with the graphs of C_α'/C_α and OCR.

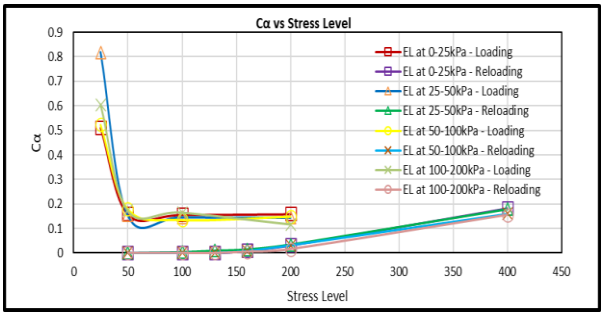

Fig. 5. C_α Variation with Stress Level – Rowe Cell

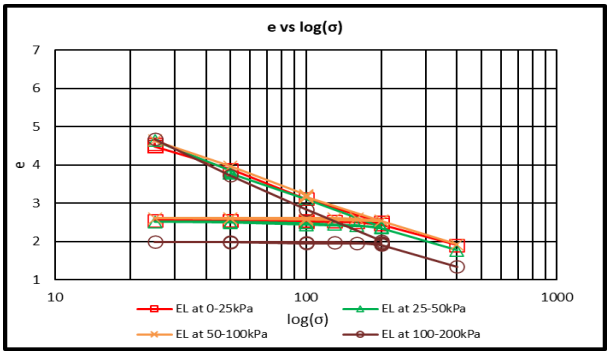

Fig. 6. Void Ratio vs Stress Level (Rowe Cell)

The e vs log (σ) plots carry loading, unloading and reloading increments of all samples in Rowe Cell are presented in Fig. 6. The plot indicated that the recompression index C_r value is in the range of 10-12% of the compression index C_c for all the four samples. This confirms the reduction that can be achieved in primary consolidation settlements due to preloading.

The reduction of C_α due to the effect of preloading was quantified by the plot of C_α'/C_α vs OCR presented in Fig. 7 for Oedometer and Fig. 8 for Rowe Cell. Here C_α' corresponds to reloading increment.

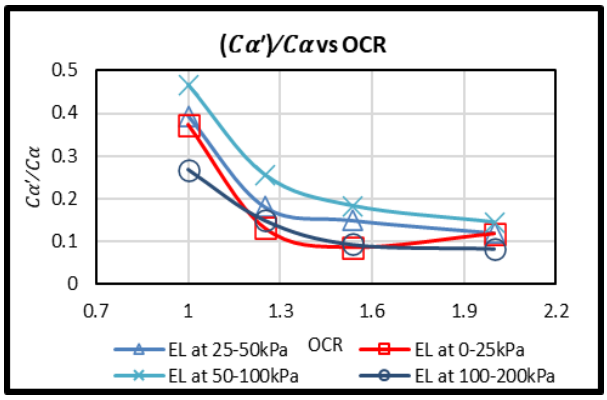

Fig. 7. $C\alpha'/C\alpha$ vs OCR - Oedometer

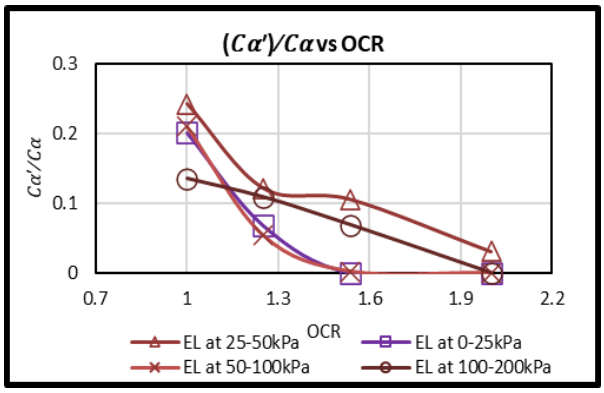

Fig. 8. $C\alpha'/C\alpha$ vs OCR – Rowe Cell

These plots confirmed that the pre-consolidation by preloading causes a significant reduction in the secondary consolidation coefficient C_α. This reduction increase with the achieved OCR. Even an OCR of 1.0 has resulted in a significant reduction of C_α. This effect increased with increasing OCR at a lesser rate. A further reduction due to prolonged loading is noticeable only when the extended loading increment was at higher stress levels of 100 kPa, 200kPa.

Following the C_α/C_c concept proposed by Mesri et al (1997) the values obtained for the different segments of the loading increments is summarized in Table 3 for the Oedometer and the Rowe Cell. The ratio has not decreased appreciably after an extended load increment.

Table 3. C_α/C_C Values

Sample		C_α/Cc values		
		25-50	*50-100*	*100-200*
ELat 0-25kPa	OM	0.0551	0.0450	0.0453
	RC	0.0811	0.0605	0.0787
ELat 25-50kPa	OM	0.0407	0.0516	0.0404
	RC	0.0553	0.0656	0.0597
ELat 50-100kPa	OM	0.0457	0.0425	0.0484
	RC	0.0800	0.0546	0.0719
ELat 100-200kPa	OM	0.0501	0.0480	0.0396
	RC	0.0550	0.0558	0.0433

6 CONCLUSION

In the preloading process which is done in stages the loading may be left for a longer time due to issues in project planning. The specific objective of this research is to investigate whether any further reduction of C_α can be achieved due to this prolonged loading. As such, in this research consolidation tests with loading/unloading and reloading were done with an extended loading shifted over the different loading increments. The tests were done on four remolded samples prepared in the same manner. The results of the study confirmed that the reduction in C_α achieved by preloading is proportional to the OCR achieved. Prolonged loading at early stages did not provide any further reduction but the prolonged loading at higher stress levels seem to cause a further reduction in C_α. This is useful finding practically as in a construction project it could be planned to keep the final loading stage for a longer period before the removal of surcharge.

REFERENCES

Ahmed, M. (2018). Secondary Consolidation Characteristics of Peaty Clay. Final Year Research Project at University of Moratuwa

Fernando, R. M., & Kulathilaka, S. A. (2015). Effect of Preloading on Secondary Consolidation of Peaty Clay. ICGE Colombo Conference Paper

Karunarathne, J. (2018). Secondary Consolidation Characteristics of Peaty Clay. Geotechnical Engineering Project Day - SLGS

Mesri, G., Stark, T. D., Ajlouni, M., & Chen, C. S. (1997). Secondary Compression of Peat with or without Surcharging. Journal of Geotechnical Engineering, ASCE, Vol123 No GT5, 411-421.

Rowe, P., & Barden, L. (1966). "A New Consolidation Cell" Geotechnique, 16(2), pp. 162-170.

Sarojini, W. A. (2014). Improvement of Sri Lankan peaty clays by deep mixing and electro-osmosis. MEng Thesis submitted at University of Moratuwa.

Effect of sea breeze on the performance of coastal rail functionality

S. Sajitthan and U.P. Nawagamuwa
Department of Civil Engineering, University of Moratuwa, Sri Lanka

ABSTRACT: This paper discusses the effect of sea breeze on the physical properties of ballasts in the coastal railway. The degradation of ballast has already been studied by several researchers. However, the impacts of sea breeze on the ballasts in coastal railway have not been studied so far. This study is a comparison of the collected samples of ballast from Moratuwa (in-land area) and Mount Lavinia (coastal area) segments of the Southern rail line. The properties of ballasts were tested by Los Angles Abrasion Value (LAAV) and slake durability tests. This was to compare the rate of ballast degradation in coastal and inland areas. In addition, Ballast Breakage Index was also determined through sieve analysis. The vibrations of ballasts were measured in the field and the impacts by the sea breeze on ballasts were analyzed. Sea breeze leads to an accelerating rate of degradation of the railway ballasts, which in turn reduces the resonance frequency of the ballasts. Therefore, the critical speed of moving train in coastal railway lines for the respective resonance frequency of ballasts will be reduced. These results hence indicate that the Sri Lankan coastal railway lines must be maintained more frequently compared to the inland lines, by the appropriate authorities.

1 INTRODUCTION

The national transport statics (September 2015 volume-V) by Sri Lanka National transport commission states that rail transport acts as a major transport mode in Sri Lanka, which is engaged in passenger and freight transport service giving 4.3 percent contribution to the transport sector in the National Economy. However, a report by Sri Lanka Railway in 2018 shows that Sri Lanka Railway Department operates at a net loss. Therefore, it is not possible to conduct routine maintenance as frequently as required. Thus, the durability and workability of railway components decrease with time due to the lack of maintenance. Ballasts are the predominant component of railway lines which provide adequate drainage and distribute the load from the sleeper to a large area of formation.

Various methods had been indicated in past literatures to determine Ballast deformation and degradation. The degradation of ballast is commonly measured by standard laboratory tests such as Los Angles Abrasion (LAA) tests and Large Scale triaxial Tests(Nålsund et al., 2013). The degradation of ballasts can be compared by observing the morphological properties such as angularity, flatness, elongation and surface texture through aggregate image analysis approach (Moaveni et al., 2016).

Studies have not been conducted considering the continuous effect of saline water in conditions like sea breeze on ballasts closer to coastal areas. This paper discusses the effect of sea breeze on coastal rail ballast coupled with vibration of ballast bed with the aim of bridging the gap left by the past studies related to degradation of ballast.

In railways, the dynamic load creates as an elastic wave through the body and creates natural vibration modes to the body. Ballasts are used to absorb the vibration more among the other components of the rail track and attenuate the transmission to the ground. The ballast layer acts as an elastic one-directional spring in the vertical direction. This is called the elastic shrinkage natural vibration mode. The physical theory of elastic first-order vibration mode is proportional to E/ρ where E and ρ respectively denote ballast layer's Young modulus and packing density (Aikawa, 2018). Practically, the interlocking aspects of materials should be of concern for ballasts' vibration.

In this paper, the Los Angeles abrasion test, slake durability test and sieve analysis were done to compare the rate of ballast degradation in coastal railway and in-land railway by testing the physical properties of the ballasts. The water content of ballasts was determined to compare the porosity of ballast since the larger the internal surface area higher the porosity and less durable is the rock (Hudec, 1989). The effect of sea breeze on ballasts in coastal railway was analyzed through the results obtained by the tests. The dynamic behavior of railway ballast was measured (in the unit of acceleration) under different velocity of moving train loads (dynamic loads) by an accelerometer with a special protection box over the ballast bed. The change of resonance frequency of ballasts with respect to train velocities in coastal and inland areas were recorded and compared.

2 METHODOLOGY

It was assumed that the ballasts tested – both in-land as well as coastal were laid at the same time and they had undergone same load and train volume since both the areas picked were under Moratuwa Railway Station maintenance program.

2.1 Materials

Ballast samples were collected from railway tracks to determine the physical properties of existing ballasts in every location. The distance between seashore and locations where the ballast sample had been collected are given in Table 1.

Table 1. Locations of samples collected and the Distances to the sea

Location	Distance (m)	Coastal/ In-Land
Mount Lavinia	15-20	Coastal
Moratuwa	160-200	In-Land

The fresh ballast samples were collected in 'Metal Mix quarry' situated in Galpotha which is the main sub-contractor of Moratuwa Railway Station. Those ballasts from the quarry are categorized as charnokitic biotite (gneiss). The existing ballasts of Mount Lavinia and Moratuwa were taken from the same quarry.

2.2 Sieve Analysis

The sieve analysis of the collected samples was compared with gradation of Indian Railway Standard (Mundrey, 2018). The fresh ballasts from quarry were found to be within lower bound and upper bound however the collected existing ballasts samples were not fitting, as presented in Figure 1.

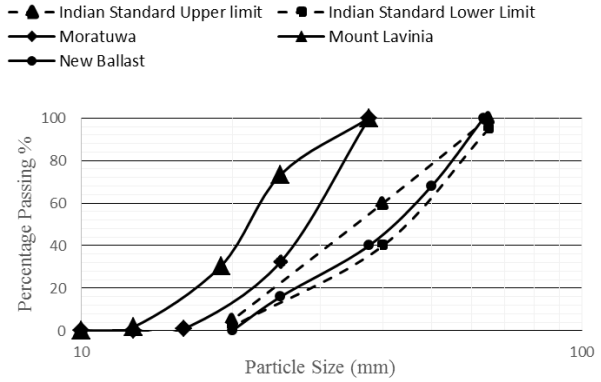

Fig. 1 Sieve analysis of Ballasts samples collected from different locations, compared to the standards

2.3 Los Angeles Abrasion Value (LAAV) Test

The collected ballast samples in Moratuwa were relatively larger in sizes than Mount Lavinia ballast samples. Therefore, the LAAV test was conducted in two test methods as mentioned in Table 2.

Table 2. LAAV test standard test procedure

Description	Ballast Taken Location	
	Mount Lavinia	Moratuwa
Size Grading	Small(<37.5mm)	Large(>19mm)
ASTM Standards	ASTM-C-131-03	ASTM-C-535-03
Categorized Grading	Grading-A	Grading -2
Number of sphere balls	12	12
Revolutions	30 to 33 r/min for 500 revolutions	30 to 33 r/min for 1000 revolutions
Time	15 min	30 min

2.4 Slake durability test and moisture content

Slake durability test was proceeded in ASTM D 4644-04 for two cycles to both in-land and coastal ballast samples. The total weight of the test specimens was measured before and after the tests (Table 3). The moisture content was also measured after the tests.

2.5 Vibration Measurement of top ballast bed

The vibrations were measured with calibrated vibration measuring device at Mount Lavinia and Moratuwa. Velocities and vibrations of 5 trains each in Mount Lavinia and Moratuwa were measured. Two vibration measuring devices were used to measure in Mount Lavinia and Moratuwa. In this situation, the average acceleration was obtained. The experiment was done keeping same time period in both areas. Therefore, the exerted load by the train can be considered to be same in all three areas. The average acceleration vs. time of Moratuwa ballast at 23km/h has been shown in Figure 2. Likewise, it was repeated and measured the velocities of train in both areas.

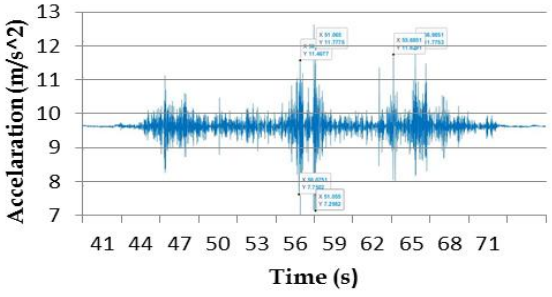

Fig.2 Average Acceleration vs. Time of Moratuwa ballast at 23km/h

3 RESULTS AND DISCUSSION

3.1 Ballast Breakage Index

The ballasts had undergone degradation due to the cyclic loading of the train for a particular time period. It is notable that the Mount Lavinia ballast curve has shifted to the left than Moratuwa ballast curve from the new ballast curve. The ballast breakage index (BBI) is a suitable method for representing ballast degradation (Indraratna et al., 2005).

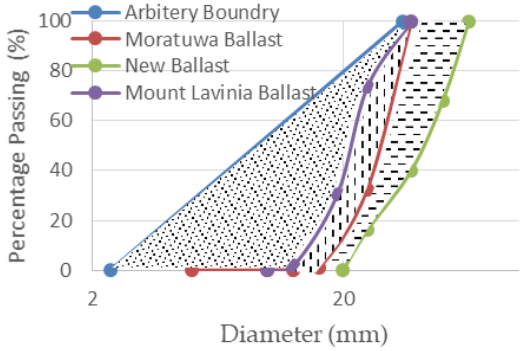

Fig.3 Particle size distribution for calculation of BBI

The values obtained from the Fig. 3 indicates that the ballast degradation is higher in the coastal railway (i.e.: Mount Lavinia –BBI = 0.41) than the inland railway (i.e.: Moratuwa- BBI = 0.25). Therefore, it provides an evidence that the sea breeze has a significant effect on ballast degradation and degradation rate compared to the general case.

3.2 Slake Durability Index and Moisture Content

Rocks can absorb water by capillary action (Moaveni et al., 2016). The absorption depends on the grain size (pore size). The finer-grained rocks absorb water at a rate nearly twice that of coarser-grained rocks, especially in the first few minutes of their contact with water. Moisture content and degree of saturation play a significant role in the durability of rock. Rocks may fail (slowly) by wetting and drying. The larger specific surface area increases the amount of water absorbed which indicates of having a large number of pores, microcracks and capillary pores (Ionescu, 2004).

Table 3. Slake Durability index calculation

	Cycle-1		Cycle-2		
Location	Wet Sample (g)	Dry Sample (g)	Wet Sample (g)	Dry Sample (g)	$I_{d(2)}$
Moratuwa	518.0	515.6	516.0	514.2	$\frac{514.2}{515.6}\% = 99.73\%$
Mount Lavinia	518.1	515.7	517.0	513.6	$\frac{513.6}{515.7}\% = 99.59\%$

Moisture content of the collected samples was measured based on ASTM D 2216- 10 standard test methods which is used for laboratory determination of moisture content (MC) of rock by mass. From these test results, it is considered that higher the moisture content, higher the porosity. The test results were 0.08% MC in Moratuwa and 0.25% MC in Mount Lavinia. These results clearly show that the existing ballasts in Mount Lavinia railway tracks have significantly larger porosity than Moratuwa ballasts. (Dhakal et al., 2004), have explained that the Slake durability index of a rock decreases with the increase in porosity. Therefore, it is reflected that larger porosity will result in less durability of rock.

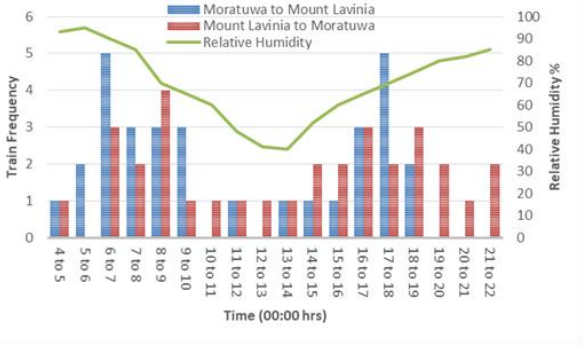

Fig.4 Train Frequency and Relative humidity vs. Time

The collected data from Department of Meteorology Sri Lanka indicates that the coastal areas have higher humidity of 70%-90% and it is high in the morning and evening. During that period, the daily traffic volume is also high which can be obtained by Fig. 4 in the Southern railway lines of Sri Lanka. Therefore, the ballasts in the coastal areas have a higher absorption rate and it leads easily to degradation and breakage into fine particles by the dynamic loading.

2.6 Vibration of ballast bed

The vibrations were measured with calibrated vibration measuring device at Mount Lavinia and Moratuwa.

The maximum and minimum acceleration were determined with respect to the train velocity. The natural frequency induced by train is proportional to the train velocity. The measured accelerations were observed in Mount Lavinia and Moratuwa for approximately same train velocities in both locations. As a result, ballasts in Mount Lavinia have higher acceleration than the ballasts in Moratuwa.

The predominant component for vibration of railway tracks is subgrade soil and ballast. Vibration in ground depends on two properties of the soil - shear modulus and damping ratio (Shih et al., 2017). Damping ratio is related to normalized shear modulus (Diego and Oronzo, 1997). Elastic modulus is directly proportional to shear modulus.

Through empirical equations, elastic modulus can be obtained from collected borehole Standard Penetration Test values. From the test results it has been observed, elastic modulus of ballast in Mount Lavinia was higher than Moratuwa.

It can be theoretically interpreted that there should be higher vibration due to weak soil in Moratuwa than in Mount Lavinia. However, the results obtained from vibration on railway tracks at Mount Lavinia have a higher value than Moratuwa. Therefore, it could be arrived at that the ballasts act as a major role, even though subgrade soil is an important component in the check of vibration.

The results obtained in the coastal areas and the inland areas do not show a linear variation between the train velocity and vibration. Resonance takes place when the train induced frequency and the natural frequency of the ballasts become the same. In Mount Lavinia area, it was observed that the maximum vibration occurs when the train is moving at a critical speed of 35km/h to 38km/h and in Moratuwa, between 37km/h and 42 km/h.

2.7 LAAV and Surface, Angularity, and flatness index

A detailed experimental study was conducted on characterizing ballast aggregate degradation using aggregate image analysis approach and LAAV tests (Qian et al., 2014) which produce fine ballast through accelerating ballast degradation. In that study the surface index, angularity index and flatness and elongation ratio were shown to decrease with the acceleration of ballast degradation. Therefore, from the above results, it can be concluded that there is a significant difference between Moratuwa (LAAV=0.3) and Mount Lavinia (LAAV=0.53) ballast and it is higher in Mount Lavinia. This shows that the surface index, angularity index and flatness and elongation ratio can be expected to be less in Mount Lavinia than Moratuwa. It increases the tendency of vibration with less interlocking ability within the ballast particles.

3 CONCLUSION

This research proves theoretically and experimentally that the natural frequency of ballast could be reduced due to the higher degrading rate of ballast when it is placed near coastal railway tracks. Therefore, even in the low velocity of train, the ballast achieves the resonance frequency and maximum vibration at such locations. The optimum velocity of a train for the resonance frequency of ballasts decreases in coastal area than inland area. Thereby, railway tracks in coastal area are in a more critical condition due to the higher degradation of ballasts. Therefore, maintenance of rail racks should be done on more frequent basis in those areas.

4 ACKNOWLEDGEMENT

I gratefully thank the technical officers of Moratuwa Station, National Building Research Organization and Metal Mix quarry for providing relevant information. I also thank the technical staff of the soil mechanics laboratory of University of Moratuwa.

REFERENCES

Aikawa, A., 2018. Vertical Natural Vibration Modes of Ballasted Railway Track, in: Yalciner, H., Noroozinejad Farsangi, E. (Eds.), New Trends in Structural Engineering. IntechOpen. https://doi.org/10.5772/intechopen.79738

Dhakal, G.P., Kodama, J., Yoneda, T., Neaupane, K.M., Goto, T., 2004. Durability Characteristics of Some Assorted Rocks. J. Cold Reg. Eng. 18, 110–122. https://doi.org/10.1061/(ASCE)0887-381X(2004)18:3(110)

Diego C.F.Lo, P., Oronzo, P., 1997. Damping ratios of soil from laboratory and in situ tests.

Hudec, P.P., 1989. Durability of Rock as Function of Grain Size, Pore Size, and Rate of Capillary Absorption of Water. Journal of Materials in Civil Engineering 1, 3–9.

Indraratna, B., Lackenby, J., Christie, D., 2005. Effect of confining pressure on the degradation of ballast under cyclic loading 4.

Ionescu, D., 2004. Ballast degradation and measurement of ballast fouling. 7th Railway Engineering Proceedings 169–180.

Moaveni, M., Qian, Y., Qamhia, I.I.A., Tutumluer, E., Basye, C., Li, D., 2016. Morphological Characterization of Railroad Ballast Degradation Trends in the Field and Laboratory. Transportation Research Record 2545, 89–99. https://doi.org/10.3141/2545-10

Mundrey, J.S., 2018. Indian railway tracks - A track engineering compendium, 5th ed. Dr. Frank August Wingler, Leverkusen, Germany.

Nålsund, R., Tutumluer, E., Horvli, I., 2013. Degradation of railway ballast through large scale triaxial and full scale rail track model tests - Comparison with mechanical laboratory tests. 15.

Qian, Y., Boler, H., Moaveni, M., Tutumluer, E., Hashash, Y.M.A., Ghaboussi, J., 2014. Characterizing Ballast Degradation through Los Angeles Abrasion Test and Image Analysis. Transportation Research Record 2448, 142–151. https://doi.org/10.3141/2448-17

Shih, J.Y., Thompson, D.J., Zervos, A., 2017. The influence of soil nonlinear properties on the track/ground vibration induced by trains running on soft ground. Transportation Geotechnics 11, 1–16.

Use of shredded scrap tyres in gabion wall construction

W. A. B. C. Desilva and U.P. Nawagamuwa
Department of Civil Engineering, University of Moratuwa, Sri Lanka

ABSTRACT: In this study, the applicability of gabion walls with shredded scrap tyres as a lightweight fill material is investigated. Scrap tyres are dumped throughout the world leading to health and environmental hazards because of limited reuse and recycle methods available. Nevertheless, such stockpiles of dumped scrap tyres could be effectively utilized in energy recovery or recycling methods. Henceforth, this study focuses on proposing a novel technique to use scrap tyres by shredding them and applying to construct earth retaining structures, namely, gabion walls. This suggested method enables to act as a lightweight solution of earth retaining structure that is ideal for resting on weak soil layers. The lateral displacement, vertical displacement and bulging patterns are tested for the shredded tyre included gabion units and the results are compared with `

1 INTRODUCTION

Scrap tyres are being dumped every day in large numbers around the world. Due to its' size and inherent inability to compress large portions of dumping sites are acquired by such scrap tyres. According to 2017 US Scrap Tire Management Summary (USTMA, 2018) 255.61 million of scrap tires are generated in US in 2017. According to USTMA scrap tyres are used to derive fuel, production of ground rubber and civil engineering applications mainly. In 2017 only 39 million tyres were disposed to landfills in US (USTMA, 2018). Derivation of fuel and recycling of rubber to by-products take up more energy whereas utilization for civil engineering applications require less energy for end product, which is beneficial in the long run.

According to CEA, 2.1 million tyres per year were imported and produced in Sri Lanka and no methods of disposal are found (CEA, 2005). In Sri Lanka waste tyre disposal is not being carried out properly which results in mosquito breeding grounds and inadequate space for tyre dumping. The tyre collects rainwater and maintains damp interior allowing the vermin to grow. Currently there is no proper practice to shred tyres before dumping which elevates the prevailing issues. There are few organizations where reuse and recycle of used tyre is done for industrial purposes, but many are dumped improperly.

The use of scrap tyre in civil engineering applications is gaining popularity as a solution for lightweight fill in embankments and economical earth retaining structures. Many studies have descriptively mentioned use of scrap tyres. The suitability of tire chips and sand as a lightweight fill material to be used in embankment fill or backfill of an earth retaining structure is studied in 1996 (Masad, 1996). A company, SULCAL Construction Pvt Ltd has obtained the patent for constructing a retaining wall using individual tyre units (Jayawickrama, 2000).

In 1994, several projects of shredded tyre and whole scrap tyre usage was mentioned descriptively (Drescher, 1994). In Riverside county whole scrap tyres were placed in a mat configuration in layers to work as a wind barrier. The use of scrap tyres as an embankment fill in Minnesota is also mentioned in Drescher (1994).

The above-mentioned reuse methods have evidently given a value to tyre waste. Nevertheless, the lightweight nature and the compressibility obtained by shredding the tyres, instead of using the tyre as a whole unit need to be investigated to arrive on innovative solutions for lightweight yet safe earth retaining structures. Thereby, this study is focused on evaluating the capacity of gabion structures constructed using shredded scrap tyres. A detailed calculation for the designed gabion structure is performed and consequently experiments are conducted to test the performance of the new gabion units.

2 OBJECTIVES

The focus of this study is to introduce a new technique for the effective utilization of shredded scrap tyres in civil engineering applications. Therefore, the objectives include designing of the shredded tyre gabion structure, evaluating the suitability of the shredded tyre gabion units by conducting packing tests and load-deformation tests, and finally to discuss the suitability of this proposed application.

3 METHODOLOGY

Firstly, the possibility of the inclusion of shredded scrap tyre pieces is checked using calculations done for a designed gabion wall retaining structure. Subsequently, the minimum unit weight per gabion unit (i.e. gabion box) is derived and the packing tests of gabion units with different sizes of tyre pieces and rock pieces are carried out. After finalizing on the suitable packing arrangement, physical testing is performed to obtain the deflection and bulging pattern of a gabion unit for a given stress. The testing was carried out for a standard rockfill gabion unit and a tyre included gabion box, such that a comparison can be done.

3.1 Calculations to obtain the minimum unit weight for the gabion unit

The gabion wall taken for the analysis is 3 units in depth and 3 units in height and is a stepped gabion wall with a backfill (Figure 1). The most critical soil properties are chosen for the backfill and basal soil for a conservative estimate. The arrangement of the units is selected to represent the most commonly used gabion wall type in Sri Lanka.

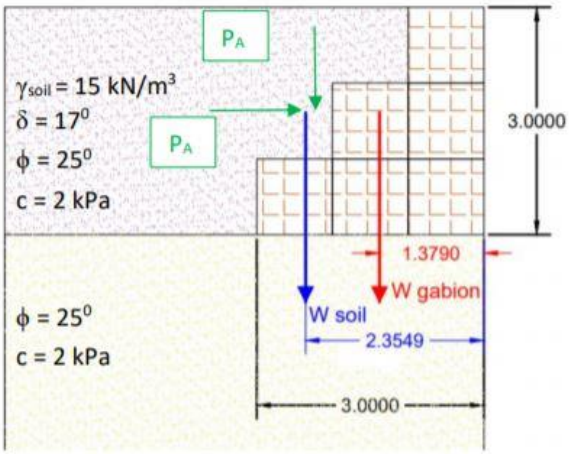

Fig. 1 Arrangement of the gabion structure selected for the study (PAV = Vertical force on the gabion structure, PAH = Horizontal force on the gabion structure, P'AV = Vertical pressure on the gabion structure, P'AH = Horizontal pressure on the gabion structure)

The calculation is carried out to ensure the factor of safety on sliding, factor of safety on overturning and factor of safety on bearing pressure is met.

A factor of safety of 1.5 was maintained for overturning while a factor of safety of 1 was maintained for sliding and bearing pressure. The factor of safety on bearing pressure was not taken as a critical value since with lightweight structure the factor of safety is increased.

$$tan\,\emptyset' = \frac{tan\,\emptyset_{max}}{1.2} \quad (1)$$

$$\emptyset' = 21.24^0$$

$$tan\,\delta_{design} = 0.75 \times tan\,\emptyset' \quad (2)$$

$$\delta = 16.25^0$$

$$P'_{AH} = \gamma\, z \times k_a \quad (3)$$

$$P'_{AV} = P_{AH} \times \tan\delta \quad (4)$$

FOS on sliding =

$$\frac{(6\gamma_g + 3\gamma_{soil}) \times tan\,16.25 + c \times 3}{P_{AH} \times 1} \quad (5)$$

FOS on overturning =

$$\frac{P_{AV} \times 3 + 6 \times \gamma_g \times 1.167 + 3 \times \gamma_{soil} \times 2.167}{p_{AH} \times 1} \quad (6)$$

FOS on bearing pressure =

$$\frac{q_{allowable}}{\sigma_v} \quad (7)$$

$$q_{allowable} = \frac{1}{2} \times B \times \gamma \times N_\gamma + c \times N_c \quad (8)$$

$$\sigma_v = \frac{R_v}{B} \times \left(1 + \frac{6e}{B}\right) \quad (9)$$

According to the analysis the minimum γ_g that can be obtained is 8.18 kN/m^3. A unit weight of 8.2 kN/m^3 was used for deciding the packing arrangement and carrying out the physical testing for the gabion unit.

The density of rock pieces used was taken as 2.86 g/cm3 and tyre pieces as 1.15 g/cm^3. The expected void ratio for the gabion unit was 0.3 - 0.4. The void ratio changed according to the packing arrangement, workmanship, and the sizes of tyre and rock used.

3.2 Determining the packing arrangement for the gabion unit

In order to get a unit weight of 8.2 kN/m^3 and a void ratio in between 0.3 - 0.4 the required weight of tyre and rock is obtained. To measure the void ratio and decide on a packing arrangement a glass box of 50 cm × 50 cm × 50 cm in dimension is taken. The displacement of water when placing rocks and tyre pieces is used to arrive at the void ratio.

Size for the rock pieces was taken as the largest dimension of rock in between 75 mm to 100 mm. First attempt was to shred the scrap tyres to 100 mm × 100 mm pieces and check the packing arrangement. At first the packing was done one layer by one layer of tyre and rock. The void ratio that could be achieved was 0.54. Since the void ratio was very high this arrangement could not be used. The second arrangement was to place tyre pieces in between rock pieces in one layer. The obtained minimum void ratio was 0.45 for this method of arrangement.

Since obtaining a void ratio of 0.3 - 0.4 was not possible using 100 mm × 100 mm the size of tyre pieces was reduced to 50 mm × 100 mm. Then a minimum void ratio of 0.4 was obtained in packing tyre pieces in between rock pieces (Figure 2).

Fig.2 Packing arrangement of shredded tyre and rock for a unit block

3.3 Load testing for the two gabion units

A gabion basket of 50 cm × 50 cm × 50 cm was prepared using the standard mesh. Then rock pieces were arranged in the gabion basket where the largest dimension is in between 75 mm to 100 mm. After the packing of the rock pieces apparatus was fixed for the loading and dial gauges were located around the gabion basket to obtain the readings of deflection (Nawagamuwa, 2012) (Figure 3)

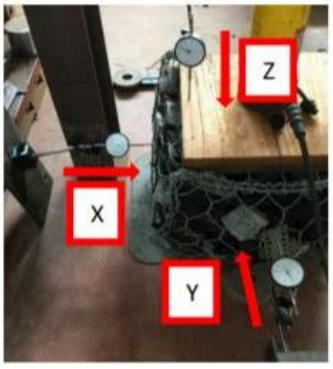

Fig.3 Dial gauges positioned around the shredded tyre included gabion unit

A similar apparatus was positioned to test the gabion unit filled with rock and shredded scrap tyres. The largest dimension of rock pieces was in between 75 mm to 100 mm and the dimension of tyre pieces was 100 mm × 100 mm. The pieces were arranged in the 50 cm × 50 cm gabion basket. Dial gauges were placed on three faces in order to read the deformation along x, y and z planes (Figure 3).

4 RESULTS AND DISCUSSION

4.1 Results obtained in the testing of standard rockfill gabion unit

The obtained results for the gabion box of 50 cm × 50 cm × 50 cm filled with rock pieces where the largest dimension was in between 75 mm to 100 mm is as follows. The load was applied in the z direction, where the x direction and y direction are perpendicular planes to z direction. The deformation of x direction and y direction are different since the gabion box had extra strengthening wire on the face of x direction. The stress was applied up to 200 kN/m^2 and the maximum deflection on x direction and y direction is 30 mm.

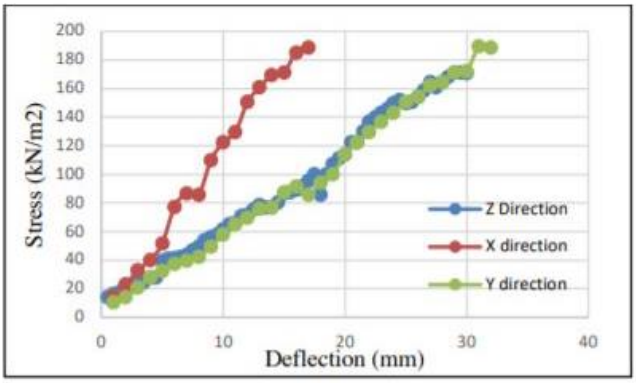

Fig.4 Stress vs deflection for x, y, and z directions in the standard rockfill gabion unit

4.2 Results obtained in the testing of shredded tyre included gabion unit

Similarly, to the standard rockfill gabion the same procedure was followed in analyzing the results for the tyre included gabion unit. The maximum stress that was applied to this gabion unit was 155 kN/m^2 since the deflection was excessive.

The load was applied to the z direction and similar to the previous testing the deflection of the face towards x direction and y direction displayed different deflections with the load application.

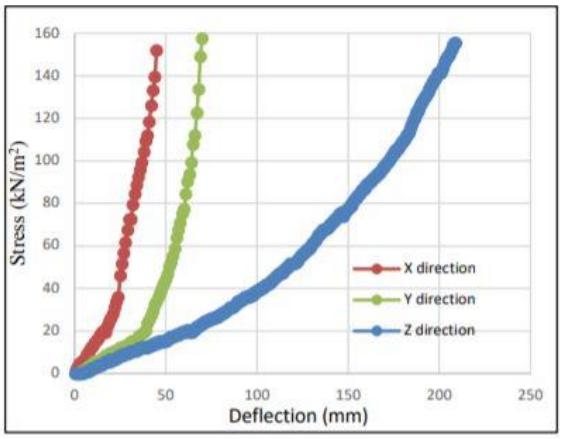

Fig.5 Stress vs deflection for x, y, and z directions in the shredded tyre included gabion unit

4.3 Analysis of results

The gradual bulking of the tyre included gabion unit for increasing stress conditions is displayed in figure 6.

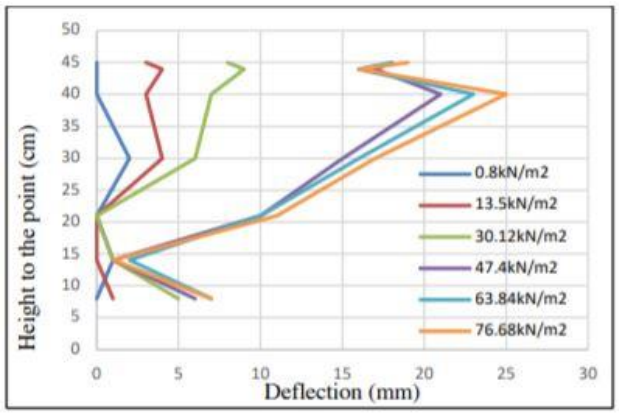

Fig.6 Height of the tyre included gabion box vs lateral deflection for shredded tyre included gabion box

Assuming the maximum deflection of the gabion unit can go up to the maximum deflection of the standard rockfill gabion box obtained in 150 kN/m^2 stress which is 9 mm. The stress levels the tyre included gabion box can be go up to a maximum of 30.12 kN/m^2 without exceeding the maximum allowed deflection. Hence in practical applications the tyre included gabion box will be capable of carrying the weight of 3 gabion units without exceeding the maximum allowable deflection.

5 CONCLUSIONS

This study focuses on the use of shredded scrap tyres in order to introduce a lightweight fill material for the gabion units. The minimum unit weight of a gabion unit is found out using the factor of safety calculations for the selected minimum unit weight.

According to the factor of safety calculations for the selected gabion structure with a 3 m height and a 3 m depth, it is concluded that one gabion unit can reduce the unit weight up to 8.2 kN/m^3. Approximately the unit weight with standard rockfill gabion unit is in the range of 15 kN/m^3 to 19 kN/m^3.

For the calculated minimum unit weight of the gabion unit, a void ratio of 0.4 is obtained from using 100 mm × 50 mm tyre pieces and rock pieces where the highest dimension was in between 75 mm – 100 mm. Shredded tyre included gabion unit could safely withstand 3 units of gabion units without excessive deformations.

In practice workmanship, packing arrangement and sizes of rock and tyre pieces decide the compaction of the gabion unit. Hence, it is essential to maintain the unit weight to be 8.2 kN/m3 with a void ratio of 0.3 - 0.4. If density of rocks and tyres are different from the used values, it is recommended to carry out additional experiments to check the suitability.

ACKONWLEDGMENT

My sincere gratitude goes to Dr. U. P. Nawagamuwa for guidance and support throughout the research project. I wish to express my gratitude to Dr. Praneeth Wickramarachchi of Access Engineering PLC for providing me resources for the experiment.
The assistance given by the technical staff of the laboratories in Department of Civil Engineering, University of Moratuwa is also acknowledged.

REFERENCES

United States Tyre Manufactures Association (2017). “2017 U.S. Scrap Tyre Management Summary.” < https://www.ustyres.org/sites/default/files/USTMA_scraptyre_su mm_2017_07_11_2018.pdf>

Technical Guidelines on Used Tyre Management in Sri Lanka, (2005), Central Environment Authority, Battaramulla, Sri Lanka

Masad E., Ho C.L., Taha R., and Papagiannakis A. T, (1996)., Properties of Tire/Soil Mixtures as a Lightweight Fill Material, Geotechnical Testing Journal, 19(3): 297-304

Drescher A., Newcomb D. (1994), “Development of Design Guideline for Use of Shredded Tyres as a Lightweight Fill in Road Subgrade and Retaining Walls”, University of Minnesota, Department of Civil and Mineral Engineering

Nawagamuwa U.P., Madarasinghe D.L., Goonathilake M.D.M.J., Karunarathna H.J.O., and Gunarathne M. 2012 Sustainable Reuse of Brownfield Properties in Sri Lanka as gabion fill material, Proceedings of ICBSE

COMPRESSIBILITY CHARACTERISTICS OF UNSATURATED SOILS

P.A.Y. Akalanka and S. A. S. Kulathilaka
Department of Civil Engineering, University of Moratuwa, Sri Lanka

ABSTRACT: Conventional consolidation theories are developed for saturated transported soils. Sri Lankan sub soil profiles contains mostly unsaturated residual soils that have different soil properties due to their different formation processes. Residual soils are more heterogeneous than transported soils and there is no stress history. Therefore, analysing the residual soils characteristics through the conventional consolidation theories are not reliable. In this research Consolidation characteristics of unsaturated remoulded samples brought to equilibrium at different matric suctions are studied with Rowe Cell and Oedometer. Techniques such as; Velocity method and Hyperbola method were used to analyse the results.

1 INTRODUCTION

Soils are mainly categorized under two categories according to their way of formation. Soils which are formed directly by the physical or chemical weathering of the parent rock and located above on its parent rock are called residual soils. When these residual soils get eroded, transported by various methods such as wind, water and deposited, then they are called sedimentary soils (a type of transported soil). These transported soils undergo various additional processes such as erosion, hardening, leaching, cementation, primary consolidation, secondary consolidation and produce old sedimentary soils from young sedimentary soils. Above process of transportation produces much homogeneous deposits due to the systematic sorting process. And sedimentary soils have stress history which is due to the further erosion and depositions of the soils (Wesley, 2010). It is the main factor in determining stage of the consolidation of the soil. But when considering the residual soils, it is more complex to analyse due to the absence of the homogeneity and stress history.

Except for homogeneity and stress history, there are several other reasons as well for the different properties of residual soil. In case of that, several analysis, concepts, and numerical models were proposed to analyse the compressibility characteristics of unsaturated residual soil.

2 METHODOLOGY

Considering non uniform nature and unsaturated state of residual soils, the test samples were prepared under remoulded conditions. Initially tests were done with the sample of saturated specimen which was prepared by mixing water at a water content greater than liquid limit. Then the saturated sample was brought to equilibrium under a specified matric suction in the pressure plate apparatus. Subsequently, tests were conducted on these samples.

As per the available literature, several methodologies were identified to determine the compressibility characteristics of unsaturated residual soil. Compression readings which were obtained with 24-hour long loading increments for each effective stress, were analysed by using Casagrande's method, Taylor's method, Velocity method and Hyperbola method. Soil compressibility parameters such as coefficient of volume compressibility (m_v), coefficient of consolidation (c_v), Compression index (c_c), and Recompression index (c_r) were obtained through the analysis and compared.

2.1 *Graphical Construction Methods*

Taylor's method and Casagrande's method are the usual graphical construction methods that are used in practice. Equation 01 is used to determine c_v using settlement-time curves.

$$c_v=(T_v \times H^2)/t \quad (1)$$

Where, Tv – Time factor H – Drainage path
t – Time

Settlement readings were plotted against log-time for each increment of load in Casagrande's method and settlement readings were plotted against root time in Taylor's method.

Velocity method and Hyperbola method do not require any graphical constructions as in Casagrande's method and Taylor's method. Therefore, those two methods avoid the complications present in the conventional methods of determining c_v due

to change of the shape of the curves at initial stages.

2.2 *Velocity Method*

This method compares the theoretical consolidation rate vs. time factor plot with the experimental settlement rate vs. time plot. Both axes should be in logarithmic scale (Parkin, 1978).

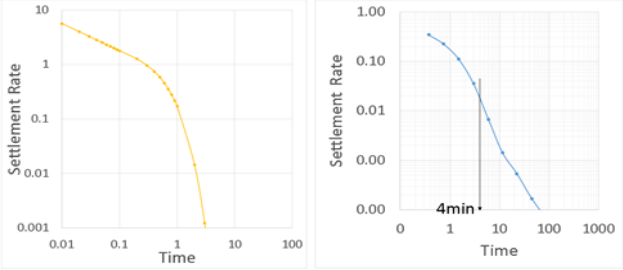

Fig. 1 Theoretical and experimental plots for Velocity method

To get the value corresponding to T=1 (100% consolidation), the theoretical curve should be superposed on the experimental curve after fitting a line with a slope of 2H:1V through initial points of the experimental curve.

$c_v=(1\times H^2)/t_{100}$ (2)

2.3 *Hyperbola Method*

Hyperbola method identifies that Terzaghi U-T relationship is a rectangular hyperbola over a wide range of T (Shukla et al., 2009). In this method, graph should be plotted in the form of t/u vs. t (Fig. 2) to obtain a straight line in between U=60% and U=90% (Prakash et al., n.d.). Slope (m) and intercept (c) should be measured to determine the c_v by using following equation.

$c_v=(0.24\times mH^2)/c$ (3)

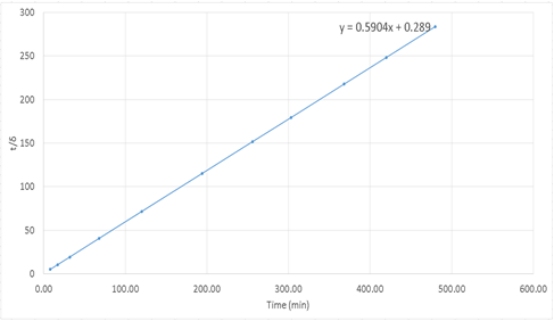

Fig. 2 Sample graph for Hyperbola method

3 EXPERIMENTAL PROGRAM

Consolidation tests were carried out by using both Oedometer and Rowe Cell for remoulded soil samples prepared. Since Rowe Cell apparatus accommodates much larger soil samples and has the ability of measuring pore water pressure and volume of expelled water, it is more advanced comparing to the Oedometer.

Unsaturated samples were prepared at different matric suction levels such as 25kPa, 40kPa, 50kPa. In these unsaturated sample and saturated sample tests were conducted with Loading, unloading and reloading steps. The increments are,

Loading – 25kPa-50kPa-100kPa-200kPa
Unloading – 100kPa-50kPa-25kPa
Reloading – 50kPa-100kPa-200kPa-400kPa

3.1 *Oedometer*

The standard Oedometer test is used to model the one-dimensional consolidation of a soil specimen. Settlement of a soil sample which is 50mm in diameter and 20mm in thickness can be modelled by this experiment. The soil sample is confined by the consolidation ring and two porous stones, allow drainage and settlement in the vertical direction.

3.2 *Rowe Cell*

Rowe Cell was introduced by Rowe and Barden in 1966. Diaphragm loading, pore pressure measurements, horizontal drainage, and minimized wall friction can be identified as the main features of Rowe Cell (Rowe & Barden, 1966).

The apparatus uses hydraulic pressure to apply the load on soil which is acting across a rubber diaphragm to maintain the uniformity of loading. The settlement is measured at the center of the sample by a dial gauge.

There are many advantages of Row Cell over the Oedometer such as, ability to measure volume of expelled water, ability to measure pore water pressure using pressure transducers, possibility of applying pressure up to 1000kPa, etc. (Rowe & Barden, 1966).

4 BASIC SOIL PROPERTIES

Table 1. Basic soil properties

Sand %	54
Fine %	39
Gravel %	07
Liquid Limit	46.45%
Plastic Limit	32.05%
Soil Classification	SC
Specific Gravity	2.696
Maximum dry density	1610kg/m^3
Optimum Moisture Content	20.2%

5 TEST RESULTS AND ANALYSIS

Settlement readings which were obtained by the standard Oedometer test and the Rowe cell test were used to plot void ratio vs. time graphs in fig. 3. Pore water pressure readings that were obtained by the Rowe cell test, were plotted against the time within the same axes (Fig. 4).

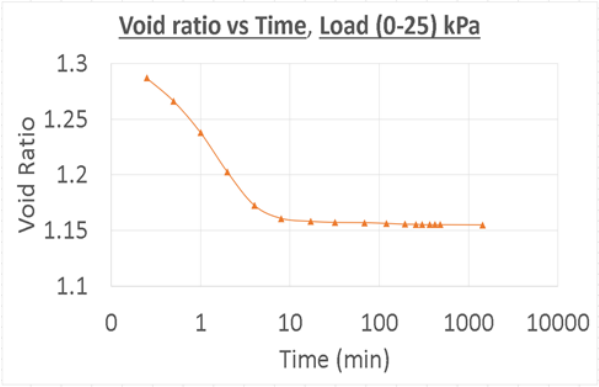

Fig. 3 Void ratio vs. time graph for Oedometer

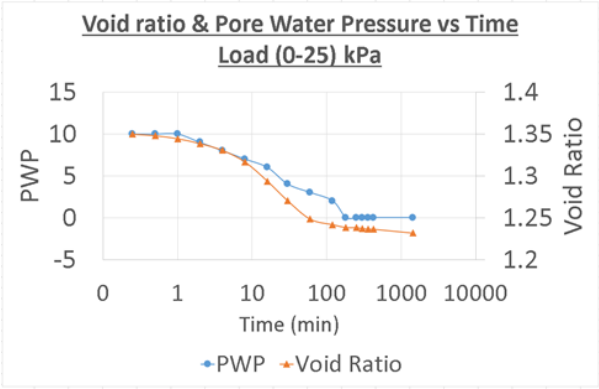

Fig. 4 Void ratio & PWP vs. time graph for Rowe cell

5.1 *Variation of Compression Index (c_c) and Recompression Index (c_r)*

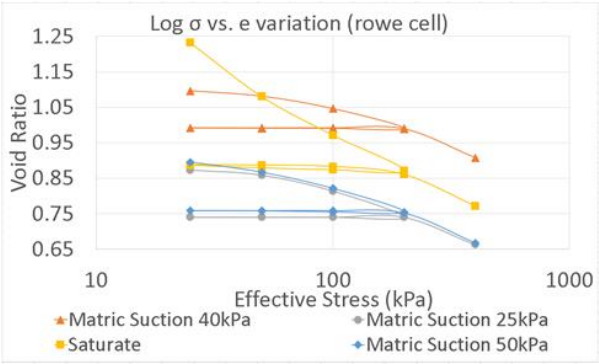

Fig. 5 Log σ vs. e variation (Rowe Cell)

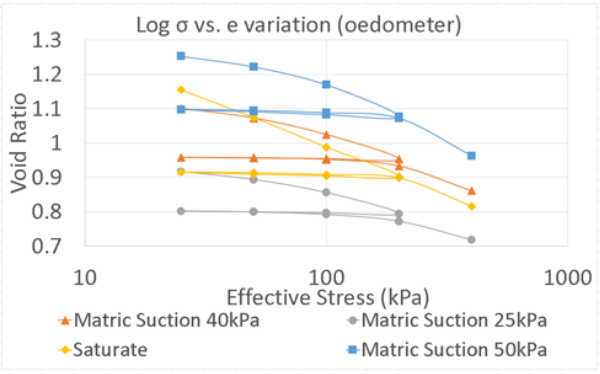

Fig. 6 Log σ vs. e variation (Oedometer)

5.2 *Variation of Coefficient of Volume Compressibility (m_v)*

Since coefficient of volume compressibility (m_v) is identified as a linear parameter, m_v is a better choice than the log parameters such as c_c and c_s when estimating settlements of soils (Wesley, 2010). Coefficient of volume compressibility values which were determined by analysing the experiment results are shown in fig. 7 for Oedometer and fig. 8 for Rowe Cell.

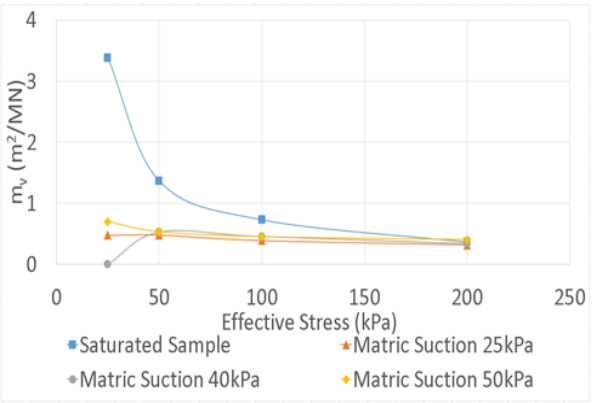

Fig. 7 m_v vs. Effective stress for Oedometer

The common observations are;

- m_v values decreases with stress increase
- m_v values for saturated sample were much higher at lower effective stresses
- m_v values of unsaturated samples with different matric suctions were at the same order
- m_v values obtained from Oedometer and Rowe Cell were at the same order

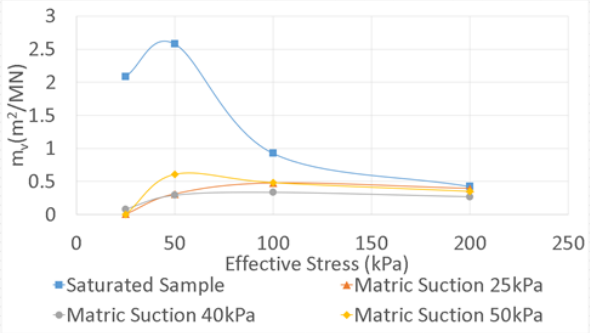

Fig. 8 m_v vs. Effective stress for Rowe Cell

5.3. *Variation of Coefficient of Consolidation (c_v)*

The settlement rate which the compression of the soil layer takes place is important in many of civil engineering projects. This rate can be determined by obtaining the value of coefficient of consolidation (c_v).

Since many factors affect c_v, the experimental behavior of soil in the one-dimensional consolidation test does not completely match with the theoretical relationship of consolidation as obtained by Terzaghi's equation, which is made use of in the curve fitting procedures (Sridharan & Nagaraj, 2004).

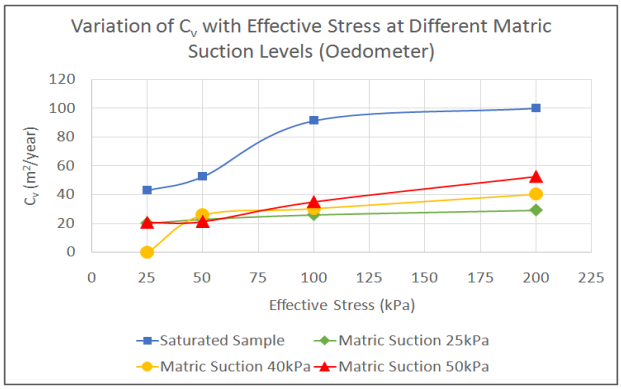

Fig. 9 C_v vs. Effective stress for Oedometer

As per the results, following facts can be concluded regarding the obtained c_v values.

- Test results obtained by the Rowe cell are generally higher than that computed by Oedometer.
- Most of the times velocity method gives lower c_v values than other three methods
- c_v values computed by hyperbola method show huge variations with the effective stress
- Most of the times c_v values computed by conventional methods behave in a similar way
- Obtaining c_v by root time method was easier than using log time method since initial part of the graphs were not necessary for the root time method
- Obtaining c_v values through Velocity method and Hyperbola method were easier than using the conventional methods which uses curve fitting methods for initial part of the graph.

6 CONCLUSION

Due to different properties of the Residual soil, it is more complex to be analysed by using conventional theories. Therefore, several other concepts, models should be adopted to determine the compressibility characteristics of Residual soil.

However, in this research the compressibility of unsaturated residual soils are assessed in the framework of Terzaghi's consolidation model.

Compression index (c_c) and Recompression index (c_r) decreases as the matric suction of soil sample increases.

All samples reach a similar m_v value at higher stresses and m_v values tend to decrease as the effective stress increases for most cases. m_v values for saturated sample shows higher values at lower effective stresses.

Different c_v values were obtained since four different methods have been used for the calculations. Most of the times velocity method gives lower c_v values than other three methods. c_v values computed by hyperbola method show huge variations with the effective stress and c_v values computed by conventional methods behave in a similar way at most cases.

ACKNOWLEDGMENTS

I would like to thank Prof. S.A.S.Kulathilaka for the immense support given to make the research project successful and I would also like to acknowledge the staff of Soil Mechanics Laboratory Mr.D.G.S. Vithanage, Mr. Ajith, Mr. Isuru Theekshana and Mrs.Pradeepa for their enormous support in conducting the laboratory tests.

REFERENCES

Parkin, A. K. (1978). Coeffcient of consolidation by the velocity method. Géotechnique, 28(4), 472–474.

Prakash, K., Murthy, N. S., & Sridharan, A. (n.d.). Rectangular hyperbola method of consolidation analysis. 37.

Rowe, P. W., & Barden, L. (1966). A New Consolidation Cell. Géotechnique, 16(2), 162–170.

Shukla, S., Sivakugan, N., & Das, B. (2009). Methods for determination of the coefficient of consolidation and field observations of time rate of settlement International Journal of Geotechnical Engineering,

Sridharan, A., & Nagaraj, H. B. (2004). Coefficient of Consolidation and its Correlation with Index Properties of Remolded Soils. Geotechnical Testing Journal, 27(5)

Wesley, L. D. (2010). Geotechnical Engineering in Residual Soils, Hoboken, N.J: Wiley

Establishment of Soil Water Characteristic Curves for Sri Lankan Residual Soils

W. K. Muthuhettige and S.A.S. Kulathilaka
Department of Civil Engineering, University of Moratuwa, Sri Lanka

ABSTRACT :All of the Sri Lankan slope failures are trigged by excessive rainfalls. Predicting threshold rainfall intensitiesis essential to identify the safety of slopes during the period of heavy rain. Soil Water Characteristic Curve (SWCC) which relate the matric suction prevailing to the moisture content in the soil is an essential tool in modelling the infiltration of rainwater into the slopes. The variation of permeability with moisture content can also be established with this curve. Therefore, it is important to establish soil water characteristic curves (SWCC) for different soil typeswith sufficient accuracy. There are several experimental methods to determineSWCC. In addition to that there are several empirical methods to derive SWCC. Fredlund and Xing method, Arya and Paris method and Zapata method are some suchempirical methods. Since experimental methods are quite elaborate and time consuming, with the comparison of results from twoapproaches, it would be possible to establishprocedures to use empirical methods with confidence.

Keywords: Soil Water Characteristic Curve, Matric Suction, Volumetric water content

1. INTRODUCTION

Soil water Characteristic curve can be defined as the relationship between the soil water content and the matric suction.Saturated soil has only two phases, soil and water. But unsaturated soil has air phase and air water interface in addition. Air water interface(contractile skin)can make a tensile pull in the soil behaving as anelastic membrane. It is under a tension applied through the soil. This phenomenon result in a greater air pressure than the water pressure.

Most of soil layer which are close to ground surface or drying environment, arein an unsaturated state. Most of the geotechnical engineering problems are found in unsaturated soil. The soil Water Characteristic Curve (SWCC) of a soil indicates how matric suction varies with the volumetric water content. It can also relate how the permeability will change with moisture content.

2. SOIL WATER CHARACTERISTIC CURVE

SWCC defined as the relationship between the matric suction and volumetric water content. Volumetric water content θw is the ratio between water volumesof the soil to the total volume. Hence SWCC illustrate the capability of retaining moisture in soil structure with the different matric suctions.Air entry value and the residual water content are the most important points in the SWCC.(Figure 1). As shown in figure1prior to air entry value, soil is saturated or nearly saturated. Beyondresidual water content value, there is very small amount of water remaining in the soil, and the effects of water content or negative pore-water pressure on soil behaviour may be negligible. In the study of rain induced slope failures, the focus will be between these two stages.

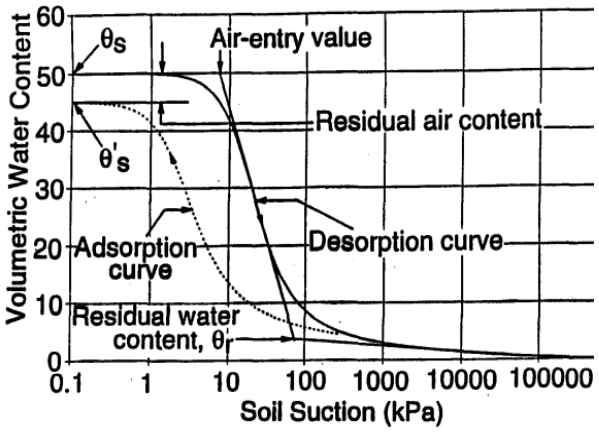

Figure 1: Idealized soil water characteristic curve

ESTABLISHMENT OF SOIL WATER CHARACTERISTIC CURVES.

Establishment of soil water characteristic curve is essential in modelling the infiltration of rainwater into slope. Research was started at University of Moratuwa to establish SWCC for different type of soils encountered in Sri Lankan slopes made of residual soils. Over the previous years some studies were done on soils with high fine content. In this research an attempt is made to establish SWCC for river sand and manufactured sand. These material will be used to form capillary barriers to minimise infiltration in a parallel research project.Manufactured sand obtained from crushing of rock and rock particlesare sieved through 1.18mm size sieve. Then two samples of coarse fraction and the fine fraction were obtained.

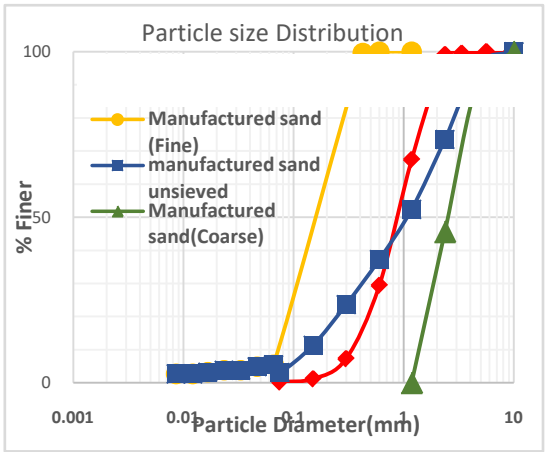

Figure 2: Particle sizedistributions

Particle size distribution curves for three different soil types are presented in Figure 2. Dry sieve analysis was carried for manufactured sand(coarse) and river sand. Both dry sieve analysis and hydrometer analysis was carried out for fine manufactured sand. All soil types are consider as non-plastic soil for the analysis of empirical method.

3. ESTABLISHMENT OF SWCC USING PRESSURE PLATE APPARATUS

A soil specimen can be brought to equilibrium under a specified matric suction in the pressure plate apparatus.The bottom of the apparatus has a high air entry disk under saturated condition and exposed to atmosphere (which is a pressure of around 100kPa). After closing the lid a desired air pressure is applied(u_a) and sample is brought to equilibrium under a (u_a-u_w) value where U_w=100kPa (Atmospheric pressure). At a given time three specimen can be placed in the apparatus. Specimen of three soil types were tested in the pressure apparatus. Test results of the pressure plate apparatus method are presented in the Figure 3.

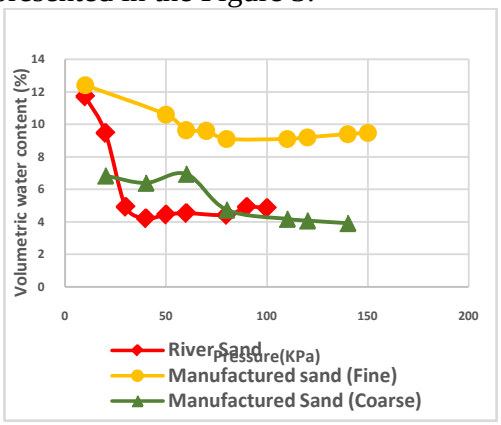

Figure 3: SWCCs from Pressure Plate Apparatus

4. ESTABLISHMENT OF SWCC USING METHOD OF CONTINUOUS MEASUREMENT

Matric suction of the soil is measured by a miniature tensiometerswhich developed at Kasetsart University, Thailand continuouslywhich connected directly to soil sample**.** This tensiometer is consisting of Micro Electro Mechanical 8 System (MEMs) pressure sensor, 1 BAR High-Air-Entry porous ceramic and transparent acrylic tub.Sample was compacted in a Perspex cylinder and apparatus was setup as the shown figure 4 Miniature tensiometers were setup in two places, top and middle layers of the cylinder for record the matric suction.Testing was carried out for both wetting and drying paths. In the drying test the sample was initially saturated and allowed to dry by evaporating into the atmosphere. In wetting curve, water drops added to the sample using a burette until the tensiometer reading comes its maximum value. Flow of water to atmosphere is measured by weight loss of the sample. Used web cameraforrecord the change of weight of the sample continuously.

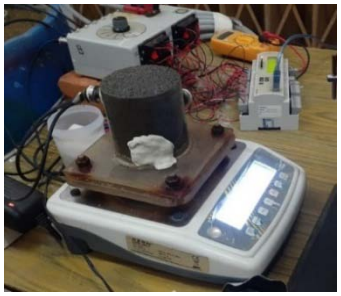

Figure 4: Soil sample connected with tensiometers

SWCCs were obtained for three types of soils in the method of continuous measurement are present in Figure 5.

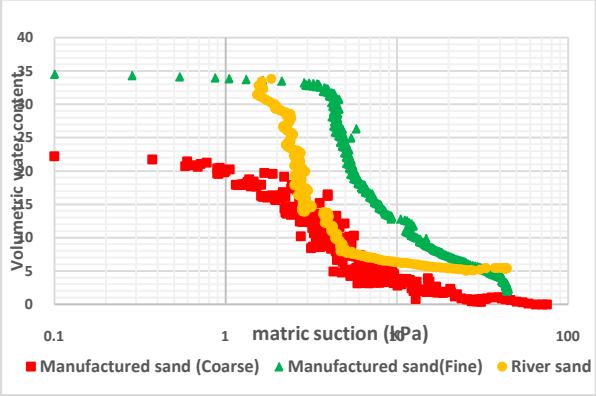

Figure 5 SWCCs from Method of continuous measurement

5. ESTABLISHMENT OF SOIL WATER CHARACTERISTIC CURVE USING FREDLUND AND XING METHOD

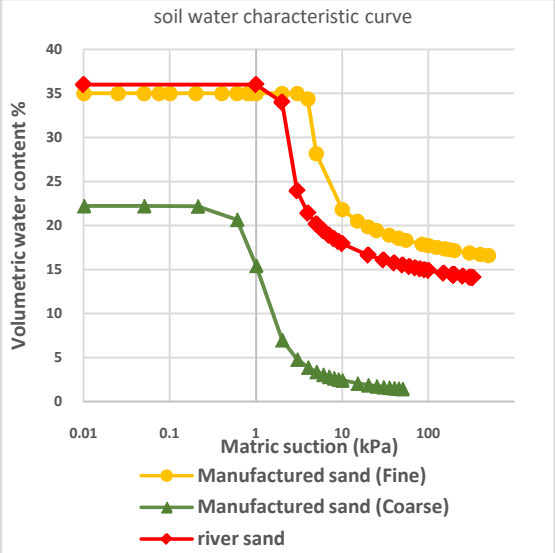

Fredlund and Xing (1994) has derived empirical equations to obtain soil water characteristic curve as to,

$$\theta = \theta_s \left[\frac{1}{\ln[e + (\psi / a)^n]} \right]^m$$

Θ=Volumetric water content
Ψ=Matric suction
Θs = Saturated volumetric water content
a, n, m = Fitting parameters obtained from predetermined SWCC from method of continuous measurement.

6. ESTABLISHMENT OF SOIL WATER CHARACTERISTIC CURVE USING ZAPATA METHOD

Zapata model(1999)is based on the particle size distribution and plasticity index properties. In this study all soil types were considered as non-plastic soil. There are certain set of equations to derive the fitting parameters using particle size distribution.

$$\Theta_w = C(h) x \left[\frac{\Theta s}{\left[ln\left[exp(1) + \left[\frac{h}{a} \right]^b \right] \right]^c} \right]$$

$$C(h) = \left[1 - \frac{ln\left[1 + \frac{h}{h_r}\right]}{ln\left[1 + \frac{10^6}{h_r}\right]} \right]$$

Θ_s=saturated volumetric water content
Θw=volumetric water content
a,b,c, hr = fitting parameters(Obtained from particle size distribution curve)

Obtained SWCCs for different soil types shown in figure 7.

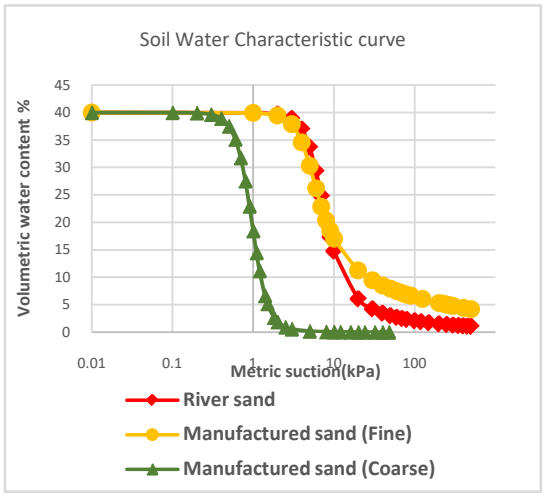

Figure 7: SWCCs from Zapata method

7. ESTABLISHMENT OF SOIL WATER CHARACTERISTIC CURVE USING ARYA AND PARIS METHOD

Arya and Paris (1981) has proposed a method to derive SWCC by using particle size distribution. In here particle size distribution is converted into pore size distribution. Pore radius for each matric suctions was obtained from numerical equation and that data was fitted for different soil types using α parameter. Fitting parameter α was obtained using the relationship graph.(Arya,1981)

Obtained SWCCs for each soil types as shown in figure 8.

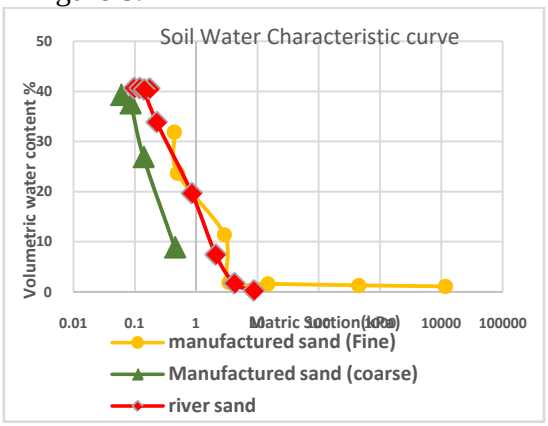

Figure 8:SWCCs from Arya and Paris method

8. COMPARISON OF RESULTS

Soil water characteristic curves derived for River sand, Manufactured sand (Fine) and Manufactured sand (Coarse) soils types from different methods are presented in figure 9 to11.

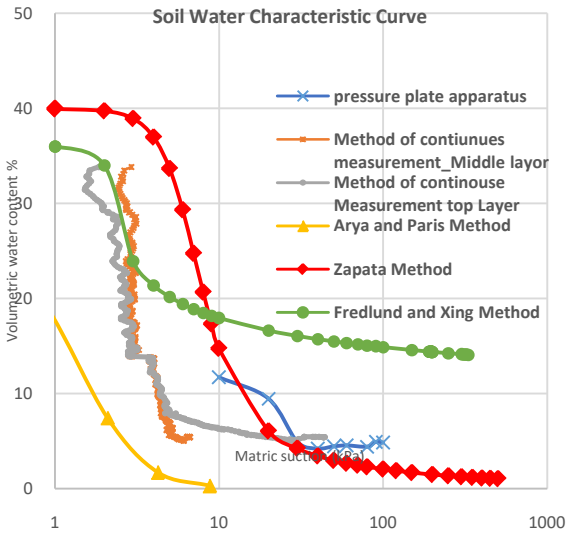

Figure 9: SWCC for Manufactured sand (coarse)

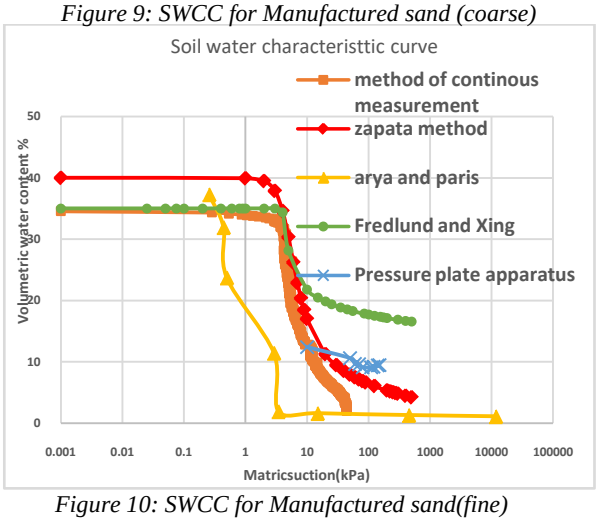

Figure 10: SWCC for Manufactured sand(fine)

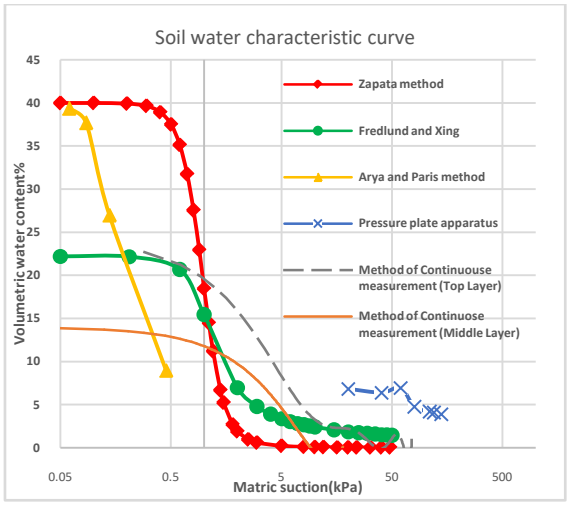

Figure 11:SWCC for undisturbed soil sample

This results shows that the air entry values are low.

9. CONCLUSION

Soil water characteristic curves from experimental methods are in reasonable agreement with the results of empirical methods. But, the three soil types are non-plastic and cohesion less, the matric suction variation between boundary effect zone and residual zone (Transition zone) is less than 10kpa. In pressure plate apparatus pressures in that low range cannot be applied. Method of continuous measurement with tensiometers, measure matric suction values lesser than 86kPa. Empirical methods by Zapata and Arya and Paris methods can extend to any high matric suction values. The results obtained from those empirical methods can be confirmed experimental methods.

REFERENCES

Arya, L., & Paris, J. (1981). A Physicoempirical Model to Predict the Soil Moisture Characteristic from Particle-Size Distribution and Bulk Density Data.

D.G.Fredlund. (1997). From Theory to the Practise of Unsaturated Doil Mechanics. *NSAT'97-3rd Brazilian Symposium on Unsaturated Soils.* Saskatoon, Sask, Canada .

Fredlund, M., Wilson, G., & Fredlund, D. (2002). Use of the Grain-Size Distribution for Estimation of the Soil-Water Characteristic Curve.

,.

Kulathilaka, S., & Dilanthi, H. (2017). *Shear strength and permeability characteristics of compacted residual soils in an unsaturated state.*

Kulathilaka, S., & Vasanthan, N. (2016). *Establishment of fundemantal characteristics of some unsaturated Sri Lankan residual soils.*

Investigation of the impact of the classification on integrity of bored and cast in-situ piles using Crosshole Sonic Logging (CSL®) test

A.G.K.P. Niwunhella and H.S. Thilakasiri
Department of Civil Engineering, Sri Lanka Institute of Information Technology, Sri Lanka

ABSTRACT: Integrity of bored and cast in-situ piles should be assessed thoroughly as tendency of occurring defects in such piles is higher due to improper construction methodologies. Crosshole Sonic Logging (CSL®) test is widely used in the industry to identify potential anomalies in order to ensure the quality and integrity of bored and cast in-situ piles. In this paper, several classification systems of bored piles based on CSL test results are identified and the effectiveness of each classification system is assessed towards the critical evaluation of pile integrity along with the assessment of anomalous regions, carried out using Tomography Analysis. The impact of the classification on the performance of piles using Tomographic Analysis is identified towards the acceptability of piles and potential reasons for the occurrence of defects are studied in Sri Lankan context.

1 INTRODUCTION

1.1 *Crosshole Sonic Logging (CSL®) test and Tomography Analysis*

Crosshole Sonic Logging (CSL®) test is a non-destructive pile integrity testing method based on transmission of an ultrasonic wave through concrete between two probes moved in pre-installed access tubes along the pile shaft. First Arrival Time (FAT) and Energy of the received signal are considered for the identification of the suspicious areas where the anomalies may be present in the pile shaft. Based on the delay of FAT and reduction in energy of the received signal, pile profiles are categorized according to the following universal pile profile categorization scale.

Table 1: Universal pile profile categorization scale

Category	FAT increase	AND/ OR	Signal reduction	Comment
G	Up to 10%	AND	< 6 dB	Good
Q	10 to 20%	AND	< 9 dB	Questionable
P/F	21 to 30%	OR	9 to 12dB	Poor/ Flaw
P/D	>30%	OR	>12 dB	Poor/ Defect

Though, CSL test reveals the existence of defects at a certain depth of bored piles, the capability is not sufficient to provide a comprehensive detail of the defect along the shaft in terms of its lateral extent and the exact location. Hence, the severity of the identified defect and its physical properties can be assessed using the Tomography Analysis. Tomography is generally defined as a mathematical simulation which provides 2-dimensional and 3-dimensional visual images of the defect along the pile based on the wave speeds obtained from the CSL test results. Basically, the pile is modelled and simulated as a grid with an assigned wave speed for each node determined from a mathematical solving algorithm of FAT along the pile depth. Tomography interprets the areas with less wave speeds in different colour schemes for easy identification of the lateral extent. The severity in terms of effective areas of the anomalies can be quantified as a threshold to assess the overall acceptability of the pile.

Based on the CSL test results, piles can be classified into several acceptance levels from worst to good condition implicating the pile integrity. Classification systems with different acceptance criterion based on the CSL test can be identified in test reports collected from the industry, from the expertise literature and the several standards around the world. It is important to study the effectiveness of different pile classification systems used in the industry based on CSL test. Huang (2018) identified a criterion for the classification of piles using CSL test under several standards around the world. Brown et al. (2010) proposed a methodology for the evaluation of defects and acceptance criteria on piles with a graphically illustrated approach.

Likins et al. (2007) carried out a study using a pile shaft with intentionally built defects and it was

shown that the defects were successfully identified with CSL and Tomography analysis. Paikowsky et al. (2000) conduted a successful programme on identifying the integrity of four piles with intentionally built defects using Pile Integrity Sonic Analyzer (PISA) along with the Tomography analysis.
The integrity of abutment foundation on Jacu-Pêsego viaduct in Brazil was thoroughly assessed using the fruitful collaboration of CSL and Tomography by Beim et al. (2005). However, it is widely known fact that the CSL measures the integrity of the pile inside of the reinforcement cage.

2 METHODOLOGY

CSL test and Tomography analysis reports on twenty five bored and cast in-situ piles were collected for the interpretation. Then, three classification systems which are integrated with pile acceptance criterion were identified from the test reports and expertise literature surveys. Key differences of the classification systems and their potential impact towards the pile acceptability were identified.

The data interpretation was carried out by classifying the collected pile sample under the different classification systems. Thereafter, the acceptability of the pile was determined in accordance with the results of Tomography Analysis. A quantitative and qualitative analytical approach were used to determine the most accurate classification system which provided the reliable prediction on the acceptability of piles according to the Tomographic analysis of the CSL profiles. The impact of the anomaly distribution along the pile shaft on the acceptability of pile was investigated. Moreover, the impact and contribution of the Tomographic analysis towards the acceptability of the piles were determined.

3 RESULTS

3.1 Identified classification systems

Following three classification systems of piles in Tables 2, 3 and 4 which were considered in the test reports sample were identified and adapted for the result interpretation.

Table 2 : Classification system 01

Rating/ Class	Criteria
A	Acceptable piles, majority of profiles falls to Category G.
B	Questionable (Q) profiles require no further action but may be considered when P/F or P/D also occurs in the same cross section.
C	Flaws (P/F) should be addressed if they are indicated in more than 50% of the profiles.
D	Defects (P/D) must be addressed if they are indicated in more than one profile and involving at least 3 tubes.

Table 3: Classification system 02

Rating/ Class	Criteria
1	Piles with majority of good profiles (G) and Q, P/F or P/D will be classified as acceptable.
2	Piles with a majority of doubtful (Q) profiles will be classified as acceptable. But they will be recommended for further analysis and remedial action if required when P/F or P/D also occurs in the same transverse direction.
3	Piles with flaws (P/F) in the same transverse cross section in more than 50% of the profiles will be recommended for further analysis and will require remedial action.
4	Piles with defects (P/D) indicated in more than one profiles involving at least three tubes will be recommended for remedial actions.

Table 4: Classification system 03

Rating/ Class	Criteria
1	Piles with majority of good profiles (G) and Q, P/F or P/D will be classified as acceptable. (Acceptance Level 01)
2	Piles with majority of doubtful (Q) profiles will be recommended for further analysis and remedial action if required. (Otherwise this category is an acceptable category). (Acceptance Level 02)
3	Piles with flaws (P/F) in more than 33% of the profiles will be recommended for further analysis and will require remedial action. (Acceptance Level 03)
4	Piles with defect (P/D) indicated in more than 33% of the profiles in will be recommended for remedial action. (Acceptance Level 04)

3.2 Classification of piles

Refer Table A-1 in Appendix A for the summarized data interpretation of sample of twenty five piles.

Classification of the piles in the sample was based on the integrity of the concrete area within the rebar cage of the pile.

4 DISCUSSION AND ANALYSIS

In classification system 01 as shown in Table 2, the localization of P/D anomalies in the same cross section is considered for the class D acceptance criterion which is critical. Piles are classified as class C when more than 50% of the profiles fall into P/F category. It implies that acceptance criterion of class C is based on the distribution of anomalies.

According to Table 3, the criterion for class D of classification system 02 is identical to the criterion of classification system 01. Also, it can be identified that the localization of anomalies in cross sections is considered for class C criterion. Also, piles are classified as class B, when majority of profiles fall into Q category. And, further actions will be recommended if P/F or P/D profiles exists on the same cross section which is more critical for the integrity.

Acceptance criteria of classification system 03 comprises with considerably different considerations compared to classification systems 01 and 02. According to Table 4, piles are classified as class D, when P/D profiles are indicated in more than 33% of the profiles. The distributed presence of P/D profiles along the shaft is considered which is critical during the evaluation, as the severity of P/D profiles are fairly high. Also, piles are classified into class C, when P/F profiles are indicated in more than 33% of the profiles which indicates the distributed presence of P/F profiles. It is more conservative than other systems, as it allows 33% of profiles with flaws (P/F) for the consideration where other two systems are based on 50% of profiles.

It can be identified that classification system 03 in Table 4 is comparably conservative than the other classification systems. In classification system 03, the acceptability of the piles in both level 3 and 4 are critical, due to the consideration of less P/D and P/F profiles in the acceptable criteria.

88% of the piles in the sample with localized presence of anomalies within the same transverse cross sections are determined as unacceptable. It reflects that localized presence of the anomalies within cross sections enhances its severity and results in the overall unacceptability of the pile.

According to Table A-1 in Appendix A, it can be identified that 64% of piles in the sample are considered unacceptable based on the effective areas of anomalies from Tomography. The class wise allocation of twenty five piles in the sample for each classification system can be identified as follows.

Table 5: Class wise allocation of pile sample

Classification system	Class wise allocation			
	Class A/ 1	Class B / 2	Class C/ 3	Class D/ 4
Classification system 01	-	01	04	20
Classification system 02	01	01	04	19
Classification system 03	02	03	01	19

It can be observed that majority of twenty five piles are classified as class D under all three classification systems according to Table 5.

Following observations are also made in accordance with Table 5 and Table A-1 in Appendix A. In classification system 01, the overall integrity of 25% of piles in class C and D are determined as acceptable, based on the effective area from Tomography analysis. 30 % of piles in class 3 and 4 are considered acceptable in classification system 02. Also, in classification system 03, 20% of piles in class 3 and 4 are determined as acceptable from Tomography. It indicates that classification system 03 has a lower percentage on predicting inaccurate acceptance using CSL test results.

Severity and extent of the identified anomalies were evaluated from Tomography analysis by using 2D and 3D images of both longitudinal and transverse sections. Final acceptability of each pile was concluded based on the effective area of anomalies. Several piles which are initially considered as unacceptable in classification systems were considered as acceptable based on the effective areas of anomalies from Tomography analysis. It reflects the significance of the Tomography analysis towards mitigation of the unnecessary further analysis and remedial actions. Fig. 1 shows the accurate contribution of each classification system on predicting the overall acceptability of the piles in the sample.

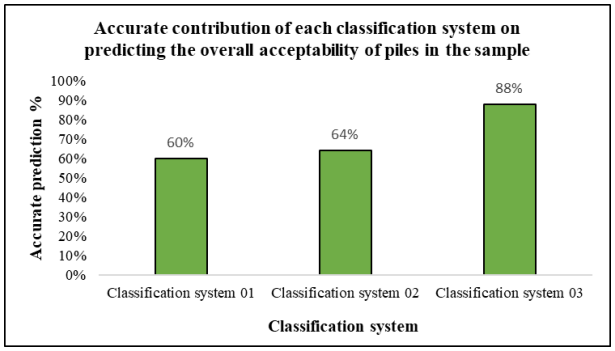

Fig. 1 Accurate contribution of each classification system on predicting the overall acceptability

According to Fig. 1, classification system 03 has a considerable accuracy and effectiveness on predicting the overall acceptability of piles. The use of the conservative approach during the interpretation anomalous profiles in classification system 03, may have increased the potential of predicting the pile integrity accurately.

It was identified that 80% of the piles in sample indicated major defects in the toe region with unacceptable integrity, which may have occurred due to the improper quality control measures taken during the construction rather than the natural causes. The main reason for the soft toe condition can be considered the due to the presence of soil and other debris in the bottom region which are not subjected for proper cleaning prior to the concreting work of the pile.

Rest of the piles indicated the occurrence of intermediate defects along the pile shaft. Such defects are likely to occur due to the delay in the arrival of concrete trucks. When the consecutive concrete truck is delayed, the tremie pipe should be taken out and kept back again to commence the concrete work after the arrival of truck. Concrete in the pile will be hardened and generation of air voids will be increased during the delay time causing anomalies in the region.

5 CONCLUSIONS

Classification system 03 in Table 4 has provided more accurate and reliable interpretation on predicting the acceptability of the piles using CSL test results. The application of conservative acceptance criteria based on the severity, distribution and frequency of anomalies has increased the potential accuracy of classification system 03.

Tomography analysis has imposed a major impact on the performance of pile by accepting the piles which are initially considered unacceptable from classification systems. Such piles are evaluated to ensure the presence of adequate integrity using the effective areas of anomalies. It mitigates the potential of taking the unnecessary remedial actions and the additional cost regarding the further analysis.

This distribution and localization of the anomalies impose a certain impact on the severity of the anomalies. Piles with localized anomalies within the cross sections are likely to be unacceptable as it enhances the severity. Also, the distributed presence of anomalies along the shaft imposes a less influence on the severity. And, those pile are likely to be acceptable except the considerable distribution of Poor/Defect (P/D) anomalies which denotes a severe condition.

Majority of the defects in bored and cast in-situ piles in Sri Lanka are occurred at toe region due to improper quality control measures. Intermediate defects along the pile are likely to occurred due to lack of planning. Hence, thorough quality control measures should be maintained during the pile construction in order to mitigate the occurrence of defects in piles.

ACKNOWLEDGMENTS

The authors would like to convey their sincere gratitude to Piletest Consultants (Pvt) Ltd. for the provision of the field data and the assistance to carry out the study successfully.

REFERENCES

Beim, J.W., Debas, L.F., Kormann, A.C.M., Martinati, L.R. and Neto, L.A. (2005). Tomography: A New Technology for Quality Control of Deep Foundations, GEO3 Construction Quality Assurance/Quality Control Technical Conference: Dallas/Ft. Worth, TX, pp.323-328

Brown, D., Turner, J. and Castelli, R. (2010). Drilled Shafts: Construction Procedures and LRFD Design Methods, NHI Course No. 132014, Geotechnical Engineering Circular No. 10, Report No. FHWA-NHI-10-016, Federal Highway Administration, Washington, DC.

Huang, K., (2018). A research for Class II defect Bored Pile's Accept Criteria; A case of Penang Second Marine Bridge, IOP Conference Series: Earth and Environmental Science, Volume 128, p. 012080.

Likins, G., Rausche, F., Webster, K. and Klesney, A. (2007). Defect analysis for CSL testing, Geotechnical Special Publication No. 158, American Society of Civil Engineers: Reston, VA.

Paikowsky, S. G., Chernauskas, L. R., Hart, L. J., Ealy, C. D., and DiMillio, A. F. (2000). Examination of a New Cross-Hole Sonic Logging System for Integrity testing of drilled shafts, Proceedings of Sixth International Conference on the Application of Stress-Wave Theory to Piles, Niyama S. and Beim J. edt, pp. 223-230.

APPENDIX A

Summarized classification of the pile sample

Interpretation of data including the classification of twenty five piles under all three classification systems with overall acceptability based on the minimum effective area from Tomography analysis can be summarized as follows,

Classification of the piles in the sample was based on the integrity of the area within the rebar cage of the pile.

Table A-1: Classification of the pile sample

Pile No	Pile classification			Tomography Analysis		Overall pile acceptability based on Effective area from Tomography	Accurate Classification system
	Classification system 1	Classification system 2	Classification system 3	Identified Anomalous region	Minimum Effective area of the cross section		
1	B	1	1	2.09m	99%	Acceptable	3
2	C	3	4	13.63m to 16.42m	51%	Not acceptable	3
3	D	4	4	18.60m to 19.0m	89%	Acceptable	None
4	D	4	4	18.25m to 19.10m	44%	Not acceptable	All
5	C	3	2	0.32m-0.38m	87%	Acceptable	3
6	D	4	4	17.50m to 18.5m	63%	Not acceptable	All
7	D	4	4	14.8m to pile toe	3%	Not acceptable	All
8	D	4	4	14.9m to 15.5m	38%	Not acceptable	All
9	C	3	4	14.1m to pile toe	2%	Not acceptable	3
10	D	4	2 & 3	11.5m to pile toe	71%	Not acceptable	All
11	D	4	4	7.18m to pile toe	70%	Not acceptable	All
12	D	4	4	12.0m to pile toe	0%	Not acceptable	All
13	D	4	4	11.75m to pile toe	0%	Not acceptable	All
14	D	4	4	18.0mto 18.60 m	52%	Not acceptable	All
				21.2m to 21.3m	31%		
15	D	4	4	0.0m-0.94m	62%	Not acceptable	All
				8.8m to pile toe	37%		
16	D	4	1	17.2m to 17.3m	95%	Acceptable	3
17	D	4	2	19.1m to 19.9m	90%	Acceptable	3
18	D	4	4	2.01m to 2.22m	79%	Not acceptable	All
19	C	2	2	16.2m to 16.7m	81%	Acceptable	2 and 3
20	D	4	4	1.35m to 2.2m	92%	Acceptable	All
				3.8m to 4.42m	92%		
				16.78m to pile toe	85%		
21	D	4	4	5.2m to 5.87m	53%	Not acceptable	All
22	D	4	4	13.54m to 13.89m	82%	Acceptable	All
23	D	4	4	6.5m to 6.8m	36%	Not acceptable	All
24	D	4	4	7.33m to 8.23m	80%	Acceptable	None
25	D	3	4	7.10m to 7.94m	54%	Not acceptable	All

Accuracy of commonly used pile integrity testing methods in Sri Lanka

T.V. Sanjula and H.S. Thilakasiri
Department of Civil Engineering, Sri Lanka Institute of Information Technology, Sri Lanka

ABSTRACT: In Sri Lanka, the use of pile foundations has amplified, with the rapid construction of high-rise structures. Construction difficulties and improper quality control measures cause anomalies in pile shaft which reduces the load-carrying capacity. Among various integrity determination methods available, Pile Integrity Test (PIT®), Pile Driving Analyzer (PDA®), Cross-hole Sonic Logging (CSL®) and pile coring are the most commonly used procedures in Sri Lanka. In this paper, test results of bored and cast-in-situ piles in different development projects in Sri Lanka were collected and analyzed to identify the capabilities and accuracy levels of different testing methods. In this respect, the accuracy of identifying the defect, severity and location of the defect of CSL tests were investigated by comparing with tomographic analysis and coring results. Limitations of PIT and PDA were identified by comparing with CSL, tomographic and/or coring of piles. Finally, reliability of the different testing methods was summarized.

1 INTRODUCTION

At present, pile foundations which are in the category of deep foundations have achieved a wide utilization in the industry, as it provides high bearing capacities and in need of less earthmoving than shallow foundations. Generally bored and cast-in-situ piles have the tendency of containing anomalies due to complications in the construction process. Hence it is vital to carry out necessary testing procedures to identify the defects present in the pile shaft. There is a wide range of available testing methods to evaluate the integrity of the piles. Among various non-destructive testing methods available, small strain dynamic testing using Pile Integrity Test (PIT), Cross-hole Sonic Logging (CSL) test, Tomographic Analysis and large strain dynamic testing using Pile Driving Analyzer (PDA) are most common in Sri Lanka as they are economical, user-friendly and time saving when compared to other similar methods. The conventional method of coring of the pile shaft, which is a destructive method of testing is also conducted to confirm the defects. Proper apprehension of prerequisites, limitations and thorough planning for conductance of these tests are important to obtain accurate evaluation on the pile integrity.

It is the common practice in the industry to conduct different integrity determination methods for the same pile profile when the obtained results are of unsatisfactory levels. The results of some of the considered tests subject to variation in different situations. Hence it is important to identify the causes for the deviations in order to evaluate the accuracy in the output result.

White et al. (2008) have tested 66 friction pile shafts using the CSL and PIT where they have indicated both similar and contradictory results. Likins et al. (2007) have also presented a case where the accuracy of CSL and effectiveness of tomography analysis has been confirmed by testing of a pile with purposely designed defects. Rausche (2004) has identified that pulse-echo method of PIT has disregarded the small defects in piles which are between 1% to 5% of the pile cross sectional area and that the CSL has identified the defects more precisely but is only limited to the area between the two access tubes. A study done by Massoudi and Teferra (2004) has appraised three case histories where PIT has been conducted to identify the anomalies present in different types of pile shafts and has concluded that PIT successfully matches with results of static load test in one of the cases. These various interpretations in the literature denote the unpredictable nature of the integrity determination methods, in different situations.

A more comprehensive analysis based on the potential capability of the PIT, PDA, CSL, Tomography Analysis and pile coring to identify the anomalies in the pile shaft is presented through this paper.

2 METHODOLOGY

Field data on piles subjected to different testing methods were collected and the data were sorted and arranged. Velocity records of the piles from the PIT, CASE method and CAPWAP method results of PDA, the waterfall diagram records from the CSL, Tomographic analysis results of corre-

sponding CSL and the coring data were acquired for analytical purposes, as available. The obtained data were sorted, arranged and compiled for concise data presentation, and overall data on thirty piles were obtained. Then, the test results of different integrity determination methods conducted to the same pile were compared and analyzed to identify the similarities, diversions and possible causes for variations in the results. Through the interpretations of the analysis, the accuracy levels of each integrity tests were evaluated. The limitations of the tests were identified through the analyzed data samples.

3 RESULTS

Field data on piles which have been subjected to two or more integrity determination methods has been obtained and the indicated data were evaluated to identify the similarities and differences in the results. The piles were categorized as follows,

i. Category A : Piles with confirmed defects
   - Combination 1 : Coring and CSL®
   - Combination 2 : Coring and PIT®

ii. Category B : Piles with semi verified defects
   - Combination 3 : CSL® and PIT®
   - Combination 4 : CSL® and PDA®

For the Category A, piles which have been subjected to coring were considered, as it provides clear visualization and confirmation of the defects present in the pile shaft.

For Category B, piles which have been subjected to CSL were considered, as the results interpreted from the CSL does not provide direct confirmation of the anomalies in the pile shaft. The interpretations from CSL results may have some uncertainty.

4 DISCUSSION

Field data on thirty piles which have been subjected to two or more of integrity evaluation methods from Pile Integrity test, Pile Driving Analyzer, Cross hole Sonic Logging test, Tomographic Analysis and pile coring have been evaluated. The field data were compared to identify whether the tests have accurately indicated the integrity of the piles. In most of the piles, the obtained data has denoted some contradiction in the final result. The quantity of piles regarded for each category and combination are presented in Table 1.

Table 1. Percentage of piles considered for each category and combination

Category	Combination	Percentage of piles in each combination	Percentage of piles in each category
A	Coring and CSL®	6.67%	10%
	Coring and PIT®	3.33%	
B	CSL® and PIT®	40%	90%
	CSL® and PDA®	50%	

By evaluating the obtained data of the pile sample, it could be observed that majority of the piles indicate the defective zone in or near the toe region of the pile. This confirms that proper cleaning and concreting of the pile toe is critical in the initial stage of pile construction. Hence, implementation of necessary quality control measures is highly recommended during construction.

The destructive method of pile coring can infer inaccurate interpretations on pile integrity when the drilled hole is not kept vertical. Even a small tilting can result misinterpretation of depths of the defects. The PIT identifies defects by the response of the pile to an impact on the pile head. To obtain accurate results and depths, it is important to receive a clear toe response in velocity records. But due to various site conditions there could be a contrast in depths to defects in different testing methods. Hence, when comparing test results of integrity tests conducted to the same pile profile, if the anomalies present in the pile shaft indicates within ±1.25m in length of one another, it was considered as “similar interpretations” in results. This allowance was adapted to consider the above-mentioned errors that can occur in the tests.

Defect interpretation ability of pile coring can be considered as a more precise approach of integrity determination if the verticality of the drilled hole is maintained. As the length of the drilled holes of piles in Category A have matched with the pile length, it can be interpreted that the output data from coring are precise.

Considering Category A - Combination 01, the two piles subjected to both coring and CSL have shown similar interpretations of the anomalies present in the pile shaft. The precision in the data interpretation ability of CSL has been confirmed by the pile coring as visualization on the defects at the indicated depth has been obtained. This proves that the accuracy of CSL and tomography are fairly high. But the evaluation of the pile integrity is limited to the concrete between the access tubes of the pile.

Conferring to the above case, it could be observed that the CSL interpretations of the consid-

ered piles are accurate. Hence, for further evaluation of test results of other integrity determination methods, it could be regarded that CSL provide considerably accurate data interpretations. But the certainty of the precision of CSL test results are lower than coring data.

In regard to Category A - Combination 02, the coring and PIT data have provided contradictory interpretations. This case opposes the ability of PIT on accurate data interpretations.

The Piles in Category B - Combination 03, has shown both similar and contradictory interpretations of PIT test results as illustrated in Fig. 1.

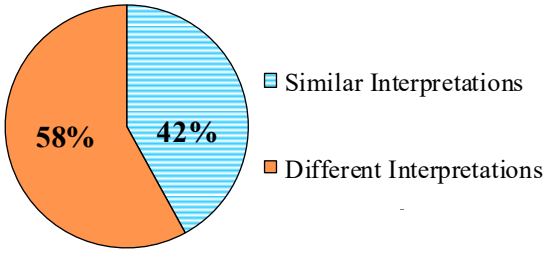

Fig. 1 Comparison of test results from PIT and CSL

As it is regarded that the CSL data provide more accurate interpretations, this demonstrates the inability of PIT to properly identify the defects in the pile shaft in certain cases.

Fig. 2 demonstrates that out of 58% piles where PIT have shown different interpretations to the corresponding CSL test results, 57% have not indicated a clear toe response in the velocity record of the pile. These data support that the precision of data interpretation in PIT is affected by the inability of the stress wave to reach the toe level of the pile.

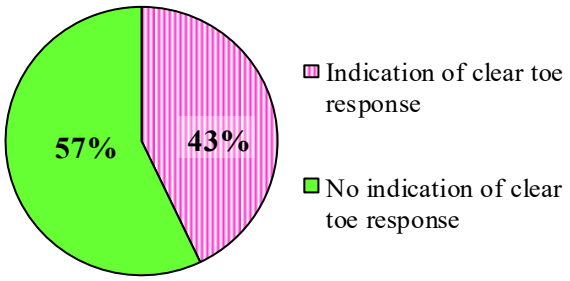

Fig. 2 Effect of toe response in contradictory data interpretations of PIT

This phenomenon mainly occurs when the soil resistance along the pile shaft and the length of the pile is fairly high. Also, when a large anomaly in the shaft is present following with a considerably small defect, the reflection of the stress pulse due to the large anomaly might mask the reflection due to the small defect. Moreover, in some cases, the defects near the pile top have not been indicated in the velocity record, which may occur due to the masking effect, where the anomaly contains within the impact pulse. As a remedial action for these cases, selection of a suitable hammer which will generate an adequate stress wave could be recommended.

Considering the fifteen piles belonging to Category B, Combination 04, the PDA test results have indicated some contradictory results than CSL by both case method and CAPWAP method or by one of the methods.

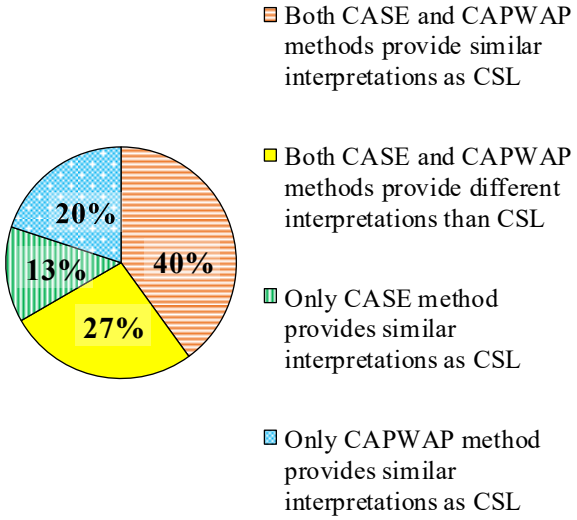

Fig. 3 Comparison of test results from PDA and CSL

Regarding Fig. 3, 73% of the piles have shown similar results to CSL by either one of CASE method or CAPWAP method, or by both methods. Hence, it could be interpreted that PDA shows considerably high accurate levels with respect to the considered pile sample. From Fig. 3 it is clear that,

- Probability of CASE method in defect identification = 53%
- Probability of CAPWAP method in defect identification = 60%

Hence, from the considered sample it can be evaluated that in PDA, CAPWAP method has higher probabilities in defect identification than CASE method.

When comparing data interpretation ability of PIT and PDA in Figs 1 and 3, it could be observed that PDA has presented high percentage of similar interpretations than PIT when compared with CSL data. Hence it can be regarded that the PDA have shown more accuracy than PIT.

Accordingly, from the evaluation of the above field data, an understanding of the accuracy of the

tests in some of the circumstances could be obtained.

5 CONCLUSION

The piles analysed in the research demonstrate cases where each considered testing methods have presented both similar and contradictory results which represent its accuracy.

As majority of the piles indicate defects near the pile toe region, it can be considered that proper pile toe construction is critical in the initial stage.

With respect to the considered pile sample, it could be regarded that CSL along with tomography analysis has provided more accurate interpretations of the anomalies present in pile shaft. The accuracy of CSL results has been confirmed by coring data.

Where PIT and coring has been conducted to the same pile, PIT has been unable to confirm the defect, resulting in uncertainty on the accuracy of PIT in certain cases.

From the evaluated test results, it is evident that PDA has shown high accuracy levels in results interpretation than PIT when compared with CSL data.

In cases where PIT has indicated contradiction to the corresponding CSL, it could be observed that majority of the piles have not shown a clear toe response.

When considering CASE method and CAPWAP method of PDA, the CAPWAP method has exhibited high probabilities of accuracy when compared with corresponding CSL data.

Consequently, it is clear that a better understanding of the defects present in the pile shaft can be obtained by utilizing a combination of integrity determination methods, rather than conducting an individual test for a pile. For the selection of a suitable testing method and result interpretation, the limitations of each test should be properly recognized.

ACKNOWLEDGMENTS

The authors would like to thank PileTest Consultants (PVT) Ltd. that supported by providing necessary field data for this study. In particular, authors wish to acknowledge Manager; Mr. R. M. Wijesinghe of the organization, for the support.

REFERENCES

Likins, G., Rausche, F., Webster, K. and Klesney, A. (2007). Defect analysis for CSL testing. In Contemporary Issues In Deep Foundations, pp. 1-10.

Massoudi, N. and Teferra, W. (2004). Non-Destructive Testing of Piles Using the Low Strain Integrity Method. Proceedings of the Fifth International Conference on Case Histories in Geotechnical Engineering: New York, NY; 1–6.

Rausche, F. (2004) Non-destructive evaluation of deep foundations (CD-ROM), Proceedings of the Fifth International Conference on Case Histories in Geotechnical Engineering, New York, NY.

White, B., Nagy, M., & Allin, R. (2008). Comparing cross-hole sonic logging and low-strain integrity testing results. In Proceedings of the Eighth International Conference on the Application of Stress Wave Theory to Piles (pp. 471-476).

Development of Local Rainfall Thresholds for Landslide Occurrence in Sri Lanka

H.T. Abeywickrama and N. H Priyankara
Department of Civil and Environmental Engineering, University of Ruhuna, Sri Lanka

ABSTRACT: In Sri Lanka, rainfall is the primary trigger of landslides that frequently cause fatalities and large economic damages, and many of these occur in central part of the country due to its geological and climatic conditions. In order to mitigate these damages, as a soft approach, rainfall thresholds are determined. As an initiation, five districts (Kalutara, Rathnapura, Galle, Hambantota and Matara) were selected for this study. Landslides which occurred in 2017 and rainfall data from rain gauges in those districts were obtained for the analysis. Then, the most relevant rain gauges for a particular landslide were selected from proximity analysis in Arc-GIS. Then Intensity- Duration Curves (I-D curves) were plotted and lower level threshold equation for each district was derived. The obtained results were verified by cumulative rainfall analysis. Based on the results, it was identified that 2-4 days cumulative rainfall was the most critical duration to saturate the soil to initiate the landslides. Further, it was found that cumulative rainfall of 200-350 mm would initiate most of the landslides in those districts. The obtained results were further verified using probabilistic analysis of Bayesian inference method. Highest probability was occurred for the lowest level threshold equation given by the I-D curve. As such, the obtained threshold values could be used as an initiation to develop an early warning system to evacuate people from the damage occurred by the landslides

1 INTRODUCTION

Landslides are commonly identified as frequent and widespread geomorphological phenomena, which account each year for enormous life and property damages in terms of direct and indirect cost due to torrential rainfall conditions. Monsoon rainfalls which are often come together with extreme cyclone conditions affect the environmental and ecological balance in many aspects. Those monsoon rainfalls are most commonly identified as they are one of the reasons for initiation or the triggering of landslides. Therefore, according to a study conducted by (Rajapaksha, et al., 2018) by considering such evidences, a concept was presented as the majority of the landslides which are experienced in Sri Lanka can be categorized as the "Rainfall induced landslides" Among the 25 districts in Sri Lanka, Badulla, Galle, Gampaha, Hambantota, Kalutara, Kandy, Kegalle, Kurunegala, Matale, Matara, Monaragala, NuwaraEliya and Ratnapura districts are identified as landslide-prone areas. When considering those districts, it is about 30% of the total land, occupied by about 38% of the total population of Sri Lanka(Kumara, et al., 2018). When investigating of the recent years which the most landslides are occurred, those years are: 2003, 2007, 2010, 2011, 2012, 2014, 2015 and 2016
They had taken nearly 1000 human lives in the country (Bandara & Pathmakumara, 2018).

According to the Sri Lankan point of view, due to the data shown previously, rainfall can be considered as a main landslide triggering factor. When it comes to the definition of landslides, landslides are defined as the movement of a mass of rock, debris or earth down a slope as a result of both natural and human induced factors. There are several factors that can be considered as the reasons for these soil failures. One of them are, the soil failure which can occur due to the individual rainfall events. They happen in areas of limited extent or in large regions. Also, these soil failures depend on the meteorological and physiographical conditions

2 MATERIALS AND METHOD

2.1 *Overall methodology of the research*

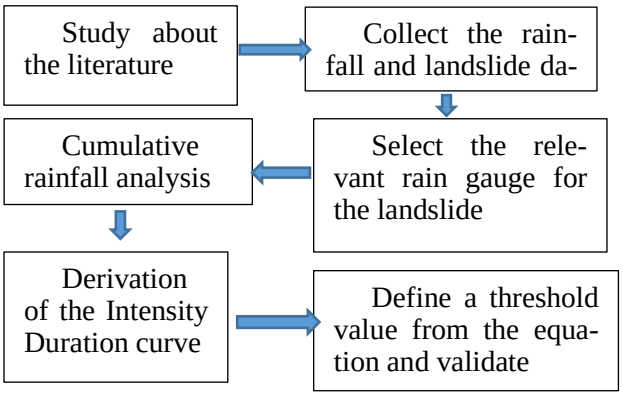

2.2 *Methods of predicting rainfall thresholds*

Most of the data regarding the landslides are in the form of average day rainfall. Therefore, in this study also, average day rainfall data are going to be used for the analysis. According to the literature review, two fair methods which were used previously by (Kumara, et al., 2018) and (Ranjan & Shuichi, 2008) are going to be used here also as they are proved to be suitable for Sri Lankan point of view.
Further, according to the literature review, it is confirmed that rainfall intensity is also a main factor which affects the initiation of landslides. To develop an intensity-duration curve the method used by (Ranjan & Shuichi, 2008) is used. Then the minimum threshold equation is derived

2.3 *Collection of rainfall and landslide data*

There are a huge number of rainfall and landslides data available in NBRO and Meteorological Department, which are not yet taken into the full use. Those data are going to be used here. In this research, Landslide data in between 1999-2018 are going to be selected which are corresponding to 200 landslides. The figure 1 shows the locations of the selected landslides and the rain fall data for the particular landslides collected by the NBRO.

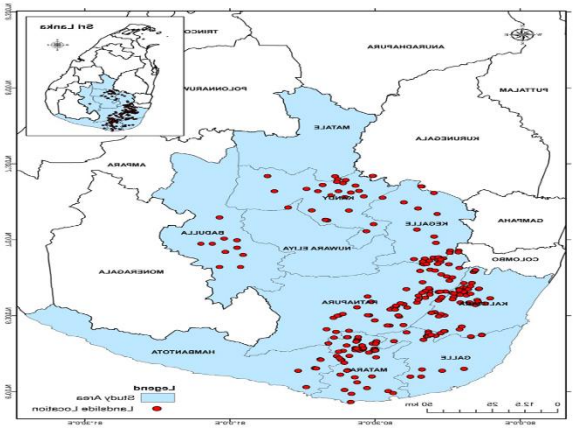

Fig. 1 Study area

2.4 *Selection of the landslide event and rain gauges*

For the study, landslide data base was extracted from the NBRO. For the landslides of Kalutara District were then selected with coordinates. Here 11 landslides were selected. Then, by considering the date of occurrence of the landslide, rain gauges and their coordinates were extracted from the Meteorological department and NBRO.

2.5 *Selection of the relevant rain gauge for the landslides*

All the coordinates of rain gauges and the landslides were plotted in arc-GIS. Then to find the relevant rain gauge for particular landslide, Proximity Analysis was done with the concept of Theisen-polygon method. According to the analysis, the most relevant rain gauge for the landslides were selected

2.6 *Event rainfall and event duration selection*

When defining the thresholds event rainfall and the event duration is important. Then below tables shows those with rain gauge Id by saying whether that rain fall event is resulted to the landslide.

2.7 *Intensity duration- Analysis*

Below figure 2 shows the graphs that are used to found the intensity duration equation obtained from the analysis

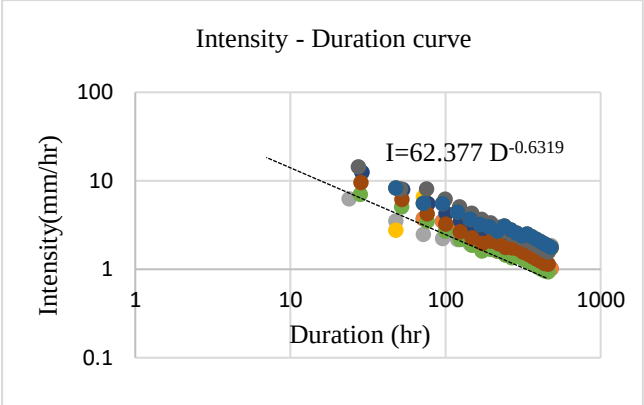

Fig. 2 Intensity duration relationship after removing outliers for Kalutara

3 RESULTS AND DISCUSSION

3.1 *Minimum thresholds*

Minimum threshold equations are shown below in table 1, then by visually observing the event period the minimum amount of cumulative rainfall was calculated for all districts

Table 1: *Threshold equations and the cumulative threshold rainfall value*

District	Equation	Days	Rainfall(mm)
Kalutara	$I= 62.377\ D^{-0.6319}$	4	335
Rathnapura	$I= 210.23\ D^{-0.899}$	4	333
Galle	$I= 71.058\ D^{-0.729}$	3	228
Hambantota	$I= 185.61\ D^{-0.9927}$	2	263
Matara	$I= 131.42\ D^{-0.881}$	3	218

From the intensity duration equation lower cumulative threshold values were obtained. Then it was compared with the al rain gauges to check the accuracy of the prediction below figure 3 also shows how accurate the prediction was

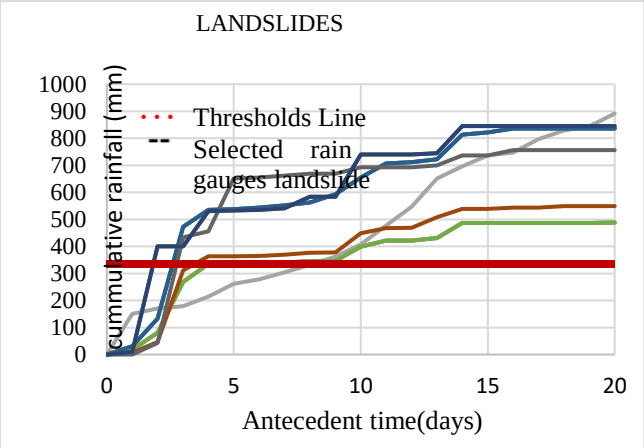

Fig. 3 Cumulative rainfall for landslide and lower threshold comparison for Kalutara

3.2 *Probability results*

This was done to validate the results found by the analysis. For that 1D Bayesian method were done with cumulative event rainfall and duration the results of the prediction shows in below table 2.

Table 2*: Highest probability range for landslide occurrence in each district*

District	Event rainfall	Event duration
Kalutara	400-500	3-4
Rathnapura	300-400	4-5
Galle	300-400	2-3
Hambantota	300	2-3
Matara	300	2-3

3.3 *Thresholds comparison*

The below figure 4 shows the thresholds comparison with already defined equation. It was clear that our derived equations are in between the already defined equations

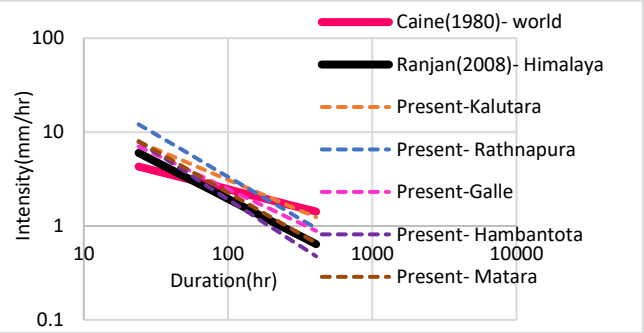

Fig.4 Comparison of thresholds

4 CONCLUSIONS

The description of the procedure which is used for the connection between landslide and rain gauge, and the clear explanation of rainfall parameters taken from rainfall records, need particular attention. Otherwise the equation derived may not be totally accurate. The results of this analysis show that, for Kalutara, Rathnapura, Galle, Hambantota and Matara district, 200-350 mm cumulative rainfall for within 2-4 days may prone to the landslide. When selecting the event rainfall, the rainfall considered should be relevant to the saturation of the soil. In intensity-duration also, event rainfall is important.

In this study it was clear that Rathnapura and Kalutara were having similar geological conditions because the event duration and cumulative event rainfall were similar in both districts. When considering the Galle, Hambantota and Matara, there were having similar event duration and cumulative event rainfall. When selecting the rainfall in this case, proximity analysis was done. for this case proximity analysis is enough because the selected period of 2017 landslides, there were not having more significant variation of the rainfall but in other cases it should be considered the other factors such as surface runoff, infiltration and elevations of the rain gauges.

When doing the Bayesian inherence by selecting the high amount of data, the results can be validated more smoothly and correctly.

REFERENCES

Bandara, R. M. S. & Pathmakumara, J., 2018. Landslide Disaster Risk Reduction Strategies and Present Achievements in Sri Lanka. Geosciences Research, Volume 3, pp. 21-28.

Guzzetti., F., Peruccacci., S. & Rossi., M., 2006. Rainfall Thresholds for the Initiation of Landslides in Central and Southern Europe. Istituto di Ricerca per la Protezione drogeologica, Consiglio Nazionale delle Ricerche, Issue National Research Council, via Madonna Alta 126, 06128 Perugia, Italy.

Kumara, G. D. D., Jayatissa, H. A. G. & Nawagamuwa, U. P., 2018. Determination of Rainfall thresholds for Landslides in Sri Lanka. s.l., National Building Research Organization.

Kumara, G. D. D., Jayatissa, H. A. G. & Nawagamuwa, U. P., 2018. Determination of Rainfall thresholds for Landslides in Sri Lanka. 9th annual symposium on innovation for bbuild back better, National Building Research Organisation, pp. 55-63.

Rajapaksha, R. M. S. D., MAK Kumari, M. A. K. & Hapuhinna, H. K. D. W. M. I. U. K., 2018. Investigation in Disaster Risk reduction for Resilience. Colombo, s.n.

Ranjan, K. D. & Shuichi, H., 2008. Representative rainfall thresholds for lanslides in Nepal Himalaya. Geomorphology, Volume 100, pp. 429-443.

Rathnayake, R. M. S. A. K., 2015. Determination of localized Rain Fall Thresholds for Landslide: A Case Study in Kaluthara District. s.l., Landslide Research and Risk Management Division, National Buildinf Research Organization, Sri Lanka

Effect of Degree of Saturation on Pullout Resistance

K.A.S.N. Fernando and N. H Priyankara
Department of Civil and Environmental Engineering, University of Ruhuna, Sri Lanka

ABSTRACT: Soil nailing is a technique which is used to reinforce and strengthen the existing ground conditions. Among the factors influencing the soil-nail pullout resistance, the degree of saturation of the soil is an important factor, especially for permanent soil-nail structures. As such, in this research study, the effect of degree of saturation on pullout resistance was studied by conducting a series of laboratory pullout tests using a laboratory pullout box. Especially designed water proof cap was used to apply back pressure to saturate the soil within the pullout box. Variation of earth pressures close to the grouted nail were observed during the tests. It was evident from test results that higher the degree of saturation of soil, lower the pullout resistance. Maximum pullout resistance was observed when the degree of saturation was near the optimum moisture of the soil. When the soil is sufficiently dry, lower pullout resistance was observed.

1 INTRODUCTION

Soil nailing is an in-situ reinforcement technique which is installed to stabilize the soil mass, such as cut and fill slopes, deep excavations, retaining structure and tunnels etc. The technique used in soil nailing is the soil reinforced with slender elements such as reinforcing bars which are called as nails and these reinforcing bars are installed into pre-drilled holes and then grouted. There are many factors affecting the soil nail pull-out resistance and the pull-out strength depends on the shear strength between grouted soil nail and surrounding soil. Among the factors influencing the soil nail pull-out resistance, the degree of saturation of the soil is an important one, especially for permanent soil nailed structures due to the fact that the degree of saturation of the soil mass will change with the variation of ground water and weather conditions, and the pull-out resistance may drop to a low level during intense rainfalls.

Few researchers have previously studied the influence of degree of saturation (S_r) on soil nail pull-out resistance. These researchers found that the soil nail pull-out resistance decreased with the increase in degree of saturation of soil. Also, in these pull-out tests, the overburden pressures were applied to the soil after the soil nails had been installed whereas in real life situations the overburden pressure existed prior to the installation of soil nails. Pradhan (2006) found from laboratory pull-out tests that with cement grouted nails in loose Compacted Completely Decomposed Granite Fill, only the nail–soil interface adhesion was reduced by a high degree of saturation. The box used by Yin et al (2005) was a simple one without good instrumentation to facilitate the saturation process. In order to overcome these disadvantages and to meet the demands for more comprehensive studies on the soil nail pull-out resistance, an innovative pull-out box was fabricated and setup in the Soil Mechanics Laboratory of the Hong Kong Polytechnic University (2006).

In the design of a soil nailing system both internal and external failure modes have to be considered. The internal failure modes consist of pullout failure, tensile failure and facing failure. Out of that pullout failure is the most critical. Usually field pull-out tests are carried out before permanent soil nail installation for the purpose of verifying the design bond strength, creep, slippage behavior and determination of whether soil nails are suitable for the ground. However, verification of pullout tests are not conducted under the worst condition in the field where soil is fully saturated. As such, the measured pullout resistance may not be a safe parameter for design. It was found out that the maximum pull-out force reduced by more than a half when the moisture content was increased from the optimum water content to the saturation moisture content by Plumelle et al (1993). Hence the significance of this research is achieving the fully saturated conditions in a laboratory setup. The main objective of the laboratory study was investigating the effect of degree of saturation on pull-out resistance. In addition, the variation of earth pressure during drilling, grouting and pull-out was investigated at different degrees of saturation. During the study four tests were conducted and 36%, 68%, 82% and 98% degrees of saturation were achieved using a laboratory set up which included a water proof front cap and special tubing ar-

rangement to facilitate application of back water pressure.

2 MATERIALS AND METHOD

The effect of degree of saturation with the pullout of soil nail was tested using a laboratory set up in this research. Commonly available lateritic soils collected from University premises were used for this research study. One nail was tested at a time. Internal dimensions of the model set up used for the laboratory tests were 600mm length, 460mm width and 600mm in height. These dimensions were enough to avoid the boundary effect. Additional extension chamber with 280mm length and a water proof front cap for the saturation process were used. Overburden pressure was applied by using a loading frame with a hydraulic jack. The applied force was measured by using a loading cell attached to the steel plate. Handle and lever system were used to distribute the load uniformly to the jacks. The modal set up used by Harshani (2018) had to be altered in order to facilitate the saturation process and to prevent the leakages (Figure 1).

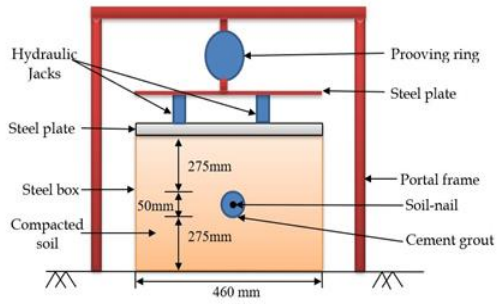

Fig. 1 Pullout model setup

2.1 *Sample preparation*

Prior to the filling of soil to the pull-out box lubricant oil was applied at the interface to reduce the friction. Maximum dry unit weight and optimum moisture content of the soil were obtained from the Standard Proctor compaction test. The soil was compacted into the steel box at 90% of maximum dry unit weight while moisture content was maintained at 3% to the drier side of optimum value. The soil was filled and compacted to layers with thickness 50mm. The amount of soil required for compaction was calculated and the corresponding amount of water was added to the soil.

Five Earth Pressure Sensors (EPS) were installed at the 3 different levels during the compaction. Then a constant overburden stress of 44.774 kPa for all experiments was applied using a load cell and hydraulic jacks and the stress was uniformly transferred to the sample using a thin steel plate.

Then the setup was kept 24 hours without drilling to achieve the equilibrium of applied overburden stress (Until EPS readings became constant). Afterwards, a horizontal hole of diameter 50mm was drilled using a hand auger. Arduino setup and a computer were used for real time recording of EPS data. Steel nail of diameter 10 mm was installed concentrically with the use of centralizers.

Grouting was done by using a pressure grouting cylinder (Harshani, 2018). The Water to cement ratio of cement grout was 0.5 by weight. In order to make grout flowable and non-shrinkage, Flowcable @ 50 was used as an admixture with 0.5% by weight of cement. 60 kPa grouting pressure was applied for all the experiments using a compressor

2.2 *Saturation procedure*

Saturation was started three days after the grouting, once the nail had acquired adequate strength. The nail head was covered with water-proof front cap. The water proof front cap was fixed to a steel plate and that plate was connected to the pullout box using bolts. In order to saturate soil, water flowed in to the pullout box by means of plastic tubes connected to a hole in the side plate. This inlet was divided into 4 lines using T joints and 7 openings were provided around the soil nail to facilitate the saturation process. Openings of the tubes were covered with filter papers to avoid clogging of openings with fine particles. A vacuum pump was used to pump out air from the voids. Vacuum was applied by connecting the vacuum pump to the valve at the front of the pullout box (near nail head). Under this suction pressure, water rose to top and filled the water proof front cap. Then using the air compressor, back-water pressure of about 30 kN/m^2 was applied to the water proof front cap which helped to saturating the soil. The same procedure was repeated but for different time intervals to achieve different degrees of saturation.

After the saturation procedure was completed pull-out test was conducted to determine the pullout out resistance of soil nail. The water proof front cap was removed and pulling-out was done with controlled rate of displacement method and, force and displacement of nail head was recorded. All EPS data during pull-out were recorded by computer and dial gauge readings were recorded manually.

3 RESULTS AND DISCUSSION

3.1 *Effect of degree of saturation on pullout resistance*

The summary of the results of variation of pullout force over pullout displacement is presented in

Fig. 2. From the curves, it can be observed that peak pullout force decreases with the increase of moisture content when the moisture content is greater than optimum moisture content.

The variation of peak pullout force over degree of saturation is illustrated in Fig. 3. Shape of the peak pullout force versus degree of saturation is very similar to compaction curve. On the contrary, displacement at peak pullout force decrease until maximum peak pullout force as shown in Fig. 2. Based on the Fig. 3, it can be noted that peak pullout force reaches to the maximum value when the moisture content is near the optimum moisture content *i.e.* S_r = 49% and is minimum in the fully saturated condition *i.e.* S_r = 98%. When the soil is at the dry side of optimum moisture content water is absorbed by the soil due to higher matric suction. This may cause more contraction of the cement grout, thus reducing the bond strength between grouted nail surface and surrounding soil. As such peak pullout force is less at dry side than that of optimum moisture content. Due to the limitations of the apparatus the pullout was done only up to a displacement of 60-65mm.

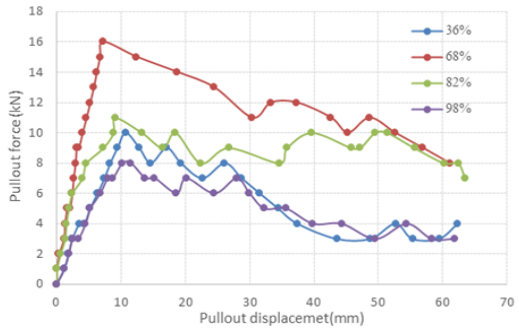

Fig. 2 Pullout force versus displacement under different moisture content

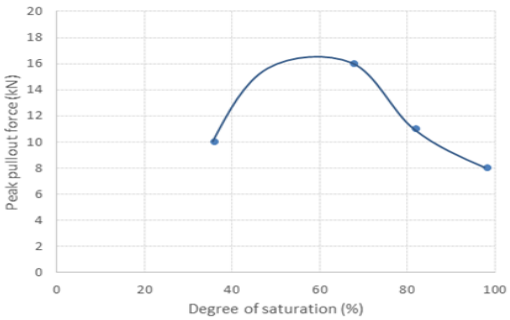

Fig. 3 Variation peak pullout force versus degree of saturation

Generally, it is believed that when the soil is dry due to higher matric suction soil has higher pullout resistance. However, it was observed that when S_r =36%, soil has lower pullout resistance than that of others. If the soil is very dry, water is absorbed by the soil from the cement grout due to higher matric suction. This will lead to contraction of cement grout and reduce the bond strength between grout surface and surrounding soil, resulting low peak pullout force.

When the moisture content of soil is more than the optimum moisture content, apparent cohesion of soil decreases. As a result, pullout resistance decreases with the increase of moisture content more than the optimum.

3.2 *Responses of earth pressure sensors*

Variation of earth pressure during the application of overburden stress, drilling, grouting, saturation and nail pullout was recorded. Fig. 4 indicates the variation of earth pressure during the pullout.

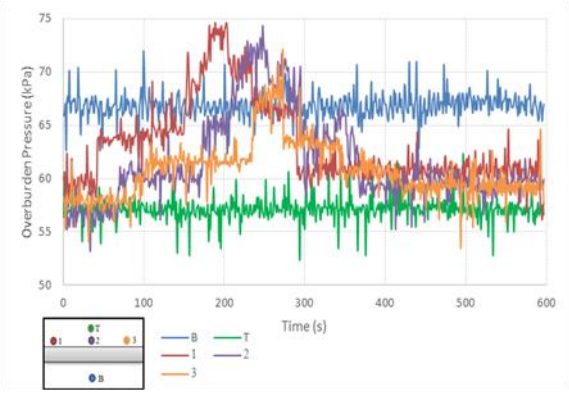

Fig. 4 Earth pressure against Sr = 82% during pullout

3.3 *Failure mechanism*

In order to study the failure mechanism of grouted nail during pullout, surface of grouted nails was investigated after the tests. Fig. 5, illustrates the failure surface (shearing plane) during pullout, at different degree of saturations. It can be seen that shearing plane has been migrated from soil-grouted nail interface outwards into the soil when the soil become saturated and it is evident from Fig. 5 as more soil is adhered to the nail after pullout when the degree of saturation is increased. This implies the migration of shearing plane from grouted nail-soil interface to soil due to decrease of soil matric suction.

The ultimate theoretical pullout resistance is 4.29 kN. It is far less than the all peak pullout values obtained for the four degrees of saturation. But this ultimate theoretical value was calculated without factoring in the parameters such as grouting pressure, matric suction etc. This behavior can be further explained with respect to the shear strength parameters of soil-grout interface.

Fig. 5 Nail surfaces after pullout for different degrees of saturation at a) 36%, b) 82% and c) 98%

4 CONCLUSIONS

Soil nailing is a technique which is used to reinforce and strengthen the existing ground conditions. This is done by installation of closely spaced, passive, structural inclusions known as nail into the soil and these nails helps to improve the overall shear strength of soil. The nail pullout force is the shear resistance of the grout-soil interface. Soil nailing technique is one of the economically advantageous method.

In order to study the effect of degree of saturation of soil on pullout resistance, a series of laboratory soil nail pullout tests were conducted by varying the moisture content. Especially designed waterproof cap was used to apply back pressure to saturate the soil within the pullout box. Variation of earth pressures close to nail head, middle and tail were observed during the experiments. In addition, to compare the experiment results with analytical results, interface shear strength parameters were determined using direct shear apparatus.

Based on the laboratory experiments and results, following conclusions can be made.

1. Pullout force is highly dependent on the degree of saturation of soil. Higher the degree of saturation, lower the pullout resistance.
2. Maximum pullout force is occurred when the moisture content of the soil is close to the optimum moisture content.
3. When soil is sufficiently dry (dry side of optimum moisture content), water within cement grout is absorbed by the soil due to higher matric suction, thus reducing the bond strength between grout surface and surrounding soil resulting low pullout resistance.
4. During drilling hole to install soil-nail causes stress release in the surrounding soil. However, during the drilling process, stress of soil increases due to outward pushing of the soil by the drill bit. During the pressurized grouting, earth pressure was initially increased and then gradually decreased. This was due to hardening of cement grout and dissipation of pore water. During Saturation earth pressure gradually increased due to the pore water pressure and the pressure near the nail showed sudden increments when the back pressure was applied. During the pullout of soil – nail, earth pressure near the nail head was increased and then decreased. This increment of earth pressure was occurred due to dilation effect of the nail which is dependent on soil suction, soil density and interface roughness. Hence soil dilation is one of the influence parameters in pullout resistance of soil nail.
5. It should be noted that number of tests were limited in this research; study and more soil-nail pullout tests with more degree of saturation should be performed to examine the effect of degree of saturation on pullout resistance accurately. Further it is necessary to measure matric suction during pullout tests to analyze the effect of degree of saturation.

REFERENCES

David-Suits, L., Sheahan, T., Chu, L., and Yin, J., (2005)., A Laboratory Device to Test the Pull-Out Behavior of Soil Nails, Journal of Geotechnical Testing , 28:1097-1107

David-Suits, L., Sheahan, T., Yin, J., and Su, L., (2006)., An Innovative Laboratory Box for Testing Nail Pull-Out Resistance in Soil, Journal of Geotechnical Testing , 29:451-1107

Harshani, R.G.F. (2018). “The Effect of Grouting Pressure on Pullout Resistance of Soil Nails.” Undergraduate Thesis, University of Ruhuna, Galle, Sri Lanka.

Pradhan, B., Tham, L., Yue, Z., Junaideen, S., and Lee, C.,(2006)., Soil–Nail Pullout Interaction in Loose Fill Materials, Journal of Geomechanics, 6:238-247

Schlosser, F., Unterreiner P., and Plumelle, C., (1993)., Validation des méthodes de calcul de clouage par les expérimentations du Projet national CLOUTERRE, Journal of Française de Géotechnique, 64:11-20

Su, L., Chan, T., Shiu, Y., Cheung T., and Yin, J., (2007)., Influence of degree of saturation on soil nail pull-out resistance in compacted completely decomposed granite fill, Canadian Geotechnical Journal,44: 1314-1328

Comparison of different philosophies on Design of Geosynthetic Reinforced Piled Embankment (GRPE)

H.D.S. Mithila and N. H Priyankara
Department of Civil and Environmental Engineering, University of Ruhuna, Sri Lanka

ABSTRACT: Designing structures such as highway embankments over soft compressible soil or weak foundation soil results in many issues such as intolerable settlement, potential bearing failure and global and local instability. In order to face these issues, many ground improvement methods are in use such as wick drains, surcharge loading and gravel column etc. But among these methods Geosynthetic Reinforced Piled Embankment (GRPE) stands out due to its efficient load transfer mechanism and less construction time. In terms of design of GRPE, though there are various analytical methods, most feasible method is not yet established. Thus, this research presents a justification to obtain the best analytical method to design GRPE by performing parametric study between most commonly used analytical methods BS 8006 and New German method (EBGEO) and their results were compared with Plaxis-2D FEM plain strain numerical simulation. Based on the analysis, it was revealed that EBGEO method is the most suitable analytical method to design GRPE since it approaches Plaxis 2D design outputs better than that of BS 8006.

1 INTRODUCTION

Geosynthetic reinforced piled embankment(GRPE) utilizes geosynthetic reinforcement with high tensile properties, to span the clear distance between adjacent piles resulting in increase of efficiency of load transfer from soil to pile.The embankment load is transferred through geosynthetic reinforcement to piles ensuring negligible load is transmitted to soft soil between piles avoiding any excessive differential settlement. (kempfert et al.,1997).

Embankment load is transferred to underlying piles mainly through mechanisms of soil arching and tension membrane developed in geotextile as illustrated in Figure1. Fluet et al.(1986), studied the effect of geogrid on the base of embankment. This study concluded that geogrid layer promoted arching process whereas if geogrid was removed no significant arching could be observed. In terms of designing GRPE, different analytical methods would provide different values for load transferred to pile, geosynthetic tension and embankment settlement when varying input parameters such as stiffness of geosynthetic reinforcement, embankment height, pile spacing, pile width stiffness soft soil directly below geogrid. Based on these contradictions, it is uncertain to state which design method is ideal for designing GRPE.

Therefore, the aim of the study is to analyze GRPE using most commonly used analytical methods BS 8006 and EBGEO and compare its results with analysis results of FEM software Plaxis2D.

2. METHODOLOGY

This research is focused on analysing and comparing the behaviour of GRPE based on different design methods. Basically, two types of models were used for analysis which were axisymmetric model and plain strain model.

2.1Axisymmetric Study

Axisymmetric model was used to model a single pile and its results were compared with Pile Dynamic Analysis (PDA) and analytical calculations. It was performed to justify the applicability of Plaxis 2D FEM to verify analytical design methods of GRPE.validate Plaxis 2D model for pile capacity calculations. 0+332.5 R1 pile of Matara-Beliatta section of southern expressway was modelled as reference pile as shown in Figure 1.Subsurface soil profile and relevant input data was obtained from boreholes and soil test reports from southern expressway project.

As shown in Figure 1, Precast Pile with 20.9m length and 0.5m diameter was positioned along the axis of symmetry. Bottom boundary was assumed rigid and standard fixities were used at side boundaries. Since pile diameter was 0.5m, it was defined as a column with 0.25m width. Along the pile length, interface was modelled and it was extended 0.5m below pile tip to avoid stress oscillation at the stiff corner.

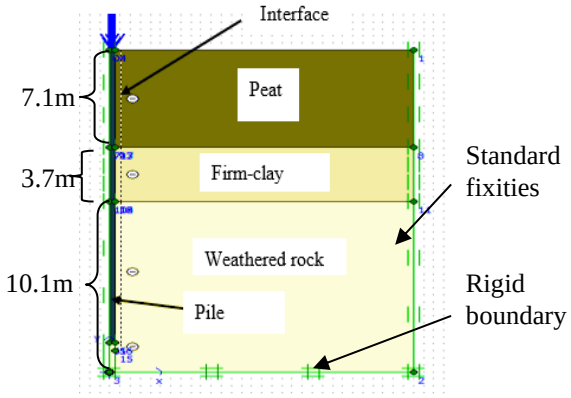

Figure 1 : Axissymetric model of single pile analysis

Then, mesh was generated for finite element analysis.Ultimately, loading was applied iteratively until failure occurs and bearing capacity and load settlement curve were obtained as outputs.Similarly, using PDA test reports and analytical calculatons load settlement curve and bearing capacity of pile was obtained was obtained for same geometry.

2.2Plainstrain Study

Plain strain model was used to model entire GRPE and perform parametric study comparing with results of analytical methods of BS 8006 and EBGEO. Interms of procedure of parametric study, input parameters such as pile width , embankment height, surcharge,geogrid and softsoil stifness were varied to observe common output parameters of geosynthetic tension and total load transferred to pile.Ultimately, by comparing proximity of results of analytical codes to that of plaxis 2D outputs the most suitable method was to be identified.

2.2.1 Plaxis 2D (FEM) – Plain strain condition

Interms of Plaxis 2D model, considering symmetry only half from the centre of geometry was modelled as illustrated in Figure 2.

In the calculation phase staged construction procedure was used for simulation of the realistic process of construction. Staged construction procedure was followedin the order of activation of piles and geogrid, Placing first embankment layer and allowing it for consolidation(14 days), Placing second embankment second layer and allowing it for consolidation (14 days) and opening road to traffic for 1 year.

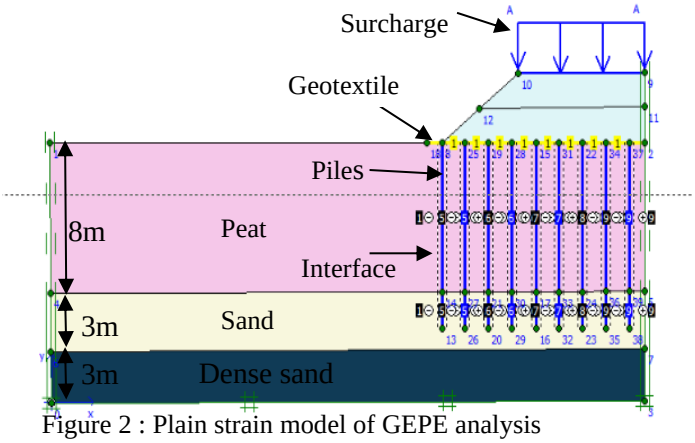

Figure 2 : Plain strain model of GEPE analysis

2.2.2 BS 8006 method

Case 01: Total load on pile

Total stress developed on pile is obtained as,

Total stress on pile top (σ_v) =γH +P (1)

Where,
γ is Unit weight of embankment soil, **H** is Embankment height and **P** is Traffic load (Surcharge)

Since, BS8006 method neglects the support from soft soil. It considers total load induced on equivalent pile grid is ultimately transferred to pile.
Therefore,

Total load on pile = σ_v x S^2 (2)
Where,
S is centre to centre pile spacing

Case 02: Geosynthetic tension

Equation 3 is used to obtain the the line load on the strips of reinforcement between adjacent piles (W_T) and Equation 4 is used to obtain tensile stress in geosynthetic reinforcement (T_{rp})which depends on W_T.

$$W_T = \frac{1.4\,S\gamma\,(S-a)}{S2-a2} \times \left(S^2 - a^2\left(\frac{P_c}{\sigma_v}\right)\right) \quad (3)$$

Where,
a is Pile width

$$T_{rp} = \frac{W_T\,x(s-a)}{2a} \times \sqrt{1+\frac{1}{6\xi}} \quad (4)$$

Where,
ξ is Estimated strain in geogrid

2.2.3 EBGEO method

Case01: Load on pile

Figure 3 is used to obtain the the normal stress developed on geosynthetic between piles ($\sigma_{Z0,k}$) due to embankment loading condition.

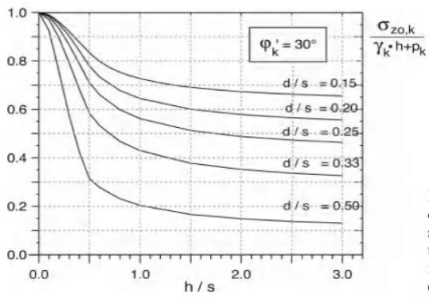

Figure 3 :Graph for obtaining Normal stress between piles(EBGEO,2011

Where,
h is Embankment height ,**s** is Maximum spacing between piles and **d** is Equivalent pile width

Equation 5 is used to obtain stress developed on piles due to arching.

$\sigma_{ZS,G+Q,K} = ((\gamma h + P_{,K}) - \sigma_{ZO,G+Q,K}) \times A_E/A_S + \sigma_{ZO,G+Q,K}$ (5)

Where,
$\boldsymbol{\sigma_{ZS,G+Q,K}}$ is stress developed on piles due to arching ,$\mathbf{A_E}$ is Equivalent area for single pile grid and $\mathbf{A_S}$ is Cross sectional area of a single pile

So, Direct load on piles due to arching,

$= \sigma_{ZS,G+Q,K} \times A_S$ (6)

Case02: Geosynthetic tension

Unlike in BS 8006 , EBGEO integrates the support from soft subsoil into calculation of geogrid tension.

$$K_{s,k} = \frac{E_{S1} \, x \, E_{S2}}{E_{S1} \, x \, t1 + E_{S2} \, x \, t2} \quad (7)$$

Where,
$\mathbf{K_{s,k}}$ is mean modulus of subgrade reaction , $\mathbf{E_s}$ is constrained modulus of stratum and $\mathbf{t_w}$ is thickness of considered stratum

Figure 4 is used to calculate the maximum strain developed in the geogrid

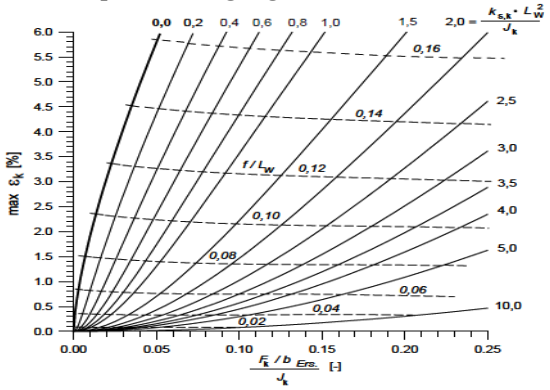

Figure 4 :Maximum strain in geogrid (EBGEO,2011)

Where,
$\mathbf{J_k}$ is Tensile stiffness of geogrid.,$\mathbf{L_w}$ is Clear distance between two piles ,$\mathbf{b_{Ers}}$ is Pile width, $\mathbf{F_k}$ is Resultant vertical strip load on geogrid and $\boldsymbol{\xi_k}$ is Maximum strain in geogrid

Ultimately, from equation 8 mobilized geosynthetic tension on geogrid ($E_{M,k}$)can be obtained.

$E_{M,k} = \xi_k \times J_k$ (8)

3 RESULTS AND DISCUSSION

3.1 *Axisymmetric study*

Load-settlement graph obtained by Pile Dynamic Analysis (PDA) test report of considered and Plaxis 2D FEM analysis results is shown in Figure 5.

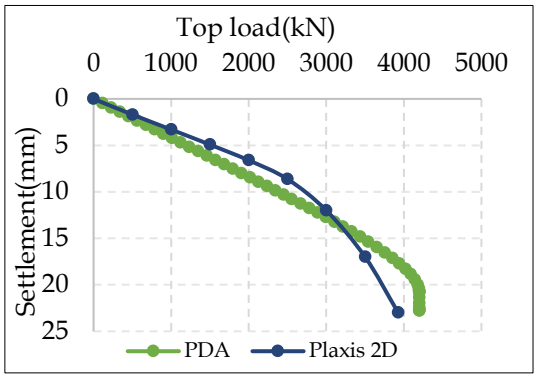

Figure 5 : Load settlement curve obtained by PDA and Plaxis 2D results

Total bearing capacity obtained by Plaxis 2D model , PDA test report and analytical calculations is illustrated in Figure 6.

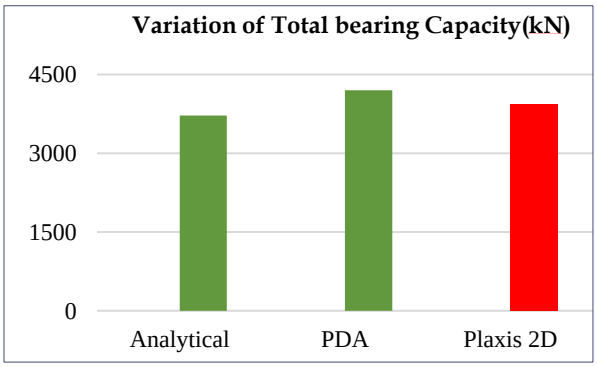

Figure 6 : Variation of Total bearing capacity

When observing the above results it is quite clear that Plaxis 2D simulation result are quite close to in situ test results of PDA and analytical calculations. Therefore , Plaxis 2D is applicable for modelling pile behaviour and it is justifiable to be used

as base of validation for plain strain GRPE modelling.

3.2 Plain Strain Study

Figure 7 depicts the variation of total load when varying input parameters of surcharge and pile width. It can be noted that BS 8006 results are significantly conservative compared with other methods.Also,BS 8006 results suggest total load on pile is independent from pile width which is not agreed by Plaxis 2D and EBGEO.

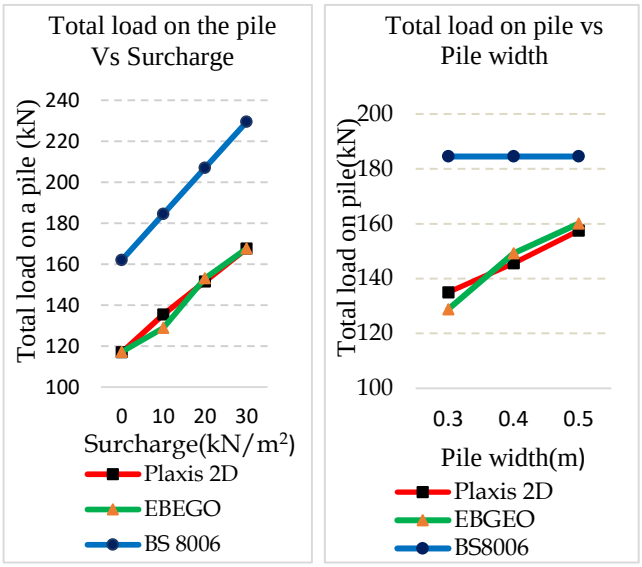

(a) (b)

Figure 7 : Variation of Total load on pile with (a) Surcharge and (b) Pile width

Figure 8 depicts the variation of geogrid tension when varying input parameters of Peat layer stifness(Softsoil layer directly below geogrid), geogrid stiffness,surcharge and embankment height.Similarly as with total load on pile BS 8006 provides conservative values for geogrid tension.

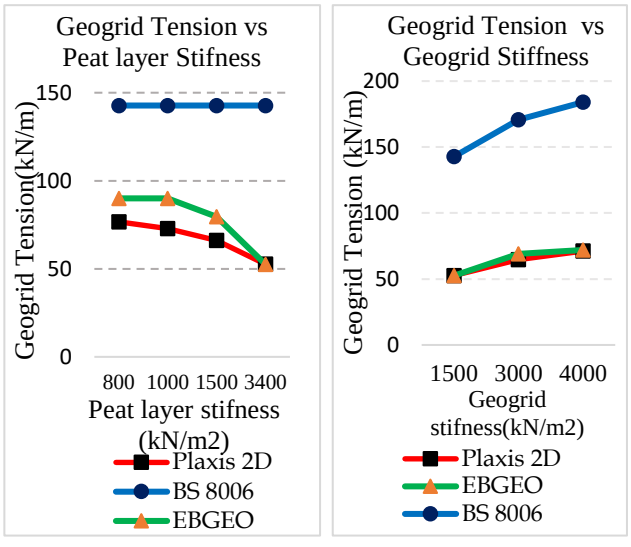

(a) (b)

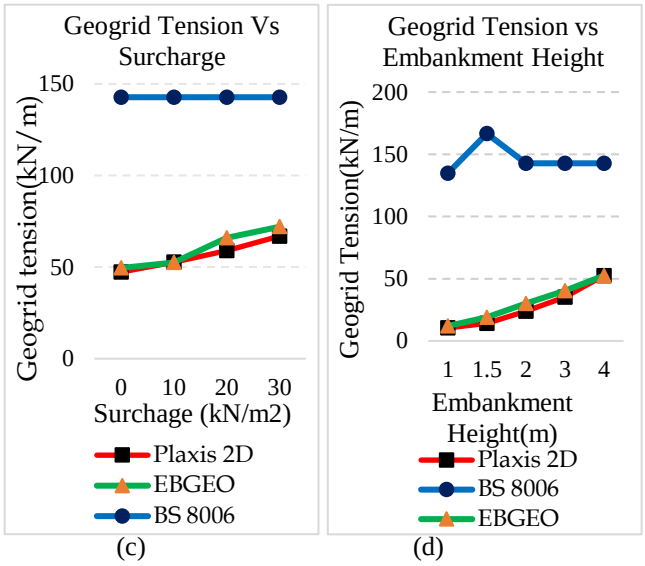

(c) (d)

Figure 8 : Variation of Geogrid tension with (a)peat layer stiffness ,(b)Geogrid tension, (c) surcharge and (d) Embankment height

4 CONCLUSIONS

This study was carried out to verify and obtain the most suitable analytical method to design GRPE.In the process, parametric study was performed using BS 8006, ,EBGEO and Plaxis 2D to identify most suitable design method between BS 8006 and EBEO.

Results clearly showed that BS 8006 is much more conservative than other methods. Therefore, designing in compliance with BS8006 is not economical. Also, Stiffness of soft soil layer directly below geogrid was found to be an influential parameter in designing of GRPE which is neglected by BS 8006.It assumes total embankment load is ultimately transferred to piles due to negligence of support from soft soil.

Since Parametric study clearly depicted that EBGEO complies considerably well Plaxis 2D results, it can be concluded that EBGEO is the best and most economical method to design GRPE considering its compliance with Plaxis 2D results.

REFERENCES

British Standards BS 8006: 1995 “Code of practice for strength ened/Reinforced /Reinforced Soils and other fills”,Section 8.3.3 ,British Standard Institution.

EBGEO(2011): “Recommendations for Design and Analysis of Earth Structures Using Geosynthetic Reinforcements”, Translation of the 2nd German edition,German Geotechnical Society

Determination of Fundamental Characteristics of Unsaturated Residual Soils in Sri Lanka

B.P.S. Harishchandra and N. H Priyankara
Department of Civil and Environmental Engineering, University of Ruhuna, Sri Lanka

ABSTRACT: Sri Lanka, a tropical country mostly consists of residual soil, disturbed soil samples collected from a landslide in Southern expressway near Beliatta was used for this research. The Soil Water Characteristic Curves (SWCCs) and permeability relationships were developed for the soil using laboratory tests with tensiometers. The continuous drying and wetting paths were developed to represent the natural soil under dry and rainy seasons. Further, shear strength parameters under different moisture contents were determined using direct shear tests. As such, variation of shear strength parameters with matric suctions were obtained. Further, SWCC was developed using Arya-Paris empirical model. The results depicted cohesion kept decreasing and friction angle kept constant with the increasing of saturation of soil on wet side. Further, cohesion and the suction show a nonlinear relationship. The empirical and test-generated SWCCs were approximately equal within considered suction range. Permeability results shows a rapid increment when suction reduces.

1 INTRODUCTION

As only a limited range of unsaturated soil properties are available and to predict the landslides. As Sri Lanka is a tropical country mostly consist of residual soil, it experiences drying and wetting conditions. Methods available for slope stabilization techniques in Sri Lanka are not cost effective and accurate. Therefore, an accurate and deep studies about unsaturated soil is necessary. As a result, this research was conducted to achieve following objectives.

- Determination of the unsaturated shear strength parameters.
- Development of the Soil water characteristic curves
- Development of the permeability function

To achieve the above characteristics and parameters, a series of experimental program is to be designed. By that following experimental categories have to be conducted to achieve the task.

Conventional direct shear tests have to be carried out with varying normal loads and moisture contents in order to find the shear stress relations with normal stress, shear strain and Apparent cohesion and friction angle with Saturation and water content. Then compare the shear strength parameters with suction obtained using tensiometers.

Soil Water Characteristic Curve (SWCC) is to be generate using tensiometers and compare them with the results of Arya-Paris empirical model.

- Continuous measurement methods using data logger.
- For both drying and wetting paths that address the dry and rainy conditions.

Development of permeability relationships using data of wetting and drying paths with few calculations.

2 BEHAVIOUR OF UNSATURATED SOIL

2.1 *Basic properties*

The unsaturated soil consists of four phases as soil, water, air, air-water interface/contractile skin according to investigations of Fredlund and Rahardjo (2012), shows complex engineering behavior. Fig. 1 presents the phases of unsaturated and saturated soils. Matric suction which is the main factor accounts for properties of unsaturated soil is the difference of pore air and pore water pressures.

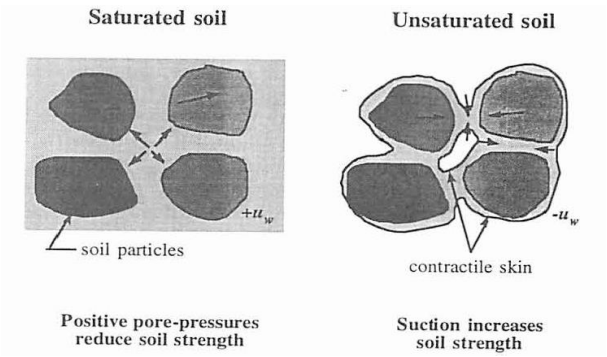

Fig. 1 Phases of saturated and unsaturated soil

2.2 *Unsaturated shear strength with matric suction*

There have been made several tests to get the failure envelop with relevant to suction which is non-linear. But at lower suction values the failure envelop is linear under drained conditions as long as the soil remains saturated. This happens at the suctions below the air entry value (the suction at which air starts to replace water in the voids). Above the air entry value the envelop is non-linear.

This is the easiest way to determine the parameters related with the unsaturated soils. SWCC is the graph of water content versus matric suction (or total suction= matric suction + osmotic suction). The SWCC consist of two paths as wetting and drying and with different zones as shown in Fig. 2.

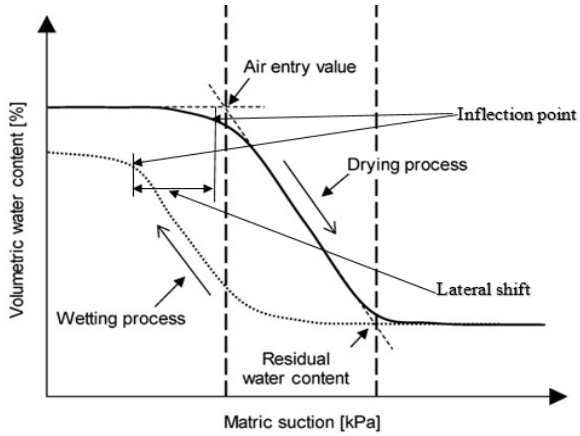

Fig. 2 Idealized Soil Water Characteristic Curve

2.3 *Permeability in unsaturated soil*

Permeability is a major parameter to be determined for the study of slope stability because the infiltration of the rainwater depends upon this. The coefficient of permeability is a widely varying engineering property.

When a rainfall prevails for a long time the infiltration diminishes the soil suction to zero at a critical depth and frequently become a triggering mechanism of shallow slope failure as presented by Springman, Jommy, and Teysseire (2003) and Godt, Baum and Lu 2009). In addition to that perched water table (Figure 2.18) can be induced by heavy rainfall at a shallow depth in soil slopes as a result of wetting front being impeded by zones of much lower permeability in drier unsaturated soil or impervious rock underneath according to Vaughan (1994).

3 METHODOLOGY AND EXPERIMENTAL SETUPS

3.1 *Methodology*

According the research objectives of finding unsaturated soil parameters a series of experiments were conducted. In addition, empirical method was also used to compare the results. The chart in Fig. 3 below depicts the methodology of how the research was conducted.

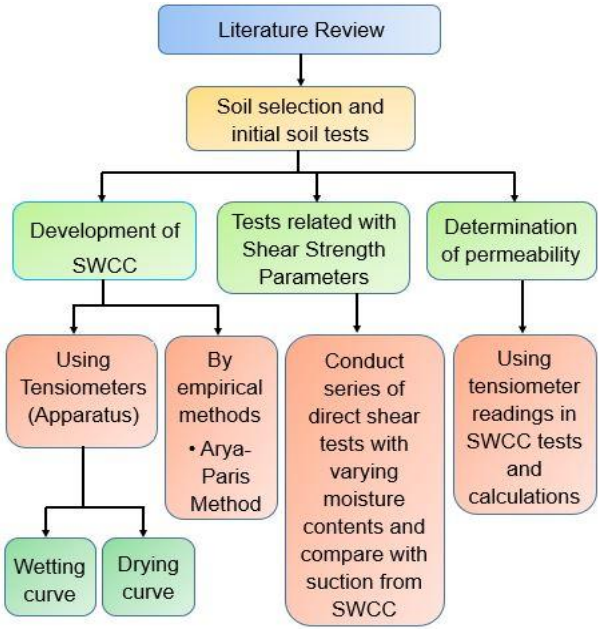

Fig. 3 Flow chart of the research methodology

For the test samples, 85% of the maximum dry density derived from proctor compaction test was used.

3.2 *Experimental setup*

An experimental setup was developed with tensiometers and an Arduino circuit.

Tensiometers were bought from Kasartsart University(KU) of Thailand and for data acquisition an Arduino circuit system was developed.

In developing of SWCC using the tensiometers by direct measurements of matric suction, a container connected with tensiometers was used as shown in the detailed arrangement in the Fig. 4.

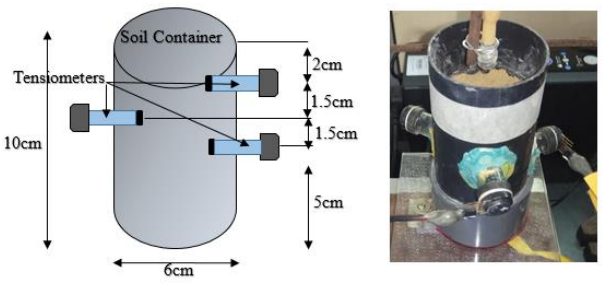

Fig. 4 Arrangement of tensiometers in the soil container

The experimental setup for the development of SWCC for drying path with all the components were presented in the Fig. 5 below. A modification was done for the soil container by providing a constant water flow in order to develop the wetting path SWCC for the soil sample.

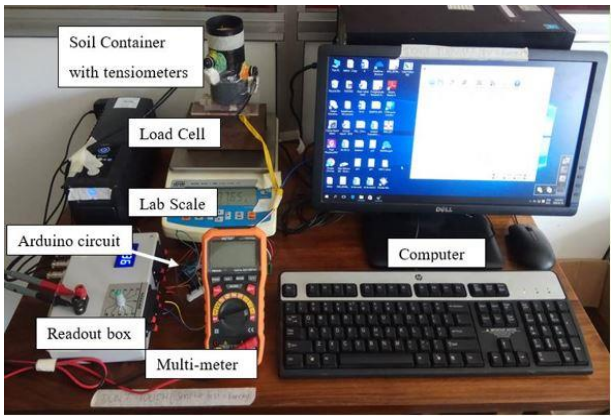

Fig. 5 Instrument Setup for SWCC drying path

4 RESULTS AND DISCUSSION

4.1 *Basic soil test results*

A set of tests were carried out to find the basic soil properties and soil type. Based on the above results, the soil was classified according to the Unified Soil Classification System. The soil was classified as CL – Inorganic clays of low to medium plasticity, gravelly, sandy and silty clays.

4.2 *Direct shear test results*

For the determination of unsaturated shear strength parameters (Friction angle and Cohesion), the direct shear tests were carried out by varying the moisture contents. Here, the moisture contents are selected such that the whole soil moisture range is covered. The graph in Fig. 6 shows the variation of cohesion and friction angle with soil saturation.

The unsaturated shear strength (Apparent cohesion) was getting reduced with the increase in saturation and friction angle kept constant on the wetting side (when saturation>50%). This means the shear strength reduced with the loss of matric suction due to saturation.

The graph in Fig. 7 shows the variation of Cohesion with Suction. There, the non-linear increment of cohesion with suction shows the increasing of strength of soil when saturation get reduced.The two points in right side were neglected as the tensiometers are not accurate at the suctions greater than 80kPa.

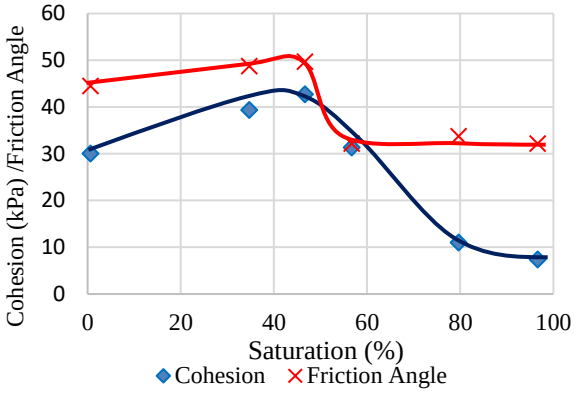

Fig. 6 The graph of cohesion & friction angle vs saturation

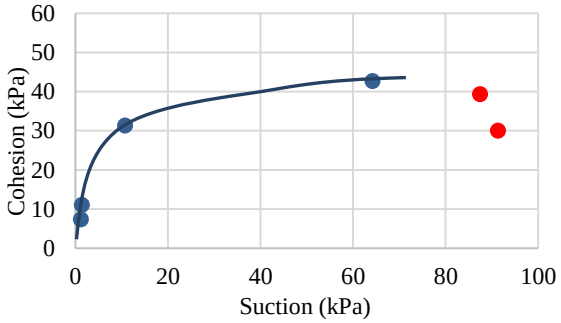

Fig. 7 Graph of cohesion vs. suction

4.3 *SWCC for drying path*

The SWCC obtained for the drying path in Fig. 8 is justified with the literature and it shows a smooth graph with less scatter. As such, this setup gives more accurate data for drying path.

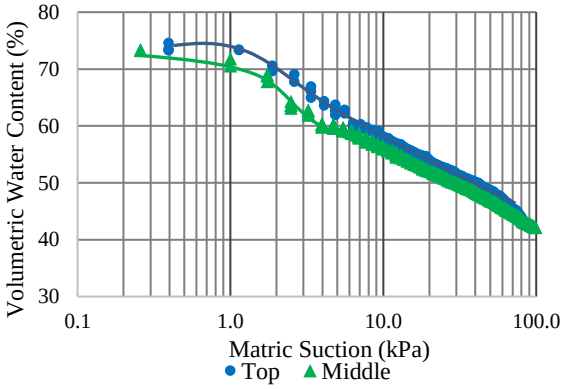

Fig. 8 SWCC for the drying path

4.4 *SWCC for wetting path*

In the development of wetting curve, the data scatter is larger and shows spikes as there were small variations which are not sensitive for the Arduino circuit setup as presented in Fig. 9.

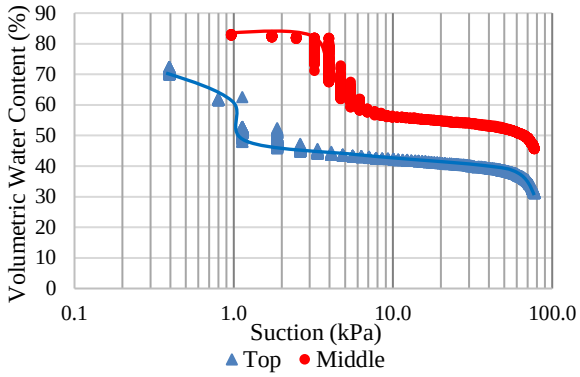

Fig. 9 SWCC for the wetting path

4.5 *SWCC by Arya-Paris model.*

Most commonly used method for development of empirical curve as shown in Fig. 10 for soil water characteristics is the Arya-Paris method. Here the particle size distribution of the soil was converted to a pore size distribution.

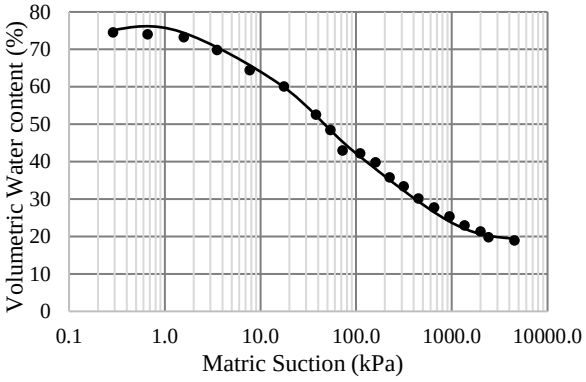

Fig. 10 SWCC using Arya-Paris model

The Fig. 11 below shows the combination all of SWCC graphs

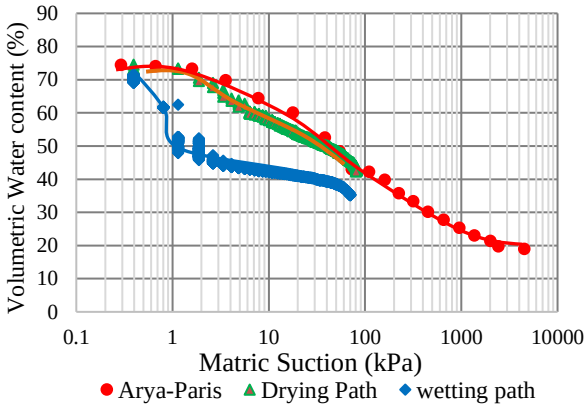

Fig. 11 SWCCs for all methods

4.6 *Permeability relationships*

The permeability relationships were developed using the equations in the Figure 6 and using the data obtained from SWCC tests as in Fig. 12.

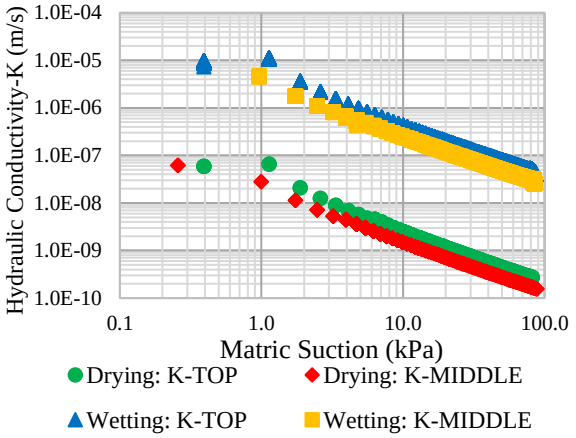

Fig. 12 Graph of hydraulic conductivity vs suction

5 CONCLUSIONS

The Cohesion of soil decreases with the increase of the saturation, this confirms the slope failures in wet(rainy) weather. Friction angle does not show any involvement in slope failure as it kept constant on wet conditions.

Modelled Soil Water Characteristic Curves can be used to implement EWS. But at higher suctions (>80kPa) the empirical models cannot be validated as the tensiometer are inaccurate and incapable of measuring higher suctions.

The permeability increases at lower suctions. Therefore, water infiltrate more when soil is getting saturated, reducing the cohesion rapidly causing slope failures.

These data can be used to develop an accurate Early Warning System by finding the safety factors for different types of slopes at different conditions.

ACKNOWLEDGMENTS

The authors would like to thank, Mr. Lilanka Udayana of NBRO for providing valuable information on the research and Perera W.A.A.I.D.P.D for Arduino coding.

REFERENCES

Fredlund, M.D., Rahardjo, H. & Fredlund, M.D., 2012, Soil mechanics for unsaturated soils,John Wiley & Sons, Inc., Hoboken, New Jercy.

Springman, S.M., Jommy, C. & Teysseire, P., 2003, Instabilities on moraine slopes induced by loss of suction: a case history, Geotechnique, 53, pp 3-10.

Godt, J.W., Baum, R.L. & Lu, N.,2009, 'Landsliding in partially saturated materials', Geophysical Research Letters, 36, 1-5.

Vaughan, P.R, 1994, Assumption, prediction and reality in geotechnical engineering, The 34th Rankine Lecture, Geotechnique, 44, pp 573-609

Deformation Behavior of Soil Cement Column Improved Ground

Thenuwara T.H.M.N and N. H Priyankara

Department of Civil and Environmental Engineering, University of Ruhuna

ABSTRACT: Greater Colombo Wastewater Management Improvement project is an ongoing project, with the major task lay sewer line in Colombo city. When soil properties were analyzed prior to lay pipes via micro tunneling, it was identified that in some areas soft soil layer extends up to 13m depth. Casting of soil columns to such a depth is problematic as there is a higher chance of bulging. This research focused on analyzing the viability of soil-cement columns in the influenced area and whether it is applicable in the field. In the first part of the research study, laboratory tests conducted to identify properties of the soft soil, after that scale down version of soil columns were casted in the laboratory and an apparatus is prepared to apply loading to the model soil-cement columns to simulate the actual field conditions. In the final part of the study, a numerical analysis in Plaxis 2D software was developed to validate the experimental results.

1 INTRODUCTION

Peaty clay is a problematic soil which frequently encountered in the construction field. In the early days, Engineers avoided peaty lands due to low bearing capacity. Problematic peat soil exhibits high compressibility, medium to low permeability, low strength and volume instability. Consequently, it is widely regarded as the worst foundation soil for supporting man-made structures (S. Hebib and E. R. Farrell .2003)

Soil-cement columns can be used, effectively to improve soft soil. According to Antonio and Hwang,(2011) this method was firstly developed in Japan and Sweden in 1960s and around 1980s. Due to its economical design and easiness of usage, it has been widely practiced in all around the world. Nevertheless, in Sri Lanka soil–cement columns have not been successfully used in the construction industry yet. It was proposed to use soil- cement columns in the Greater Colombo Water and Wastewater Management Improvement Investment Project, in some parts as, the ground consists of soft peaty clay soil. In the section of Kirula, Narahenpita ,Thalakotuwa Gardens: when the construction was carried out the pipe head has settled and when the soil condition was analyzed ,it was found that the soil in the area is soft peaty clay and the soft soil thickness may varies between 6 m -13 m. It has been identified that the construction cannot proceed without improving the soft ground in the area.

As a remedy it has been proposed to cast underground soil columns and lay the pipe line on it. Usually this is an acceptable practice, as casting of soil cement column is an economical method of ground improving. But the soft soil layer thickness is extending up to depth of 13 m. Hence there is a high possibility of buckling of columns when they are casted to a greater depth. On the other hand, according to many researches such as Wardani and Muntohar (2011), casting of soil column may improve the soil surrounding the soil columns radially and vertically for a greater limit, this factor might help columns to support the load on the outside. In academia there are various positive and negative opinions suggested on this matter.

Despite number of researches have conducted to analyze behavior of the soil columns, with respect to soil type and cement and various other stabilizing agents such as fly ash, lime etc. None have attempt to predict the behavior of soil column and its vertical deformation relating to a real-time application. Since this is an ongoing actual project, it is necessary to adopt a reliable method of construction

2 BASIC PROPERTIES OF PEATY CLAY

Prior to analyzing the degree of soft soil improvement, it is mandatory to identify the basic properties of peaty clay. Soft peaty clay for this research study was selected from Nilwala flood plain. From the laboratory test results basic properties of the peaty clay were identified and they are depicted in the Table 1. Based on laboratory test results, it is noted that that peaty soil consists of high-water content of about 171 % and organic content of 20% According to ISO 14688-1(2002) and ISO 14688-2 (2004) (International Organization for Standardization) classification system, if the organic content is greater than 20 %, soil is categorized as of ‘high organic content’. As such the peaty soil that has been used to

cast soil cement columns can be categorized as 'high organic peat'. Further this peaty soil can be classified as 'moderate acidic' as pH values is in between 4.5 to 5.5 according to ASTM-D 4427(The American Society of Testing Materials).

Table 1. Basic properties of peaty clay

Property	Value
Saturated moisture content	171 %
Bulk unit weight	14.4 kN/m^3
Organic content	20 %
Liquid Limit (LL)	94 %
Plastic Limit (PL)	67 %
Plastic Index (PI)	27%
Linear shrinkage	12 %
pH value	4.6
Cohesion	22.5 kPa
Friction Angle	0 degrees
Elastic Modulus	1800 kN/m2

3 SOIL CEMENT COLUMNS & APPARATUS

In order to predict the behavior of soil cement columns in advance, it is needed to conduct plate load test for model soil cement columns. For that model small scale soil- cement columns were casted and experimental apparatus was prepared to occupy the columns and conduct the loading process

3.1 *Mix Design*

In the actual field, soil column are prepared with a 0.75 w/c and casted in-situ ,but in the experimental study columns are installed separately and when preparing model columns it has observed that the soil cement slurry will be highly viscous, therefore pouring of cement slurry in to soil cement mold became fairly difficult. Thus, the mix design has altered to 1.5 w/c.

3.2 *Soil column Preparation*

After preparing the mixture it is poured to mold under three stages using a funnel. After each stage soil cement mixture is tampered for 10 times. In the research study greater consideration was given to simulate the actual scenario. As circular shape soil cement columns casted in the actual field, in the experimental study also circular shape model columns were casted.

Conduit PVC pipes were used as molds and the 23 mm diameter conduit pipes were selected in accordance to model diameter. Firstly, the conduit pipes were cut in to the required lengths and then were split in to two as shown in Figure. 1. And applied mold oil in the two pieces of each column and the two pieces were kept together and bound with the binding tape.

.

Fig. 1. Splitting of PVC pipes

3.3 *Mold Removal*

After pouring the mix, molds were kept 24 hours outside to harden and after that the columns were submerged in a curing tank for 28 days of period time. The curing procedure is shown in the Fig. 3. Soil cements columns were removed after the curing period. When removing the molds only, 6m & 8m model columns were retrieved from the molds, however 13 model columns were unable to separate from the molds due to its' flimsy nature. Hence for the experimental study only 6m and 8m columns were used.

a-Soil cement columns b-Curing process

Fig. 2. Column curing process

3.4 *Method of Loading*

In the actual scenario columns are supporting by a sewer pipe with a 1.2 m diameter, to simulate that effect, a modeled steel pipe with a diameter of 55 mm was used. The Steel pipe is made with a welded plate to hold on to the proving ring. Hence after placing the proving ring on top of the pipe the load is applied via the hydraulic jack. The loading method is shown in Fig. 3. After laying the pipe, loading is applied gradually. Total loading apparatus is shown in Fig.4. For the loading box dimensions; width, length & height selected are 500 mm ,1200 mm & 800 mm respectively minimizing the end effects.

Fig. 3. Loading method

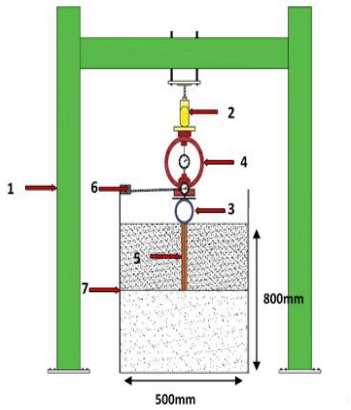

1-Steel Frame
2-Hydraulic Jack
3-Steel Pipe
4-Proving Ring
5- Soil Columns
6-Settlement Gauge
7-Steel Box

Fig. 4. Loading Apparatus

4 RESULTS AND DISCUSSION

When analyzing the results of the loading test, only 6m columns were able to withstand the design load and 8m columns were failed. From the post mortem study conducted for the failed columns had identified that the columns were failed due to a bulging failure. Figure 5 shows the failed soil cement columns .Given below, several relationships discovered through the loading test

Fig. 5. Failed Soil Cement Columns

4.1 *Settlement Reduction*

When sum-up the settlement characteristics of the unimproved ground and the improved ground, it can be said that soil columns have been contributed to the settlement reduction in the soft soil and the settlement has been reduced approximately up to 90%. Figure 6 shows the settlement curves with comparison to unimproved ground and 6m column installed grounds.

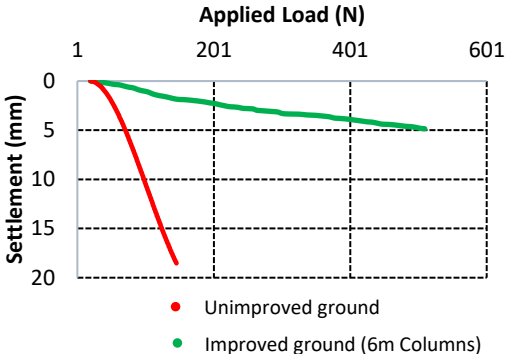

Fig. 6. Settlement Reduction

4.2 *Effects of the Length*

When analyzed the influence of the column length in soil cement columns, it has been noted that the both 6m and 8m columns behave in the same manner (Figure 7).However since the 8m columns were cracked while reducing the settlement, it can be interpreted that, when the slenderness ratio is more than 12,soil-cement columns carry the load while buckling the columns

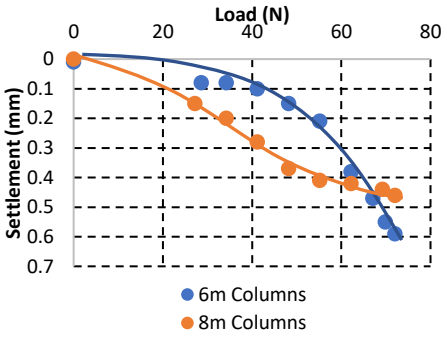

Fig. 7. Effect of the Length

4.3 *Effect of Loading Time*

By analyzing the settlement graph of 8m columns for different curing periods it can be identified that, when the loading duration increases settlement of the columns has reduced due to the contribution of the confining pressure from the soil. Figure 8 shows the column loading time curves.

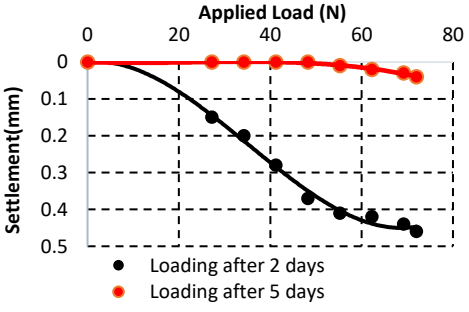

Fig. 8. Effect of Loading Time

4.4 *Numerical Results*

It is vital to validate the experimental results through a numerical analysis, such that increases the accuracy of the experimental results. In this section discusses about the result of the numerical analysis which is done through Plaxis 2D software. The soil columns were modelled in plain strain condition and plate elements used to model soil-cement columns (PLAXIS Version 8 Tutorial Manual .2005)

4.4.1 Unimproved Ground

When the results obtain from the numerical analysis and the experimental analysis are plotted as given in the Fig. 9; It can be seen that the numerical resultant values for unimproved ground was initially resemble to each other. But when the loading increased the experimental results showed a slightly higher settlement that the numerical results. Overall, it can be said that the numerical and experimental result on unimproved grounds show the same behavior

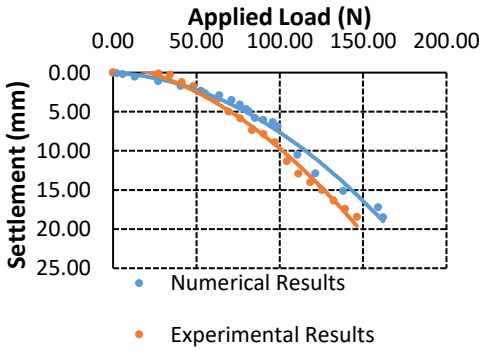

Fig. 9. Unimproved ground settlement

4.4.2 Column Improved Ground

From Fig.10 reflects the comparisons of numerical and experimental results for 6m soil cement columns. When analyzed the curves it can be identified that the behavior of modeled and the laboratory results are not exactly same, the main reason for such a difference is that in the Plaxis platform the soil cement columns are modeled as plate elements and it is unable to customize the characteristics of plate elements to a greater extend. However, the settlement values don't vary much.

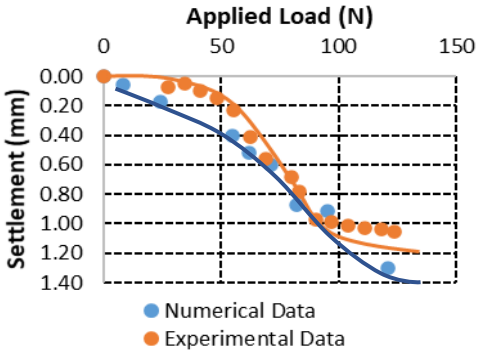

Fig. 10. Improved ground settlement analysis

5 CONCLUSION

Based on this experimental research study following conclusions can be made;

1. By mixing the about 35% of the cement with very soft peaty clay, compressive strength of the peaty clay can be improved significantly. The undrained shear strength of unimproved peaty clay is 22.5 kN/m2 However after improvement, unconfined compressive strength has been increased to 350 kN/m2 after 28 days of curing. Moreover, the initial elastic modulus of 1800 kN/m2 has been increased to 20000 kN/m2.
2. Installing soil-cement columns up to the hard stratum, settlement due to intended load (Design load, 2 x Design load) can be drastically reduced. In other words, by installing soil-cement columns, bearing capacity of the soft peaty clay can be significantly improved. Further it can be concluded that settlement in the unimproved ground under design load can be reduced by 90% after installation of soil-cement columns.
3. When the soft soil thickness is less than 6m soil-cement carry the pipe load without any failure in the columns. However, when the slenderness ratio is more than 12, soil-cement columns carry the load while buckling the columns. Even though, soil-cement columns were failed settlement under the design load is very less that of unimproved ground and that is within the allowable limit.
4. Failure pattern of the soil-cement columns indicated that, buckling occurred at 2/3 of the height of the base.
5. Numerical analysis validates the experimental data such that it proves the credibility of the experimental pipe load testing results.

REFERENCES

Antonio Bobet C.T.J and Hwang J (2011), One5dimensional_consolidation_b.PDF, NRC Research Press, p. 16

Hebib S. and Farrell E.R (2003), Some experiences on the stabilization of Irish peats, Can. Geotech. J., vol. 40, no. 1, pp. 107–120

Toit D , Kradenburg V and Lochner F (2005),PLAXIS Version 8 Tutorial Manual, *Plaxis*, pp. 1–16,

Wardani P.R. and Muntohar A.S (2011),Laboratory Model Test on Improved Soil Using Lime-Column, no. May, pp. 271–275